UKRI Science and Technology Facilities Council

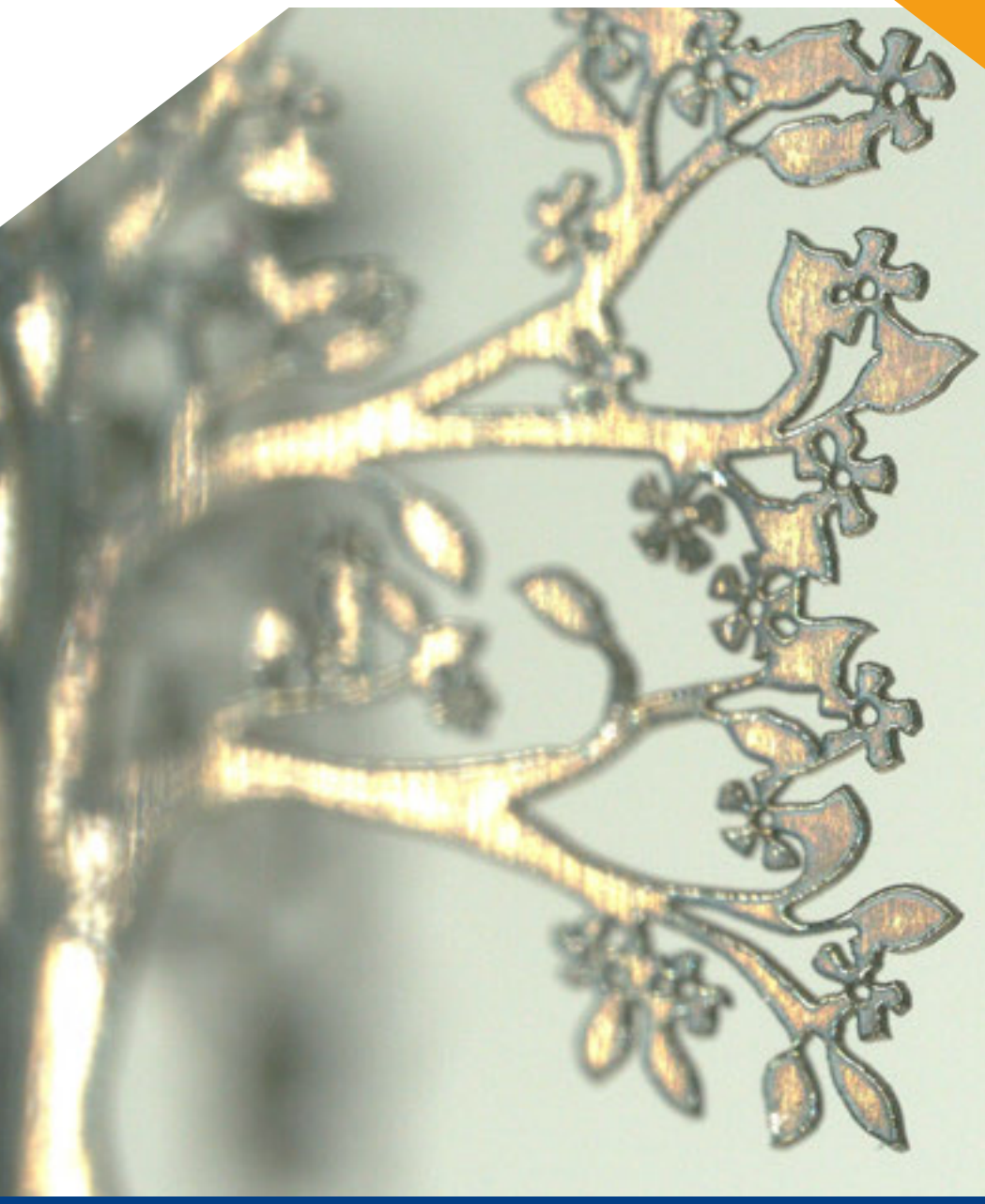

Central Laser Facility Annual Report

2021–2022

Central Laser Facility
Science & Technology Facilities Council
Rutherford Appleton Laboratory
Harwell Campus
Didcot, Oxfordshire OX11 0QX
T: +44 (0)1235 445647
E: clfannrep@stfc.ac.uk
W: www.clf.stfc.ac.uk

The production team for this Annual Report was as follows:

Editor: Raoul Trines

Production: Tracey Burge and Raoul Trines

Section Editors: Hamad Ahmed, David Carroll, Ian Clark, Dave Clarke, Rob Clarke, Marco Galimberti, James Green, Greg Greetham, Chris Hutchinson, Robert Lees, Ian Musgrave, Pedro Oliveira, Rajeev Pattathil, Jonathan Phillips, Tiago Pinheiro De Faria Pinto, Alex Robinson, Dan Symes, Martin Tolley, Christopher Tynan, Adam Wyatt, Tinesimba Zata

This report is available on the CLF website at www.clf.stfc.ac.uk

Design, layout and production: UKRI Creative Services

Thanks to all of the above for their contribution towards producing this report and, of course, to all of the authors for their submissions.

Front cover image: A minute 3D sculpture of a tree. The flowers on the tree are mere nanometres wide. The individual parts to it were cut out by the CLF's Microengineering group and then hand-built by our Target Fabrication team. To take this picture, we borrowed some time on a stereo microscope in the Octopus Facility, where the machine cleverly combined several layers of images into one.

Contents

Foreword

John Collier Director, Central Laser Facility, STFC Rutherford Appleton Laboratory, Harwell Campus, Didcot, UK | Email address: john.collier@stfc.ac.uk | Website: www.clf.stfc.ac.uk

The Central Laser Facility has long thrived on ideas, novelty and creativity, that are most often the product of face-to-face interaction, collaboration and sharing. Many great ideas have arisen through chance encounters or casual remarks. After the challenges we all faced through lockdowns, it has been wonderful to see staff and users returning in numbers to our facilities in 2021/22, once again fermenting that unique collective spirit that has been so successful for us. Interactions matter – they matter a great deal. They are a vital source of motivation and inspiration.

Based at the STFC Rutherford Appleton Laboratory in Oxfordshire, the CLF is the UK's national laser facility and supports curiosity-driven and applied research across a wide range of areas from fundamental physics to the life sciences. Our laser facilities – **Vulcan, Gemini, Artemis, Ultra** and **Octopus** – provide scientists with an unparalleled range of cutting-edge laser technology. We also offer a comprehensive support package for facility users, including custom experiment design and construction, computational **plasma physics, target micro-fabrication** and **engineering**, intended to help our user community to maintain their world-leading position.

We remain committed to advancing the technologies available to our user community and a number of new facilities and facility upgrades are either under construction or at the planning stage. Significant progress has been made on the new **Extreme Photonics Applications Centre (EPAC)** with the building fully complete and plans in place to begin installation of the services. Designs for the laser systems are progressing well. This is an exciting partnership between UKRI, MoD, academia and industry to develop and apply novel, laser-based, non-conventional accelerators and particle sources, delivering new opportunities for engineering, materials, and life sciences research, as well as having a large range of applications for industry and defence. A business case is being developed for **Vulcan 20-20**, an upgrade to the Vulcan facility that will increase its peak power by 20 times to deliver the highest power laser facility in the world. This will enable new areas of research, for example potentially allowing researchers to study the physics of materials under the most extreme conditions, delivering cutting-edge science in a hitherto unexplored regime, and supporting the development of laser inertial confinement fusion. **HiLUX** is a major transformation of the CLF's ultrafast laser and infrared, Raman and XUV spectrometer infrastructure and upgrades the Artemis and Ultra facilities.

In addition to its user facilities, the CLF is home to the **Centre for Advanced Laser Technology and Applications (CALTA),** which aims to deliver societal, scientific and economic impact from developments in the CLF. Alongside supporting the EPAC project, CALTA is developing the next generation of 100 Hz DIPOLE lasers as part of a Widespread Teaming project funded by the EU and the Czech Ministry of Science, with ground-breaking results expected in the coming year. The commissioning work of the DiPOLE-100X system at the European XFEL continues, and the system will be ready for user experiments in 2023. CALTA and the CLF's **Industry Partnerships and Innovation (IPI) group** also work with industrial partners to facilitate solutions to real-world problems. Embedded staff in the IPI group, who are experienced in delivering industry experiments across the facilities, drive the largest growth for the facilities with strategically aligned impact.

Our **Engineering and Technology Centre (ETC)** is almost complete. The vibrant and space-efficient working area offered by new building will allow us to co-locate all the different engineering disciplines, which will have a huge impact on the overall effectiveness of the teams in their delivery of experiments and projects, as well as in their general training and development. EPIC, the joint innovation centre with India, is proving to be essential for the CLF's ongoing facility development projects. Along with developing the control system modules and targetry solutions for our future facilities, EPIC is now exploring options for extremely cost-effective engineering manufacturing in India.

This annual report for the CLF offers an insight into some of the scientific and technical research that has been carried out by users of the CLF and its staff over the financial year 2021/22. As you will see, this research spans a broad range of science areas, and supports wide-reaching efforts to solve major scientific, economic and societal challenges. I do hope that, like me, you enjoy reading this selection of abstracts, and feel inspired by the achievements of all those involved.

Professor John Collier FLSW
Director, Central Laser Facility

Highlights of 2021/22 include:

For many cutting-edge research areas in laser-matter interactions there is a desire to increase the intensity to which high power lasers can be focused. Higher laser intensities can open up new approaches to laser-driven particle beams as well as allow us to study fundamental physics such as high field quantum electrodynamics. One method to achieve this new intensity regime is focusing the laser to an ever smaller spot size. Researchers from the University of Strathclyde have used the **Vulcan** Petawatt laser to demonstrate that the spatially-varying intensity profile of the laser focal spot strongly affects the fundamental physics of how these high power lasers are absorbed at the target interface. The research points the way to future methods of optimising (and improving the reproducibility) of laser-driven secondary sources relevant to upcoming facilities like EPAC.

An international collaboration, led by Queen's University Belfast, used **Gemini** to study plasma acceleration in solid density interactions at extreme intensity. The radiation pressure of the laser pulse produced ions with energy of 10s MeV emitted from the rear surface of the targets. In this work, the team optimised the mechanism to preferentially accelerate carbon ions over contaminant hydrogen – an important result for the use of heavy ions for radiobiology applications.

The CLF successfully held its first ever hybrid **High Power Laser** Christmas scientific meeting, with a series of talks dotted between networking and poster sessions. The meeting went very well, with 60 people attending in person and a further 40 people online.

Artemis user experiments with XUV pulses re-started in the new labs in the Research Complex at Harwell. Artemis commissioned its new 100 kHz laser system, and completed engineering work on the new XUV beamline designed to exploit it for studies of ultrafast dynamics in materials.

Octopus continues to be strong in the fields of atmospheric science, through optical trapping of aerosols to assess their morphology and composition, and life sciences, through correlative and super-resolution microscopy of mammalian and plant samples. The group contributed to the characterisation of new probes for lipids and DNA, as well as being involved in an international project uncovering the mechanisms of SARS-CoV-2 coronavirus infection.

Ultra has been developing its support for energy sciences, such as research into new catalysts. Ultra's ability to study chemistry across multiple steps of a catalytic cycle was highlighted by the Royal Society of Chemistry, for sustainable catalytic chemistry work with the University of York (Fairlamb and Lynam).

Most current laser shock peening (LSP) techniques require a confinement layer, typically water, which puts a major limitation on its accessibility to industry. **CALTA**'s in-house DiPOLE laser was used to demonstrate the ability to peen without the need for the water confinement layer, opening up LSP as a technique for real-world applications.

The **EPIC** partnership with India is developing a talent pool of control and software engineers from which we could potentially recruit. We had the first such recruit in this reporting year, for developing the data management solutions for EPAC. We have also explored cost-effective engineering manufacturing in India through EPIC; the first turning chamber for EA1 will shortly be shipped to the UK.

The CLF's **IPI group** continues to scan for innovative concepts and technology transfer opportunities, to capture and drive forward the most impactful ideas and inventions. A new patent family was filed, giving a current total of 25 active patent families, with 11 invention disclosure forms submitted for future consideration.

The **Plasma Physics Group** has continued to provide CLF users with theory and simulation support, including access to the PRISM suite and help with use of the CLF's SCARF resources. In the wake of the announcement of net gain on the NIF (USA) in 2022, Dr Robbie Scott also helped inform national media outlets of the importance of this seminal result.

The CLF's **Target Fabrication Group** has continued its support for the user community with delivery to the Vulcan and Gemini laser systems, and further developments in tape drive technology to enable direct laser irradiation for high rep rate ion acceleration experiments. It has also supported academic access to the Orion laser system and CLF-led experimental campaigns on Omega in the US.

The CLF's **Engineering Division** will shortly be moving into its purpose-built Engineering and Technology Centre. This new space will include an upgraded mechanical machine shop with a range of new CNC machines for faster and more accurate production of components, a flexible ground floor space to maintain and build large items, and a first floor space to build racks and modules.

Overview of the Central Laser Facility (CLF)

Cristina Hernandez-Gomez
Central Laser Facility, STFC Rutherford Appleton Laboratory, Harwell Campus, Didcot, UK
Email address: cristina.hernandez-gomez@stfc.ac.uk | **Website:** www.clf.stfc.ac.uk

Introduction

The CLF is a world leading centre for research using lasers in a wide range of scientific disciplines. This section provides an overview of the capabilities offered to our international academic and industrial community.

VULCAN

Vulcan is a versatile high power laser system that is composed of Nd:glass amplifier chains capable of delivering up to 2.6 kJ of laser energy in long pulses (nanosecond duration) and up to 1 PW peak power in a short pulse (500 fs duration) at 1053 nm. It currently has eight beam lines. Two of these beam lines can operate in either short pulse mode or long pulse mode, while the remaining six normally operate in a long pulse mode. The short-pulse and long-pulse systems operating jointly can be directed to two different target areas, enabling sophisticated interaction and probing experiments.

The installation of the new short-pulse OPCPA beamline (VOPPEL) has continued: this beamline aims to deliver a PW-level pulse (30 J in 30 fs) to the Vulcan Petawatt Area (TAP) in conjunction with the existing PW (500 J, 500 fs) and long pulse (250 J) capabilities. The new laser area (LA5) houses the VOPPEL Front End and initial I stages of amplification, and the commissioning of these systems in LA5 has started. In addition, building work in TAP enabled the floor to be strengthened for the new compressor chamber vessel, which has now been installed.

GEMINI

Gemini is a dual-beam Petawatt-class Ti:Sapphire laser system that provides unique capabilities for relativistic laser-matter interactions and secondary source production. Gemini is one of the leading centres for laser-driven plasma accelerators and applications. In the reporting year, Gemini managed to recover from COVID-affected operations, running a full programme of experiments. Ventilation levels in Gemini target area were also improved, which allowed us to get back to the pre-COVID levels of occupancy in the experimental area.

The highlight from this period is the production of 10s of MeV carbon ions using radiation pressure acceleration. This experiment, led by the Queen's University Belfast optimised the mechanism to preferentially accelerate carbon ions over contaminant hydrogen – an important result for the use of heavy ions for radiobiology applications.

TARGET FABRICATION

The Target Fabrication Group made the majority of the solid targets shot on the CLF's high-power lasers, and also supported target design for the academic access on the Orion Facility at AWE. Commercial access to target fabrication capabilities was available to external laboratories and companies via the spinout company Scitech Precision Ltd. The group also supported the LSF with microfabrication capabilities to enable their experimental campaigns.

A range of microtarget types were produced to enable the exploration of several experimental regimes. Fabrication techniques included thin film coating, precision micro-assembly, laser micromachining, and chemistry processes, all verified by sophisticated characterisation. STFC's advanced capabilities in both high precision micromachining and MEMS microfabrication were also utilised. The Group's processes and component tracking system provided a high level of traceability.

Further progress was made in the development and experimental fielding of a high stability, high rep-rate (HRR) tape drive, which was used on experiments in Gemini and on external facilities. In collaboration with several Indian institutions through EPIC, advances were made in the production of complex tapes for novel HRR applications and experiments. Progress continued in the robotic assembly of target arrays, and exploratory work on liquid targetry for EPAC was started in collaboration with SLAC and QUB.

THEORY AND MODELLING

The Plasma Physics Group supports scheduled experiments throughout the design, analysis and interpretation phases, as well as users who need theoretical support in matters relating to CLF science.

PPG supports principal investigators using radiation hydrodynamics, particle-in-cell, hybrid and Vlasov-Fokker-Planck codes, as well as by providing access to large-scale computing (SCARF).

Strong support of users throughout this period has continued, including the provision of the PRISM suite. Alongside the core mission of the PPG, this year also commemorated the contributions of Professor Peter Norreys to the PPG in a symposium to mark his formal retirement from STFC.

ARTEMIS

(Research Complex at Harwell)

This was the first year of operations for Artemis in the Research Complex, following the lab move and completion of the upgrade project.

The first experiments on the 1 kHz beamline started in June, gradually increasing in complexity through the year. The much higher XUV flux obtained on the fully refurbished beamline was appreciated by the users.

Commissioning of the 100 kHz laser continued throughout the year. It has now fully met specifications and continues to work reliably. Engineering work on the 100 kHz beamline was completed by commissioning of the vacuum control system in the summer. The pump laser of the 100 kHz system was used in the autumn for its first experiments. These involved a collaboration with Ultra on Kerr-gated Raman spectroscopy, exploring the advantages of pumping at much higher average power. The team also generated high harmonics with the 100 kHz laser for the first time.

The Artemis and Ultra teams resubmittted their 'HiLUX' proposal for major transformation of the ultrafast spectroscopy and dynamics facilities in autumn 2021, and this has now been approved. For Artemis, this will include replacement of the unreliable 1 kHz system with a 100 kHz Yb-based laser, and upgrades of the materials science and molecular dynamics end-stations to capitalise on the higher repetition rate. The work done to move the facility to new labs and upgrade the infrastructure puts the CLF in an excellent position to implement these new technologies.

ULTRA

(Research Complex at Harwell)

The structural dynamics facilities at Ultra explore molecular structure during changes, such as chemical reactions, or in complex environments. Ultra's unique combinations of multiple laser amplifiers provide light across UV to IR, spectrally narrow and broad, measuring dynamics across femtoseconds to seconds, to address a diverse portfolio of scientific problems. The scientific themes span the dynamics of drug binding and protein folding to structural changes in battery charging and catalytic cycles. The available techniques provide highly sensitive time-resolved vibrational and electronic absorption spectroscopies or Kerr-gated Raman spectroscopy to observe weak signals obscured by strong emission from samples.

OCTOPUS

(Research Complex at Harwell)

In the imaging area, the Octopus cluster offers a range of microscopy stations linked to a central core of pulsed and CW lasers, offering "tailor-made" illumination for imaging. Optical resolution techniques offered include total internal reflection (TIRF) and multi-wavelength single-molecule imaging, confocal microscopy (including multiphoton), fluorescence energy transfer (FRET), fluorescence lifetime imaging (FLIM), and Light Sheet Microscopy. Super-resolution techniques are also available: 2D and 3D Stochastic Optical Reconstruction Microscopy (STORM) with adaptive optics, Photoactivated Localization Microscopy (PALM), Structured Illumination Microscopy (SIM), gated 3D Stimulated Emission Depletion Microscopy (STED), 3D MINFLUX, and super-resolution cryo-microscopy. Laser tweezers are available for combined manipulation/trapping and imaging with other Octopus stations, and can also be used to study Raman spectra and pico-Newton forces between particles in solution for bioscience and environmental research. A cryo focused ion beam scanning electron microscope (FIB-SEM) is also available for 3D volume electron imaging. This forms part of a correlative light and electron microscopy (CLEM) workflow currently under development.

Chemistry, biology, and spectroscopy laboratories support the laser facilities, and the CLF offers access to a multidisciplinary team providing advice to users on all aspects of imaging and spectroscopy, including specialised biological sample preparation, data acquisition, and advanced data analysis techniques. Access is also available to shared facilities in the Research Complex, including cell culture, scanning and transmission electron microscopy, NMR, and x-ray diffraction.

ENGINEERING SERVICES

Engineering is fundamental to all the operations and developments in the CLF. The engineering division operates across all of the CLF's facilities. Mechanical, electrical and software support is provided to deliver the experimental programmes, and the research and development activities. Support can range from making small-scale modifications to existing equipment to improve its performance, through to carrying out larger scale projects, such as the design and development of commercial projects. In addition, there are active engineering collaborations with regional and international partners such as, HiLASE (Prague, Czech Republic), XFEL (Hamburg, Germany) and TIFR (Hyderabad, India).

This year, the CLF Engineering and Technology centre (ETC) building was completed and is now fully operational on the ground floor. The ETC brings all the engineering lab spaces together into a central hub. Not only will this building provide increased space to build and test infrastructures, but it will also offer space to upskill the existing teams and support the training and development of apprentices. The ground floor of the new building will focus on manufacturing from raw materials, and the building of large structures and systems. All the mechanical teams are now co-located and the electrical teams will gradually join them in the coming year.

THE CENTRE FOR ADVANCED LASER TECHNOLOGY AND APPLICATIONS (CALTA)

CALTA aims to deliver societal, scientific and economic impact from developments in the CLF, and continues to support the EPAC Project and develop the next generation of 100 Hz DIPOLE lasers as part of a Widespread teaming project. Construction of this new 100 Hz DiPOLE system is almost complete and CALTA expects to break new ground in the coming year. The commissioning work of the D-100X system at the European XFEL continues, with the first two stages of the laser amplifier chain now commissioned and operating as expected. Completion of this system will be ready for user experiments in 2023. The in-house DiPOLE 10 J laser was used to demonstrate a new laser shock peening (LSP) technique that does not require a water confinement layer, opening up LSP to a wider range of applications, particularly in combination with CALTA's DiPOLE laser system, for which the beam behaviour can be controlled closely and adapted for optimal results.

THE EXTREME PHOTONICS APPLICATIONS CENTRE (EPAC)

EPAC, which is under construction at the CLF, will enable the development of a transformational generation of laser-driven radiation sources and accelerators, and will maximise their scientific and economic exploitation through engagement of multiple end-user communities.

EPAC will initially deliver a PW laser operating at 10 Hz to dedicated experimental areas housed in a stand-alone building. In order to achieve this high peak power and repetition rate, DiPOLE technology will be used to pump a high energy Titanium Sapphire amplifier operating at 10 Hz.

The first experimental area (EA1) will be especially designed for laser wakefield acceleration (LWFA), where multi-GeV electron beams and synchrotron-like x-ray beams can be generated. The second experimental area (EA2) will be a very versatile area for fundamental science and applications with flexible focusing geometries. A third experimental area is still to be specified.

The first and second floor will also have a large office space where staff and long-term visitors will be based. The building is expected to be handed over to the CLF in May 2022.

ECONOMIC IMPACT

This year, industry contract-access projects amounted to 19 facility access weeks, delivering experimental access to Gemini, Ultra and Octopus, along with access to CLF scientific expertise. The level of interaction with industry remained lower than that prior to COVID, as this year was focused on recovering the core funded academic access. This focus will remain for the coming year, and further impact on the industry user programme is anticipated.

The Industry Partnership and Innovation (IPI) Group has been pushing to ensure that the interactions delivered are strategically aligned to the CLF and of the highest economic and societal impact to the UK. Industry access with Rolls Royce was delivered, enabling them to non-destructively test their electric rotor for aerospace. This access not only helped them to gain a better understanding the structural changes, but will also help to drive forward the technological development of EPAC. Other access has also strengthened strategic industry partnerships with Johnson Matthey, UCB Pharma and the MOD's dstl.

The CLF remains a strong department for innovation. Internationally, the CLF has driven forward its innovation policy and the growth of industry liaison offices, through shared learning and knowledge exchange across EU laser facilities as a project partner organisation on the European Horizon 2020 IMPULSE project.

ACCESS TO FACILITIES

The CLF operates "free at the point of access", available to any UK academic or industrial group engaged in open scientific research, subject to external peer review. European collaboration is fully open for the high power lasers, whilst European and International collaborations are also encouraged across the CLF suite for significant fractions of the time. Dedicated access to CLF facilities is awarded to European researchers via the Laserlab-Europe initiative (www.laserlab-europe.net) funded by the European Commission.

Hiring of the facilities and access to CLF expertise is also available on a commercial basis for proprietary or urgent industrial research and development.

Please visit www.clf.stfc.ac.uk for more details on all aspects of the CLF.

Industry Engagement and Innovation

Kathryn Welsby
Central Laser Facility, STFC Rutherford Appleton Laboratory, Harwell Campus, Didcot, UK
Email address: kathryn.welsby@stfc.ac.uk | **Website:** www.clf.stfc.ac.uk

Introduction

This article highlights the industrial user engagement, industry partnerships, and innovation activities of the Central Laser Facility for the reporting period April 2021 to March 2022.

Industrial users and engagement

During this past year, the facilities concentrated on recovery of the academic programme due to the impact of the COVID-19 pandemic. This had a knock-on effect on capacity to deliver industrial use of the facilities. Whilst the CLF delivered an increase of industry access this year compared to year 2020-21, the industry user programme is still in recovery and aims to reach the allocated 10% industry access rates by year 2023-24.

The CLF delivered 19 facility access weeks with industrial users this year, delivering experimental access to Gemini, Octopus and Ultra facilities and access to CLF scientific expertise. The CLF continues to drive impact across a wide variety of industrial sectors and to contribute advanced characterisation in industrial R&D despite the reduced operational delivery.

Over the past year CLF's Industry Partnerships and Innovation (IPI) group has also delivered multiple expertise consultations with industry partners. In 2021-22 we consulted on 14 different projects with 14 different industry partners. The industry sectors engaged with through the CLF's industry user programme include advanced manufacturing, formulation and chemical, defence and security, space, food and agritech, and biotechnology (healthcare, medical, bio-pharmaceuticals).

SME LightOx Ltd, a spin-out success from Durham University, focuses on developing light activated chemotherapy for treatment of early-stage mouth cancers. LightOx and the CLF were awarded funding through Innovate UK's Analysis for Innovators (A4I) grant to study the two-photon absorption cross-section and cellular-behaviour of their light activated probes. LightOx scientists were seconded to our facilities to learn our advanced fluorescence microscopy techniques. The experiments carried out at the CLF are helping LightOx in developing new therapeutic solutions to improve patient function and long-term outcomes.

The IPI group has also performed a number of pump-prime applications with industry and academic partners, and a number of commercial access experiments that prime future return or provide current return of investment for the facilities. We have carried out experiments for a PepsiCo sponsored PhD studentship in collaboration with Leeds University, applied advanced spectroscopy with Oxford Nanopore Technologies, and imaging and spectroscopy for the CLF's strategic partner Johnson Matthey.

Industry Partnerships

This year our Gemini facility carried out exploratory application of laser plasma acceleration to penetrative x-ray imaging for our industry partner Rolls Royce. This work is crucial to understanding how our new Extreme Photonics Applications Centre (EPAC) will be used by industry and help us to develop our technology to suit the requirements of business.

The experiment looked towards laser-produced highly penetrative x-rays used to image the rotor found in Rolls Royce's new electric engine for aerospace. Large, metallic items like Rolls Royce's rotor are difficult to image due to their size, high density and magnetic materials. EPAC will revolutionise x-ray imaging of these type of objects non-destructively, which will have applications in engineering and manufacturing industries from across the UK and internationally.

In partnership with both academia and industry, a CLF collaboration has been awarded funding through the Innovation Partnership Scheme to develop the novel application of two-dimensional IR spectroscopy as a liquid-biopsy diagnostic technique. This project will run for next three years and includes funding for regular access to our 2DIR system. Our lead academic partners at York University are developing a rapid multi-sample holder to be optimised at our Ultra facilities, and our industrial partner UCB Pharma will utilise the new technique for realising business benefits.

The CLF's long-standing laser fellowship programme with Johnson Matthey continued once more this year, successfully delivering industrial access to both the Ultra and the Octopus facilities. The fellowship highlights the importance of the work that the CLF does for knowledge transfer between large-scale facilities and industry.

Innovation

The CLF's IPI group continues to scan for innovative concepts and technology transfer opportunities, to capture and drive forward the most impactful ideas and inventions.

This year the CLF filed a new patent family, giving a current total of 25 active patent families, and 11 invention disclosure forms were submitted for consideration for future patent filing. Additionally, three proof-of-concept projects were funded or ongoing, and a new Knowledge Assets Grant Fund was awarded.

A new area of innovation for the CLF is the development of a novel VUV Light source for gas and water treatment. This project was supported this year by the governments Knowledge Assets Grant Fund. This project proposes the development of a microwave plasma to produce VUV (UV λ<200 nm). Currently, the main source of VUV commercially is from excimer lamps. The proposed microwave-sustained plasma system will push beyond current systems, remove the need for environmentally harmful mercury, and provide advantageous rates of photochemical reactions and conversion compared to other systems.

In this reporting period the CLF's spin-out company Scitech Precision Limited benefited from the recovery from the COVID-19 pandemic. Experimental campaigns restarted across the world and company sales began to recover to pre-pandemic levels. The company carried out 98 individual contracts across 32 institutions across the world, with a turnover of £239k.

Scitech sold its first target delivery system, supplying a tape drive to the SCAPA facility at the University of Strathclyde. This sale was part of the licencing agreement between SPL and the CLF that allows the CLF to support, participate and supply external facilities. The company also supplied its first targets direct to LLNL in the US, as well as continuing to support experiments at the LCLS. Scitech also supported the local scientific campus by providing services to Diamond Light Source, and other spin-out companies on the Harwell campus, as well as companies requiring micro-fabrication across the UK.

International Impact

Horizon 2020's IMPULSE programme, with participation of representatives from 15 Consortium partners from the UK and nine other European countries, continued throughout 2021-22. The project is using the IPI group's expertise to help develop and implement new industry liaison offices, processes and policy, to obtain a strong understanding and learning of how to grow and improve collaborations with industry partnerships and commercial customers to large-scale laser-based facilities.

The Extreme Photonics Innovation Centre (EPIC), a partnership between the CLF and the Tata Institute of Fundamental Research (TIFR), is proving beneficial to the CLF and TIFR alike. EPIC is developing a critical mass of skilled people in India in the technologies associated with novel accelerators, and is proving to be essential for the CLF's ongoing facility development projects, such as EPAC and Vulcan 20-20.

Communications and outreach activities within the CLF

Helen Towrie
Central Laser Facility, STFC Rutherford Appleton Laboratory, Harwell Campus, Didcot, UK
Email address: helen.towrie@stfc.ac.uk | **Website:** www.clf.stfc.ac.uk
Twitter: @CLF_STFC | **LinkedIn:** Central Laser Facility

The CLF's Communication Strategies

The role of the CLF's Impact and Engagement team is to promote CLF science and technology to some of our key audiences and share what we are capable of, to engage with our community and recruit new people. Different audiences require different types of interaction, and we have worked to develop and harness the tools needed to communicate with each effectively.

We are responsible for internal and external engagement functions, including: the CLF website and Twitter for our general science audience, staff and user community; talks, tours and activities for our general and next gen audiences; and a fortnightly newsletter for CLF staff.

Social Media

Social media, namely Twitter, has become increasingly important for interacting with our target audience. Monthly analyses of the CLF Twitter account show that we have grown in followers, and that these followers are largely within our target audience of users and the scientific community. This means that, when we share a tweet, we know that what we are sharing will impact the right people.

2019/20	587	(187 more than the year before)
2020/21	850	(263 more than the year before)
2021/22	1,067	(217 more than the year before)

A quick comparison of our Twitter follower growth over the past three years shows a steady increase.

Having reached our main goal of hitting 1,000 followers, we have now moved on to a new goal of increasing or maintaining our engagement on the tweets we share. This will involve observing which tweets do well and which do not, and adjusting our posts accordingly.

Key moments on Social Media

Not all tweets are created equal. Over the years we have learnt more about what makes our followers engage with our content, and the subjects to which they are most likely to respond.

For example, a nail-biting video of our new ~10 tonne compressor being guided through a door with only a few millimetres gap proved a success on Twitter. We also know from secondary research that videos do work well on this platform.

Another tweet that did very well (with a 12.6% engagement rate!) was a fun, casual tweet about EPAC.

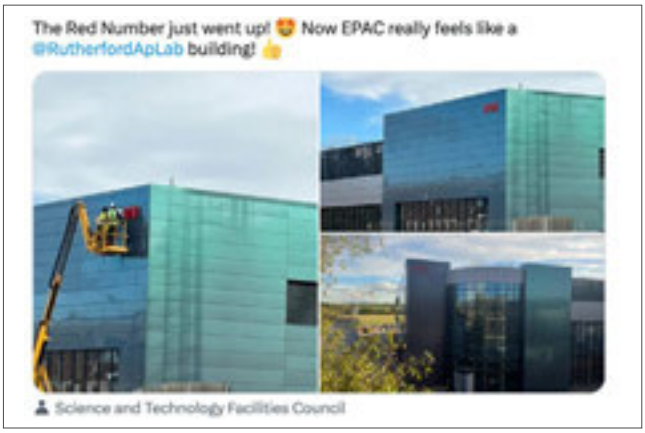

Casual tweets seem to do really well and we have found that our audience always enjoys tweets like this, particularly where combined with the subject matter of EPAC. The engagement rate was increased by the fact that there were multiple pictures, meaning that users clicked through the images.

We continue to keep in close contact with the STFC Twitter and Instagram team, through whom we can reach a more general public audience as opposed to the general scientific audience that the CLF Twitter aims to attract. To aid these discussions and others, a CLF representative attends a monthly Social Media meeting, where all the departments can communicate new ideas, campaigns and best practices.

The CLF Website

Summary Financial Year: 2021/22

Number of people who visited the website

24,488

Unique page views
(Bots subtracted)

88,593

Social referrals out of 24,488 users:

Twitter
735

Facebook
257

LinkedIn
158

YouTube
3

Instagram
1

Although the number of people visiting our website has fallen (29,000 in 2020/21), there has been a higher number of unique page views. We have also seen a further increase in the number of people coming from LinkedIn (just 20 in 2019/20 and 149 in 2020/21), with other social referrals remaining at a similar level to the previous year.

Attracting a Wider Audience

And maintaining all avenues of communication

This year has, once again, been quite different from other years at the CLF. While lockdowns have eased, COVID is still very much present and impactful in our lives.

As a result, we have continued to conduct a hybrid communications strategy and have remained as flexible as we can during this uncertain period.

We have completed an array of projects, many of which are highlighted in this summary, to help make the CLF more appealing to a wide range of audiences.

Our largest undertaking this year has been our involvement in the upgrade of the CLF Visitor Centre. The upgrade involved extending the room, adding around two metres to the south side, coupled with the addition of new interactive displays, TV screens and wall panels, and a complete information and imagery refresh.

As well as writing a fair amount of the text ourselves, our team worked closely with designers, engineers and senior staff over a number of months to collect the vast amount of information needed to refresh the internal walls.

In addition, we created a large mural that is now displayed on both outer walls of the visitor centre. This illustration took many weeks of thought and consideration, and is intended to make the CLF's visitor centre more eye-catching to passers-by, and to engage with a wide range of people.

Public Engagement Overview

As part of our goal to engage with the next gen audience, we have taken part in multiple events, often by giving tours. These events have been well attended and we have engaged with one of our key audiences – 8 - 14 year olds. This is the age at which children are starting to think about their future careers, and is also around the age when many young girls unfortunately decide that science and engineering is not for them.

Overall, from April 2021 – March 2022, we hosted 60 tours and visits to our facility. Due to the new way of hybrid working introduced by lockdowns, many of these were virtual visits via Zoom. While this has its limitations, it did mean that we were able to reach a more varied audience that was not constricted by whether they could travel to visit our labs.

Here are the stats, for April 2021 – March 2022:

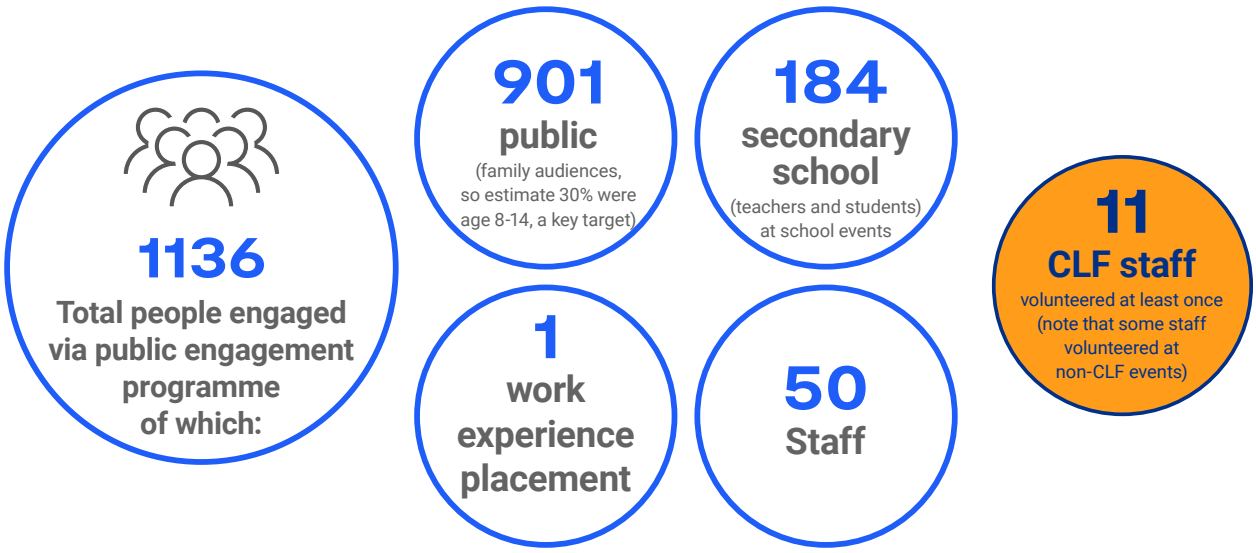

Welcoming New Staff

The CLF and other STFC departments have created a rota for hosting virtual tours for new starters. These tours take place throughout the year and are designed to show staff what is going on all around them in the place they work. It also helps CLF staff themselves, because often we find that people from one part of the CLF do not realise what is happening in another.

Below is some feedback from a New Starters' tour we hosted alongside the Technology Department. In total there were 74 attendees, with more people subsequently asking for a recording of the tour.

- **95% of attendees said the level was pitched just right for them**
- **84% of attendees said the tour was the right length for them**

Comments received include:

I feel like I was able to see a showcase of the wide variety of research that STFC's facilities help to facilitate. It was also interesting to hear about the variety of collaborations, commercial spin-offs and cutting edge technologies that STFC helps develop.

The main thing I learnt was the diversity of work being carried out at STFC.

I learnt a lot about lasers which are possibly the coolest thing at least at STFC but maybe even just in general.

Too much to write down, amazing the different research that goes on across the organization.

[I learnt about] The Size and the impact of STFC's Projects.

I thought the quality of the presentations and speakers were excellent.

I enjoyed this session and felt that it was pitched correctly to give me a perspective of parts of the RAL site that I do not use, while not requiring too much of my time.

Would like to take part again if there is a physical tour in the future.

Such positive feedback makes it feel worthwhile presenting staff tours and talks, and we are thankful for the support we have received to pull everything together.

User Leaflets

As lockdowns are easing, we have created brand new User Leaflets for our visiting users. These are available to HPL and LSF users, and contain useful information to help them find not only the labs and offices, but also coffee, food and places to relax on campus.

EPAC Open Day

Looking forward, we are preparing to host an EPAC Open Day on 25th May 2022 with around 200 predicted attendees from the CLF and surrounding buildings.

We are responsible for creating posters and signage for this event, which is a mammoth project, but a very exciting one!

Advancing towards EPAC —

a new national facility to support UK science, technology, innovation and industry

The building construction phase of the Extreme Photonics Applications Centre (EPAC) is nearing completion, with the building scheduled to be handed over to the CLF in May 2022.

EPAC will bring together academic, industrial, defence and security communities in a diverse programme of fundamental and applied research, industrial metrology and qualification, materials processing, and advanced imaging.

As a facility asset for the UK, EPAC will combine unique capabilities and will serve broad communities. It will enable novel applications leading to scientific breakthroughs and new solutions to challenging problems that will advance UK science and technology, helping to keep us safer, improve our healthcare and support a cleaner, more productive economy.

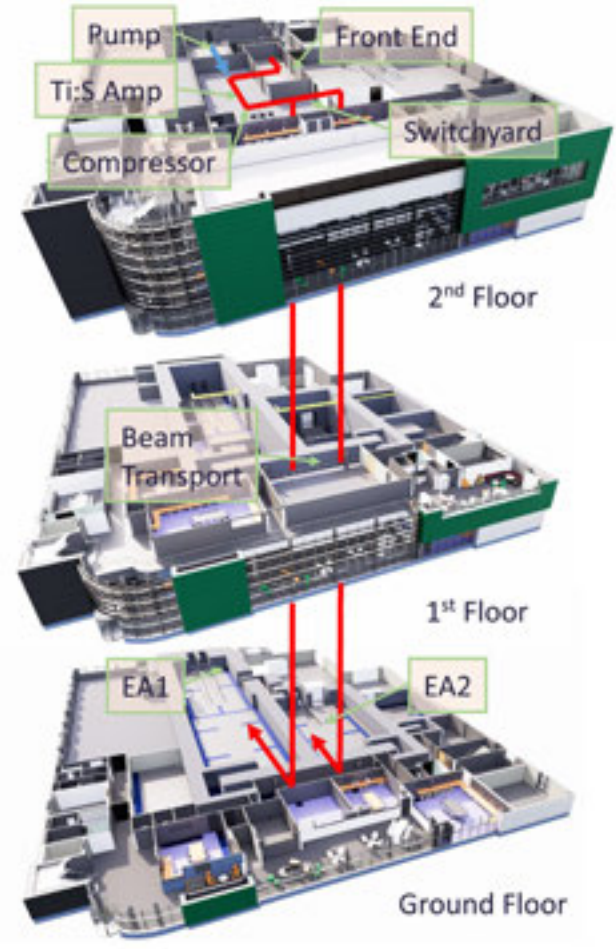

The EPAC building in April 2022

EPAC will house a state-of-the-art 10 Hz, 1 PW laser, with two independent experimental areas. It will constitute a new capability for studies of fundamental science using laser-driven secondary sources, and will focus much of its research on developing laser plasma accelerators for a range of applications in industry, medicine, defence and security.

The ground floor of the building houses three double-height radiologically-shielded experimental areas, where the laser-driven sources are created and used, plus support laboratories.

The parts of the first floor not occupied by the double height experimental areas will house services and offices.

The second floor will house the highly advanced laser technology, with a beam transport propagating the beam to the experimental areas on the ground floor.

The new facility will initially deliver a PW-class laser operating at 10 Hz. In order to achieve this high peak power and repetition rate, the CLF's DiPOLE technology will be used to pump a high energy Titanium Sapphire amplifier.

Detailed descriptions of the laser sub-systems can be found in P.D. Mason, P.J. Phillips, N.H. Stuart *et al.*, EPAC Laser Systems, in the online version of this report on the CLF website.

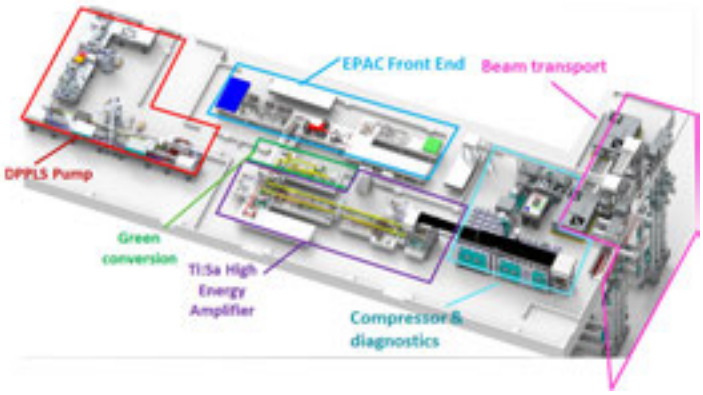

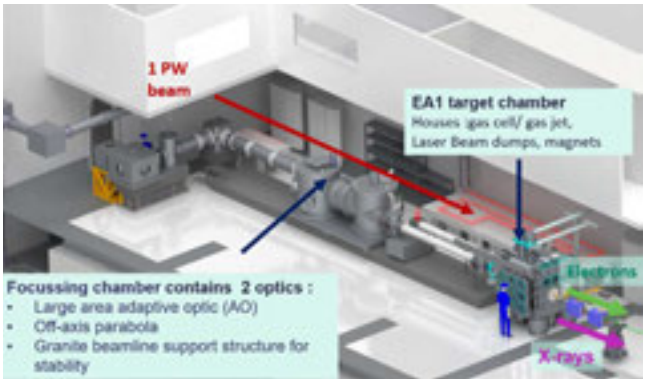

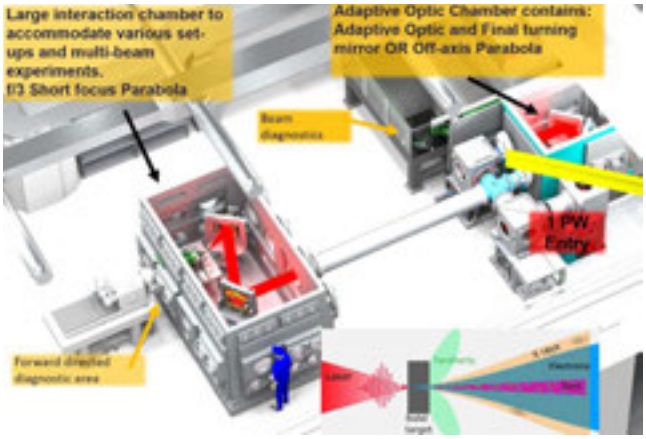

The versatile experimental areas (EAs) in EPAC can drive bright, beam-like high-energy x-ray beams and beams of high-energy electrons, protons, ions, neutrons and muons by merely changing the target geometry, enabling multi-modal imaging and probing capabilities for fundamental science and applications.

EA1 (top) has a fixed configuration, delivering a long-focus laser beamline predominantly for driving a laser-wakefield accelerator.

EA2 (bottom) contains a large vacuum chamber that can be configured in a flexible way with short, medium, and long-focus beamline options. The primary aim of EA2 will be to deliver high intensity solid target interactions; however; it will be possible to also deliver liquid and gas targetry, depending on the science or application driver.

Detailed descriptions of the experimental areas can be found in DR Symes, JS Green, *et al.*, EPAC Experimental Areas and Targetry Developments, in the online version of this report on the CLF website

Several targetry technologies remain under development for EPAC to be able to supply well-characterised targets at up to 10 Hz once user operations begin. There are many areas that need to be progressed to fully exploit the capabilities of EPAC, including rapid batch fabrication (sometimes in situ), accurate alignment, characterisation, and issues of survivability in such extreme environments. Several R&D projects are underway for both solid and liquid targetry, including several larger collaborative efforts with a number of international institutions.

Detailed descriptions of EPAC targetry can be found in W. Robins, C. Spindloe, *et al.*, EPAC High repetition-rate targetry developments, in the online version of this report on the CLF website

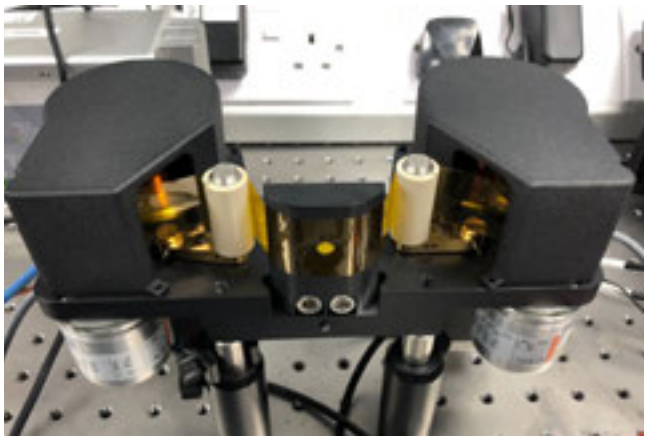

The CLF has made significant progress in the build and testing of an ultra-stable tape delivery system for targets

High energy density and high intensity physics

Generation of Intense Second Harmonic Light from Aperture Targets

E.F.J. Bacon, M. King, R. Wilson, T.P. Frazer, E.J. Dolier, M. Peat, J. Goodman, R.J. Gray, P. McKenna *(Department of Physics, University of Strathclyde, Glasgow, UK)*

T. Dzelzainis, C. Spindloe, S. Astbury *(Central Laser Facility, STFC Rutherford Appleton Laboratory, Harwell Campus, Didcot, UK)*

This report provides a summary of the development of experimental methodologies to enable the investigation of a novel plasma-based mechanism for the generation of higher order mode (HOM) at relativistic intensities, using the Gemini laser system in early 2022.

This mechanism involved the interaction between a high intensity (>10^{18} W/cm^2) laser pulse and a micron-diameter aperture target, leading to several obstacles to overcome experimentally.

These obstacles included mitigating the on-shot spatial jitter of the laser pointing, locating and accurately aligning the aperture to laser focus and a target design which would facilitate high repetition rate operation through automated or precision target placement.

Contact:
E.F.J. Bacon
ewan.bacon.2016@uni.strath.ac.uk

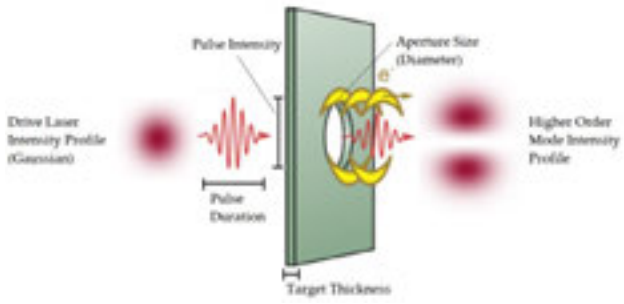

Figure 1: Schematic of the plasma-based HOM generation mechanism, adapted from [1].

*[1] E.F.J. Bacon et al. High order modes of intense second harmonic light produced from a plasma aperture. Matter and Radiation at Extremes} **7**, 5 (2022)*

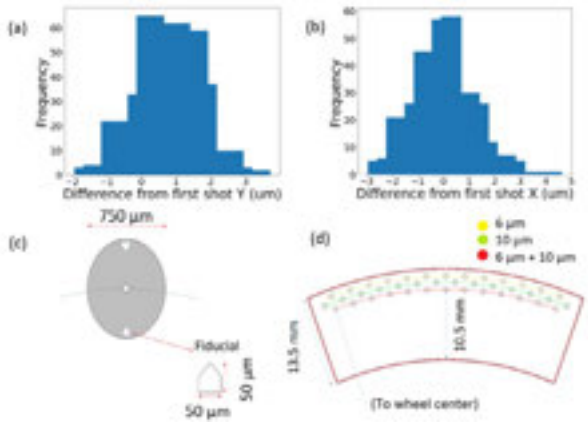

Figure 2: (a) and (b) are histograms of the movements of the focal spot between each shot in Y and X directions, respectively. (c) placement of a fiducial relative to an aperture. (d) segment of the target wheel developed for this experiment.

Effect of laser temporal intensity skew on enhancing pair production in laser—electron-beam collisions

L.E. Bradley *(York Plasma Institute, Department of Physics, University of York, UK; Central Laser Facility, STFC Rutherford Appleton Laboratory, Harwell Campus, Didcot, UK)*
M.J.V. Streeter *(The John Adams Institute for Accelerator Science, Blackett Laboratory, Imperial College London, UK; School of Mathematics and Physics, Queen's University Belfast, UK)*
C.D. Murphy, C. Arran , C.P. Ridgers *(York Plasma Institute, Department of Physics, University of York, UK)*
T.G. Blackburn *(Department of Physics, Chalmers University of Gothenburg, Sweden)*
M. Galletti *(Central Laser Facility, STFC Rutherford Appleton Laboratory, Harwell Campus, Didcot, UK; GoLP Instituto de Plasmas e Fusão Nuclear, Instituto Superior Tecnico, Universidade de Lisboa, Portugal)*
S.P.D. Mangles *(The John Adams Institute for Accelerator Science, Blackett Laboratory, Imperial College London, UK)*

Recent high-intensity laser experiments (Cole *et al. 2018 Phys. Rev. X* **8** 011020; Poder *et al.* 2018 *Phys. Rev. X* **8** 031004) have shown evidence of strong radiation reaction in the quantum regime.

Experimental evidence of quantum effects on radiation reaction and electron–positron pair cascades has, however, proven challenging to obtain and crucially depends on maximising the quantum parameter of the electron (defined as the ratio of the electric field it feels in its rest frame to the Schwinger field). The quantum parameter can be suppressed as the electrons lose energy by radiation reaction as they traverse the initial rise in the laser intensity.

As a result the shape of the intensity temporal envelope becomes important in enhancing quantum radiation reaction effects and pair cascades. Here we show that a realistic laser pulse with a faster rise time on the leading edge, achieved by skewing the temporal envelope, results in curtailing of pair yields as the peak power is reduced. We find a reduction in pair yields by orders of magnitude in contrast to only small reductions reported previously in large-scale particle-in-cell code simulations (Hojbota *et al. 2018 Plasma Phys. Control. Fusion* **60** 064004). Maximum pairs per electron are found in colliding 1.5 GeV electrons with a laser wakefield produced envelope 7.90×10^{-2} followed by a short 50 fs Gaussian envelope, 1.90×10^{-2}, while it is reduced to 8.90×10^{-5}, a factor of 100, for an asymmetric envelope.

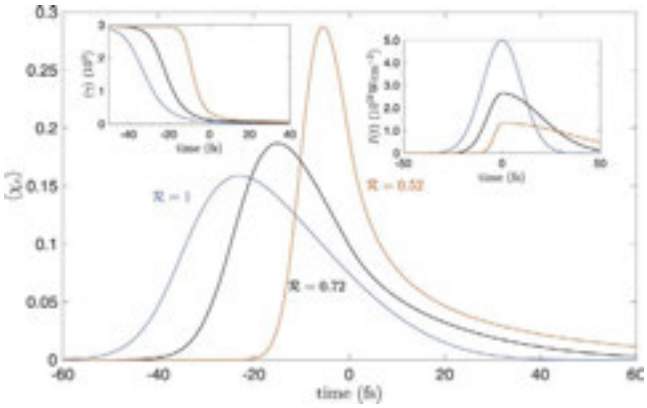

Figure 1: Average electron quantum parameter $\chi_e(t)$ for a Gaussian with different amounts of skew (right inset) using the closed form solution in equations (7) (left inset) and (8) with different reduction factors R. The equations can be found in the published paper.

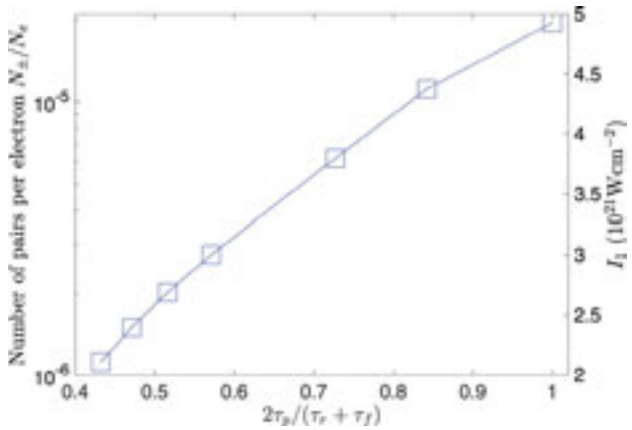

Figure 2: PIC code results showing the electron–positron pair yields per electron $N_\pm/N_e$ as the laser envelope is skewed. As the rising edge of a $I_0 = 5 \times 10^{21}$ W cm^{-2} Gaussian laser pulse becomes faster, the peak intensity drops by a factor R giving the new peak intensity $I_1 = RI_0$ displayed on the right-hand axis.

Contact:
L.E. Bradley
laurence.bradley@stfc.ac.uk

Characterisation of a laser plasma betatron source for high resolution x-ray imaging

O.J. Finlay, S. Jamison *(The Cockcroft Institute, Daresbury, UK; Physics Department, Lancaster University, UK)*
J-N. Gruse, J.M. Cole, J.C. Wood, S.P.D. Mangles, Z. Najmudin *(The John Adams Institute for Accelerator Science, Imperial College London, UK)*
C. Thornton, R. Allott, C.D. Armstrong, N. Bourgeois, C. Brenner, C. Gregory, Y. Katzir, P.P. Rajeev, D.R. Symes, D. Neely *(Central Laser Facility, STFC Rutherford Appleton Laboratory, Harwell Campus, Didcot, UK)*
C.D. Baird, C.D. Murphy, C.I.D. Underwood, M.P. Selwood *(York Plasma Institute, Department of Physics, University of York, UK)*
S. Cipiccia *(Diamond Light Source, Harwell Science and Innovation Campus, Didcot, UK; Department of Medical Physics and Biomedical Engineering, University College London, UK)*
N.C. Lopes *(The John Adams Institute for Accelerator Science, Imperial College London, UK; GoLP/Instituto de Plasmas e Fusão Nuclear, Instituto Superior Técnico, Lisboa, Portugal)*
L.R. Pickard *(National Composites Centre, Bristol and Bath Science Park, Bristol, UK)*
K.D. Potter *(Advanced Composites Collaboration for Science and Innovation (ACCIS), University of Bristol, UK)*
D Rusby *(Central Laser Facility, STFC Rutherford Appleton Laboratory, Harwell Campus, Didcot, UK; Lawrence Livermore National Laboratory, Livermore, California, USA)*
A.G.R. Thomas *(The Cockcroft Institute, Daresbury, UK; Physics Department, Lancaster University, UK; Center for Ultrafast Optical Science, University of Michigan, USA)*
M.J.V. Streeter *(The Cockcroft Institute, Daresbury, UK; Physics Department, Lancaster University, UK; The John Adams Institute for Accelerator Science, Imperial College London, UK)*

We report on the characterisation of an x-ray source, generated by a laser-driven plasma wakefield accelerator. The spectrum of the optimised source was consistent with an on-axis synchrotron spectrum with a critical energy of $13.8^{+2.2}_{-1.9}$ keV and the number of photons per pulse generated above 1 keV was calculated to be $6^{+1.2}_{-0.9} \times 10^9$. The x-ray beam was used to image a resolution grid placed 37 cm from the source, which gave a measured spatial resolution of 4 μm × 5 μm. The inferred emission region had a radius and length of 0.5 ± 0.2 μm and 3.2 ± 0.9 mm respectively. It was also observed that laser damage to the exit aperture of the gas cell led to a reduction in the accelerated electron beam charge and a corresponding reduction in x-ray flux due to the change in the plasma density profile.

Contact:
O.J. Finlay
oliver.finlay@cockcroft.ac.uk

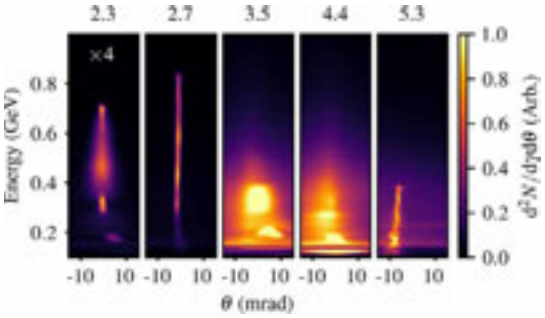

Figure 1: Angularly resolved electron spectra for different plasma densities. The plasma density given on top of each image is given in units of 10^{18} cm^{-3}. The spectrum in the left-most panel has been multiplied by 4 to make it visible on the same colour scale.

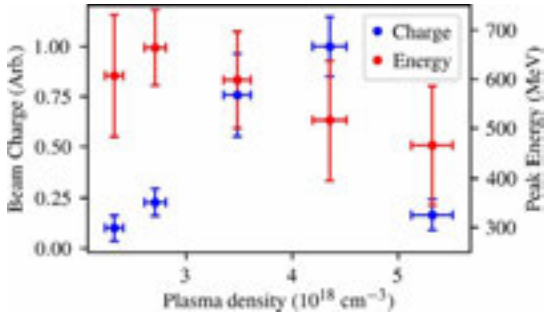

Figure 2: Dependence of the electron bunch charge and maximum electron energy on the plasma density. Each point shows the mean and standard deviation of between 16 and 21 electron spectra.

Industrial imaging using bremsstrahlung generated by a laser-plasma accelerator

M. Gear, C. Armstrong, G. Hull, S. Dann, D. Symes, K. Welsby *(Central Laser Facility, STFC Rutherford Appleton Laboratory, Harwell Campus, Didcot, UK)*

M. Streeter, G. Sarri *(School of Mathematics and Physics, Queen's University Belfast, UK)*
N. Glover, C. Boettcher, E. Chong *(Rolls-Royce plc, Moor Lane, Derby, UK)*

Laser-plasma accelerators can generate bright x-ray beams with attractive properties for imaging applications. They have the potential to surpass the image quality and acquisition rates achievable with commercially available machines – a major motivation for the Extreme Photonics Applications Centre (EPAC), under construction at the CLF. In collaboration with Rolls-Royce, we performed a proof of principle experiment in Gemini Target Area 3 to explore the capability of laser-driven bremsstrahlung x-rays to provide high quality imaging of large, high-density components.

The sample was a rotor that has been used on a demonstrator project for developing high power density electric machines. Rolls-Royce need to analyse the internal features of this rotor without disassembly because this would disturb the underlying structure. This type of non-destructive inspection (NDI) is difficult to achieve with conventional sources, and is a perfect test-case for the unique properties of the radiation beams that will be generated using EPAC.

Contact:
D.R. Symes
dan.symes@stfc.ac.uk

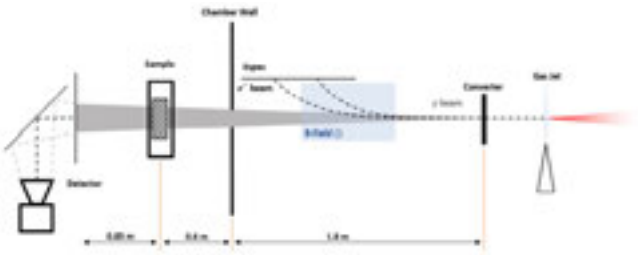

Figure 1: Experimental layout for production and use of bremsstrahlung radiation from laser wakefield acceleration.

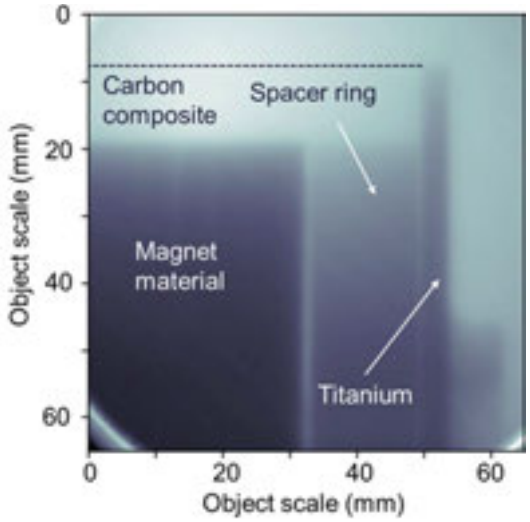

Figure 2: Radiograph of Rolls Royce rotor obtained using bremsstrahlung generated with Gemini.

Investigation of the ejected mass during high-intensity laser solid interaction for improved plasma mirror generation

G.F.H. Indorf *(Institut für Laser und Optik, Hochschule Emden/Leer-University of Applied Sciences, Germany; Central Laser Facility, STFC Rutherford Appleton Laboratory, Harwell Campus, Didcot, UK)*
G.G. Scott, D. Haddock, S.J. Hawkes, L. Scaife, N. Bourgeois, D.R. Symes, C. Thornton *(Central Laser Facility, STFC Rutherford Appleton Laboratory, Harwell Campus, Didcot, UK)*
M.A. Ennen *(Institut für Laser und Optik, Hochschule Emden/Leer-University of Applied Sciences, Germany)*
P. Forestier-Colleoni *(Center for Energy Research, University of California San Diego, USA)*
A.A. Andreev *(Institut für Laser und Optik, Hochschule Emden/Leer-University of Applied Sciences, Germany; Saint-Petersburg State University, Russia)*
U. Teubner *(Institut für Laser und Optik, Hochschule Emden/Leer-University of Applied Sciences, Germany; Institut für Physik, Carl von Ossietzky Universität, Oldenburg, Germany)*
D. Neely *(Central Laser Facility, STFC Rutherford Appleton Laboratory, Harwell Campus, Didcot, UK; Department of Physics SUPA, University of Strathclyde, Glasgow, UK)*

The interaction of very intense and ultrashort laser pulses with solid targets is a topic that has attracted a large amount of interest in science and applications. This interest is boosted by the large progress made in the development of high repetition rate, high-power laser systems. With the significant increase in average power, there is concern about how to deal with ablated debris that may lead to contamination and damage during interaction experiments with solid targets.

This issue is also highly relevant in experiments that include plasma mirrors. These are often employed to increase the contrast ratio of the intense laser pulse to unwanted laser pre-pulses from the amplifier chain and/or the background of amplified spontaneous emission.

For this reason, the present work investigates the mass ejected from the target into vacuum for different conditions, particularly those present when plasma mirrors are introduced. The total amount of ablated mass can be reduced by making use of a temporally controlled plasma expansion that enhances the plasma mirror reflectivity. In this way, high intensity laser interaction experiments can be carried out with efficient and clean plasma mirrors significantly reducing the degradation of the laser optics and plasma diagnostics placed near the interaction.

Reproduced with permission from G F H Indorf et al 2022 Plasma Phys. Control. Fusion **64** *034004, © 2022 IOP Publishing Ltd. doi: 10.1088/1361-6587/ac4939*

Contact:
G.F.H. Indorf
g.indorf@gmx.de

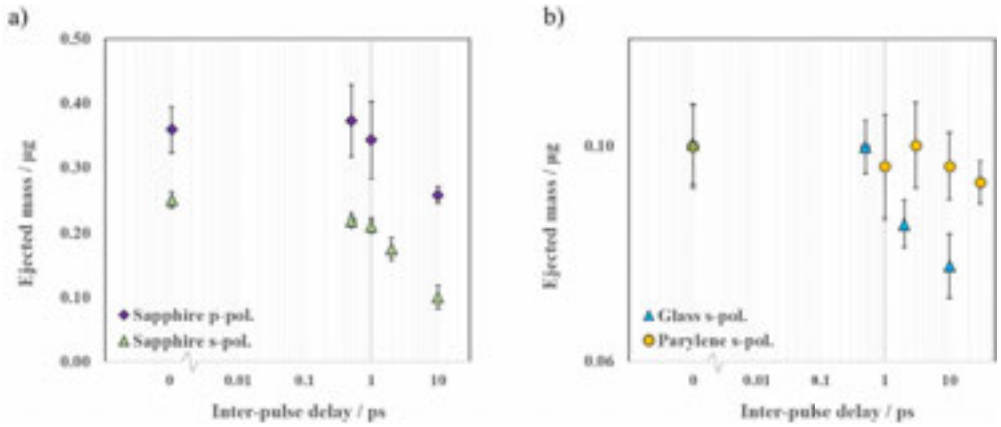

Experimental results showing the ablated mass m_{abl} from the target material ejected into the vacuum as a function of the inter-pulse delay. The first data point in both graphs at 0 ps inter-pulse delay represents a single pulse ablation. (a) Results on the ablation of sapphire showing variation with polarisation. (b) Difference between ablation of glass and parylene, both data sets were obtained in s-polarisation.

A laser–plasma platform for photon–photon physics: the two photon Breit–Wheeler process

B. Kettle, E. Gerstmayr, C. Colgan, R. Watt, S.J. Rose, S.P.D. Mangles *(The John Adams Institute for Accelerator Science, Imperial College London, UK)*
D. Hollatz, H. Harsh, F.C. Salgado, A. Seidel, M. Zepf *(Helmholtz Institut Jena, Germany; Institut für Optik und Quantenelektronik, Friedrich-Schiller-Universität, Jena, Germany)*
G.M. Samarin, A. Alejo , G. Sarri *(School of Mathematics and Physics, Queen's University Belfast, UK)*
S. Astbury, C. Gregory, Y. Katzir, P.P. Rajeev, C. Spindloe *(Central Laser Facility, STFC Rutherford Appleton Laboratory, Harwell Campus, Didcot, UK)*
C. Baird, C.D. Murphy, C. Underwood *(Department of Physics, University of York, UK)*
S. Bohlen, J. Osterhoff, K. Põder *(Deutsches Elektronen-Synchrotron DESY, Hamburg, Germany)*
M. Campbell, D. Dannheim, A. Nurnberg *(CERN, Geneva, Switzerland)*
P. Hatfield *(Department of Physics, University of Oxford, UK)*
J. Hinojosa *(Center for Ultrafast Optical Science, University of Michigan, USA)*
J. Morton *(AWE Aldermaston, Reading, UK)*
G. Pérez-Callejo *(Université de Bordeaux-CNRS-CEA, Centre Lasers Intenses et Applications (CELIA), France)*
C. Roedel *(Helmholtz Institut Jena, Germany)*
F. Roeder *(Institut für Optik und Quantenelektronik, Friedrich-Schiller-Universität, Jena, Germany)*
S. Spannagel *(Deutsches Elektronen-Synchrotron DESY, Hamburg, Germany; CERN, Geneva, Switzerland)*
S. Steinke *(Lawrence Berkeley National Laboratory, California, USA)*
M.J.V. Streeter *(School of Mathematics and Physics, Queen's University of Belfast, UK; Physics Department, Lancaster University, UK)*
A.G.R. Thomas *(Center for Ultrafast Optical Science, University of Michigan, USA; Physics Department, Lancaster University, UK)*

We describe a laser–plasma platform for photon–photon collision experiments to measure fundamental quantum electrodynamic processes. As an example we describe using this platform to attempt to observe the linear Breit–Wheeler process.

The platform has been developed using the Gemini laser facility at the Rutherford Appleton Laboratory. A laser wakefield accelerator and a bremsstrahlung convertor are used to generate a collimated beam of photons with energies of hundreds of MeV, that collide with keV x-ray photons generated by a laser heated plasma target.

To detect the pairs generated by the photon–photon collisions, a magnetic transport system has been developed which directs the pairs onto scintillation-based and hybrid silicon pixel single particle detectors (SPDs).

We present commissioning results from an experimental campaign using this laser–plasma platform for photon–photon physics, demonstrating successful generation of both photon sources, characterisation of the magnetic transport system and calibration of the SPDs, and discuss the feasibility of this platform for the observation of the Breit–Wheeler process. The design of the platform will also serve as the basis for the investigation of strong-field quantum electrodynamic processes such as the nonlinear Breit–Wheeler and the Trident process, or eventually, photon–photon scattering.

Contact:
B. Kettle
b.kettle@imperial.ac.uk

S.P.D. Mangles
stuart.mangles@imperial.ac.uk

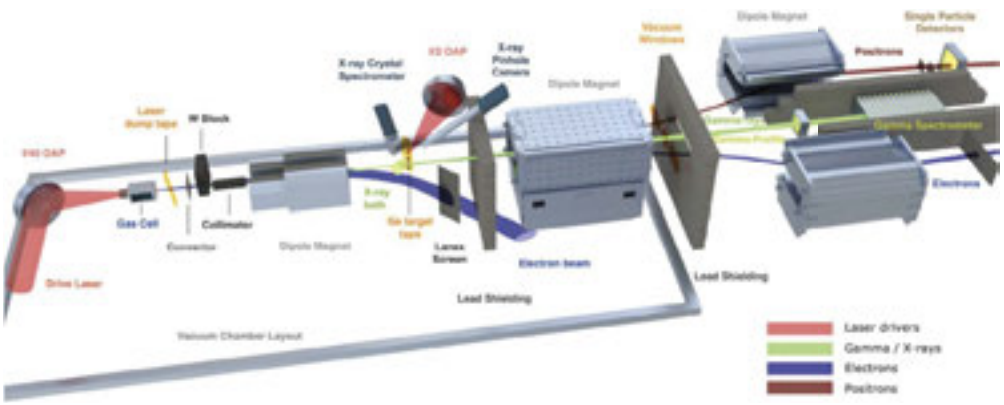

The experiment setup. An f/40 laser pulse was used to drive a laser-wakefield accelerated electron beam in a gas cell. This high-energy electron beam was used to create on axis γ-rays before being swept away by a magnet. A second laser pulse was incident on a germanium target tape, driving an x-ray bath through which the γ beam passed. Any particle pairs created in this interaction region propagate on axis and are swept away to SPDs using a magnetic transport system.

Parametric study of high-energy ring-shaped electron beams from a laser wakefield accelerator

A. Maitrallain, E. Brunetti, R. Spesyvtsev, G. Vieux, M. Shahzad, B. Ersfeld, S.R. Yoffe, A. Kornaszewski, D.A. Jaroszynski *(SUPA, Department of Physics, University of Strathclyde, Glasgow, UK)*
M.J.V. Streeter *(School of Mathematics and Physics, Queen's University Belfast, UK; Physics Department, Lancaster University, UK; The Cockcroft Institute, Daresbury, UK)*
B. Kettle, J.M. Cole, S.P.D. Mangles, Z. Najmudin *(The John Adams Institute for Accelerator Science, Imperial College London, UK)*
O. Finlay *(Physics Department, Lancaster University, UK; The Cockcroft Institute, Daresbury, UK)*
Y. Ma, A.G.R. Thomas, L. Willingale *(Physics Department, Lancaster University, UK; The Cockcroft Institute, Daresbury, UK; Gérard Mourou Center for Ultrafast Optical Science, University of Michigan, USA)*
K. Krushelnick *(Gérard Mourou Center for Ultrafast Optical Science, University of Michigan, USA)*
F. Albert, N. Lemos *(Lawrence Livermore National Laboratory, California, USA)*
N. Bourgeois, P.P. Rajeev, D.R. Symes *(Central Laser Facility, STFC Rutherford Appleton Laboratory, Harwell Campus, Didcot, UK)*
S.J.D. Dann *(Physics Department, Lancaster University, UK; Central Laser Facility, STFC Rutherford Appleton Laboratory, Harwell Campus, Didcot, UK)*
S. Cipiccia *(Department of Medical Physics and Biomedical Engineering, University College London, UK)*
I.G. González, O. Lundh *(Department of Physics, Lund University, Sweden)*
A. Higginbotham, C. Lumsdon *(York Plasma Institute, Department of Physics, University of York, UK)*
A.E. Hussein *(Gérard Mourou Center for Ultrafast Optical Science, University of Michigan, USA; Department of Electrical and Computer Engineering, University of Alberta, Edmonton, Canada)*
M. Šmid *(Helmholtz-Zentrum Dresden-Rossendorf, Dresden, Germany)*
K. Falk *(Helmholtz-Zentrum Dresden-Rossendorf, Germany; Technische Universität Dresden, Germany; Institute of Physics of the ASCR, Prague, Czech Republic)*
N.C. Lopes *(The John Adams Institute for Accelerator Science, Imperial College London, UK; GoLP/Instituto de Plasmas e Fuso Nuclear, Instituto Superior Tecnico, Lisboa, Portugal)*
E. Gerstmayr *(Stanford PULSE Institute, SLAC National Accelerator Laboratory, California, USA)*

Laser wakefield accelerators commonly produce on-axis, low-divergence, high-energy electron beams. However, a high charge, annular shaped beam can be trapped outside the bubble and accelerated to high energies. Here we present a parametric study on the production of low-energy-spread, ultra-relativistic electron ring beams in a two-stage gas cell. Ring-shaped beams with energies higher than 750 MeV are observed simultaneously with on axis, continuously injected electrons.

Often multiple ring shaped beams with different energies are produced and parametric studies to control the generation and properties of these structures were conducted. Particle tracking and particle-in-cell simulations are used to determine properties of these beams and investigate how they are formed and trapped outside the bubble by the wake produced by on-axis injected electrons. These unusual femtosecond duration, high-charge, high-energy, ring electron beams may find use in beam driven plasma wakefield accelerators and radiation sources.

Contact:
A. Maitrallain
antoine.maitrallain@strath.ac.uk

D.A. Jaroszynski
d.a.jaroszynski@strath.ac.uk

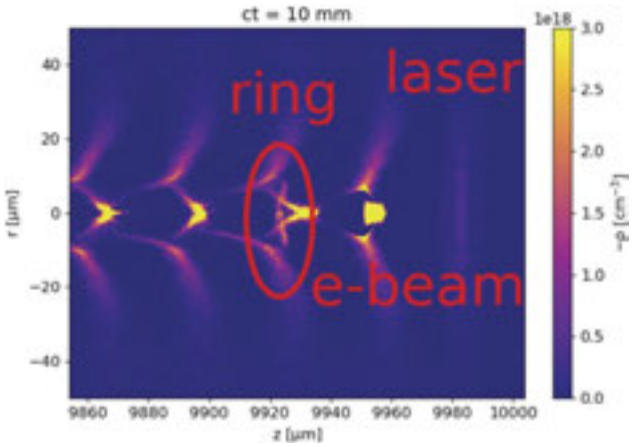

Figure 1: Electron density distribution obtained using FBPIC shows both the ring-shaped and the on-axis electron beams produced by a laser pulse with an initial a_0 = 1.35 focused inside the gas cell (at z = 3 mm). This snapshot is taken after 10 mm propagation.

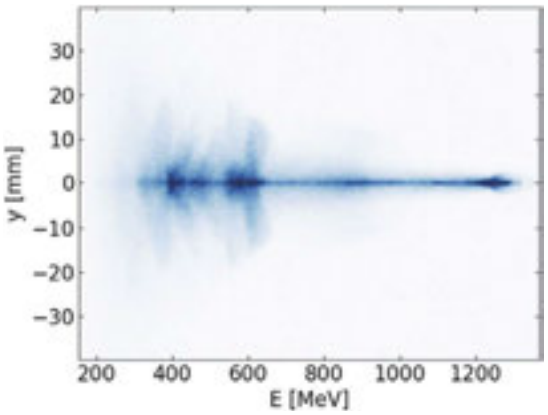

Figure 2: Electron spectrum obtained from FBPIC simulations reported in figures 9(b) and 10(b) (see published paper) transported using GPT through a set up reproducing the experimental one.

Selective Ion Acceleration by Intense Radiation Pressure

A. McIlvenny, P. Martin, S. Kar, M. Borghesi *(Centre for Plasma Physics, Queen's University Belfast, UK)*
D. Doria *(Centre for Plasma Physics, Queen's University Belfast, UK; Extreme Light Infrastructure (ELI-NP) and Horia Hulubei National Institute for R & D in Physics and Nuclear Engineering (IFIN-HH), Magurele, Romania)*
L. Romagnani *(Centre for Plasma Physics, Queen's University Belfast, UK; LULI–CNRS, Ecole Polytechnique, CEA, Universit Paris-Saclay, France)*
H. Ahmed *(Centre for Plasma Physics, Queen's University Belfast, UK; Central Laser Facility, STFC Rutherford Appleton Laboratory, Harwell Campus, Didcot, UK)*
N. Booth, G.G. Scott, D. Neely *(Central Laser Facility, STFC Rutherford Appleton Laboratory, Harwell Campus, Didcot, UK)*
E.J. Ditter, O.C. Ettlinger, G.S. Hicks, Z. Najmudin *(The John Adams Institute for Accelerator Science, Imperial College London, UK)*
S.D.R. Williamson, P. McKenna *(SUPA, Department of Physics, University of Strathclyde, Glasgow, UK)*
A. Macchi *(Istituto Nazionale di Ottica, Consiglio Nazionale delle Ricerche (CNR/INO), Research Unit Adriano Gozzini, Pisa, Italy; Dipartimento di Fisica Enrico Fermi, Università di Pisa, Italy)*

We report on the selective acceleration of carbon ions during the interaction of ultrashort, circularly polarized and contrast-enhanced laser pulses, at a peak intensity of 5.5×10^{20} W/cm^2, with ultrathin carbon foils. Under optimized conditions, energies per nucleon of the bulk carbon ions reached significantly higher values than the energies of contaminant protons (33 MeV/nucleon vs 18 MeV), unlike what is typically observed in laser-foil acceleration experiments.

Experimental data, and supporting simulations, emphasize different dominant acceleration mechanisms for the two ion species and highlight an (intensity dependent) optimum thickness for radiation pressure acceleration; it is suggested that the preceding laser energy reaching the target before the main pulse arrives plays a key role in a preferential acceleration of the heavier ion species.

Reproduced with permission from A McIlvenny et al Phys. Rev. Lett. **127**, *194801, © 2021 American Physical Society. doi: 10.1103/PhysRevLett.127.194801*

Contact:
A. McIlvenny
amcilvenny01@qub.ac.uk

M. Borghesi
m.borghesi@qub.ac.uk

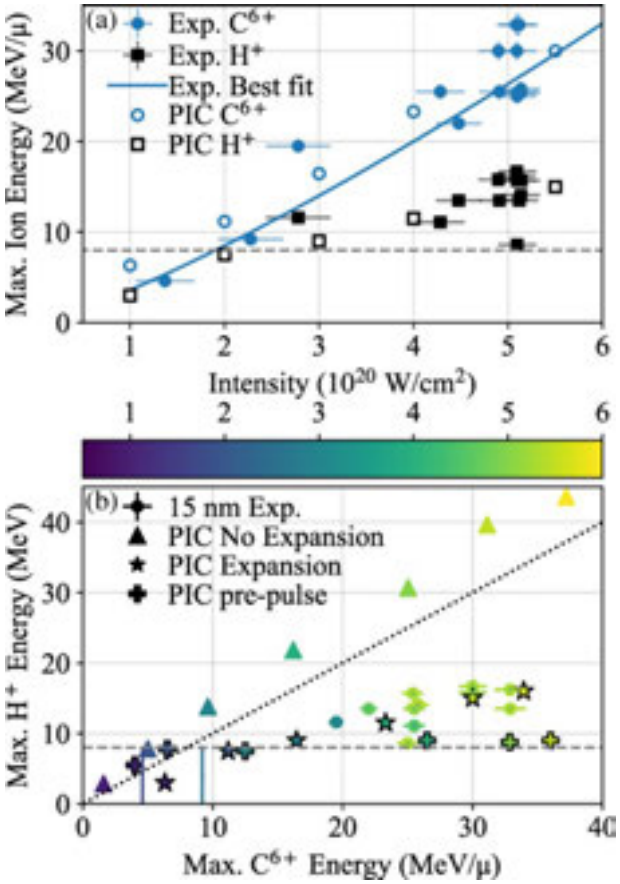

(a) Maximum ion energy as a function of laser intensity for experimental measurements of C^{6+} (filled blue circles) and H^+ (filled black squares). 2D PICs with expansion included are also shown with the same markers but empty. The solid line represents the best fit line to the C^{6+} experimental data, $\propto I^{1.2\pm0.2}$. (b) Correlation between C^{6+} and H^+ maximum energies for experimental and simulation data (marker colors indicate the laser intensity). Dotted line indicates where C^{6+} and H^+ energies are equal. The dashed line at y = 8 MeV in (a) and (b) represents the detection threshold for protons, and the maximum proton energy did not meet this threshold for the two lowest intensity shots. Crosses indicate simulations which included a prepulse with a peak intensity of 10^{17} W/cm^2 arriving on target 2.5 ps before the peak of the main pulse.

Kinematics of femtosecond laser-generated plasma expansion: Determination of sub-micron density gradient and collisionality evolution of over-critical laser plasmas

G.G. Scott *(Lawrence Livermore National Laboratory, California, USA; Central Laser Facility, STFC Rutherford Appleton Laboratory, Harwell Campus, Didcot, UK)*
G.F.H. Indorf *(Central Laser Facility, STFC Rutherford Appleton Laboratory, Harwell Campus, Didcot, UK; Institut fur Laser und Optik, Hochschule Emden/Leer-University of Applied Sciences, Germany)*
M.A. Ennen *(Institut fur Laser und Optik, Hochschule Emden/Leer-University of Applied Sciences, Germany)*
P. Forestier-Colleoni, F. Beg *(Center for Energy Research, University of California San Diego, California, USA)*
S.J. Hawkes, L. Scaife, D.R. Symes, C. Thornton *(Central Laser Facility, STFC Rutherford Appleton Laboratory, Harwell Campus, Didcot, UK)*
M. Sedov *(Joint Institute for High Temperatures of the Russian Academy of Sciences, Moscow, Russian Federation)*
T. Ma *(Lawrence Livermore National Laboratory, California, USA)*
P. McKenna *(Department of Physics SUPA, University of Strathclyde, Glasgow, UK)*
A.A. Andreev *(Institut für Laser und Optik, Hochschule Emden/Leer-University of Applied Sciences, Germany; Saint-Petersburg State University, Russian Federation; ELI-ALPS, Szeged, Hungary; Max Born Institute, Berlin 12489, Germany)*
U. Teubner *(Institut fur Laser und Optik, Hochschule Emden/Leer-University of Applied Sciences, Germany; Institut für Physik, Carl von Ossietzky Universität, Germany)*
D. Neely *(Central Laser Facility, STFC Rutherford Appleton Laboratory, Harwell Campus, Didcot, UK; Department of Physics SUPA, University of Strathclyde, Glasgow)*

An optical diagnostic based on resonant absorption of laser light in a plasma is introduced and is used for the determination of density scale lengths in the range of 10 nm to >1 μm at the critical surface of an overdense plasma. This diagnostic is also used to extract the plasma collisional frequency, allowing inference of the temporally evolving plasma composition on the tens of femtosecond timescale. This is found to be characterized by two eras: the early time and short scale length expansion (L < 0.1λ), where the interaction is highly collisional and target material dependent, followed by a period of material independent plasma expansion for longer scale lengths (L > 0.1λ); this is consistent with a hydrogen plasma decoupling from the bulk target material. Density gradients and plasma parameters on this scale are of importance to plasma mirror optical performance and comment is made on this theme.

Contact:
G.G. Scott
scott110@llnl.gov

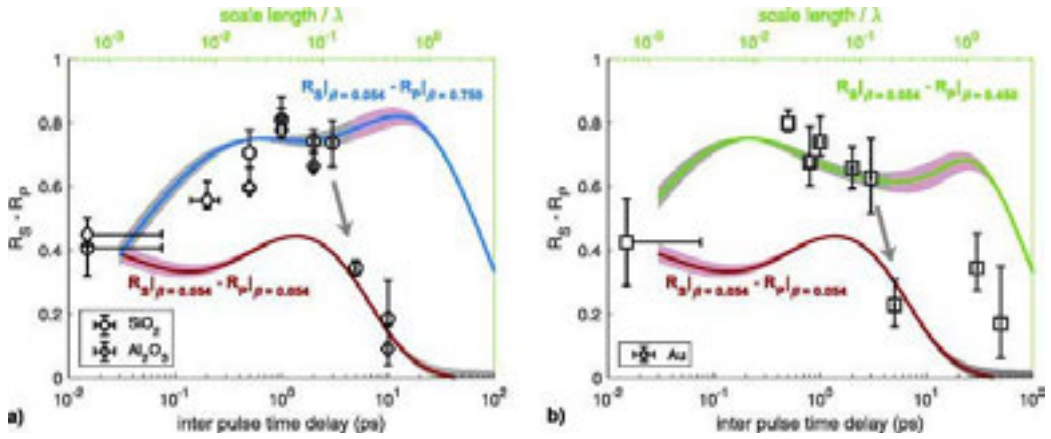

[(a) and (b)] The difference in reflected energy fraction between s- and p-polarized interactions for three different collisionality ratios as calculated from the analytic model is shown by lines. This is compared to the experimentally measured values for (a) BK7 glass and sapphire, and (b) gold. (a) $\beta_p > \beta_s$, represented by the blue line, best fits the data for scale lengths less than around 125 nm, whilst for scale lengths longer than this, the red line representing $\beta_p = \beta_s$ better fits the experimental data. (b) Qualitatively the same trend is observed for gold. In both cases, the error bar in the model represents the effect of changing the collision frequency by 10% and its colour is intended to guide the eye to its region of validity, grey being where the model fits the data, and red being where it does not. A summary of the best fitting parameters for the model is presented in Table I in the published paper.

Measuring multi-tesla, transient magnetic fields in laser-driven coils using dual-axis proton deflectometry

P. Bradford, A. Dearling , L. Antonelli , M. Khan, C.P. Ridgers , N.C. Woolsey *(York Plasma Institute, Department of Physics, University of York, UK)*
J.J. Santos *(Centre Lasers Intenses et Applications, University of Bordeaux-CNRS-CEA, 33405 Talence, Bordeaux, France)*
M. Ehret *(Centre Lasers Intenses et Applications, University of Bordeaux-CNRS-CEA, 33405 Talence, Bordeaux, France; Institut für Kernphysik, Tech. Univ. Darmstadt, Germany)*
V.T. Tikhonchuk *(Centre Lasers Intenses et Applications, University of Bordeaux-CNRS-CEA, 33405 Talence, Bordeaux, France; ELI Beamlines, Institute of Physics, Czech Academy of Sciences, Czech Republic)*
N. Booth, D.C. Carroll, R. Heathcote , C. Spindloe , R.J. Clarke *(Central Laser Facility, STFC Rutherford Appleton Laboratory, Harwell Campus, Didcot, UK)*
J.D. Moody, B.B. Pollock *(Lawrence Livermore National Laboratory, California, USA)*
S. Pikuz, S. Ryazantsev *(National Research Nuclear University MEPhI, Moscow, Russia; Joint Institute for High Temperatures, RAS, Moscow, Russia)*
M.P. Read *(First Light Fusion, Kidlington, UK)*
K. Glize *(Key Laboratory for Laser Plasmas (MOE), School of Physics and Astronomy, Shanghai Jiao Tong University, People's Republic of China; Collaborative Innovation Center for IFSA, Shanghai Jiao Tong University, People's Republic of China)*

In this paper, we show that quantitative measurements using perpendicular probing are complicated by the presence of GV/m electric fields in the target that contribute to the proton deflection and can produce significant errors in the magnetic field measurement. Probing parallel to the coil axis with fiducial grids, we demonstrate that electric and magnetic field measurements can be reliably separated by recording the rotation of the grid shadow in the proton images.

Comparing our experimental proton data with particle-in-cell simulations, we estimate that currents of order I ≈ 5 kA were generated in 1 mm- and 2 mm-diameter wire loops using a ~550 J, ns-duration laser drive from Vulcan West.

We also present an analytic model of proton deflection in electric and magnetic fields that can be used to benchmark results from particle-in-cell codes and help deconvolve the magnetic and electric field deflections using a proton energy scaling.

Building on these results, a new experimental platform for measuring multi-tesla, laser-generated magnetic fields is proposed using a single-plate target with a miniature coil integrated into the target support.

Contact:
P. Bradford
philip.bradford@u-bordeaux.fr

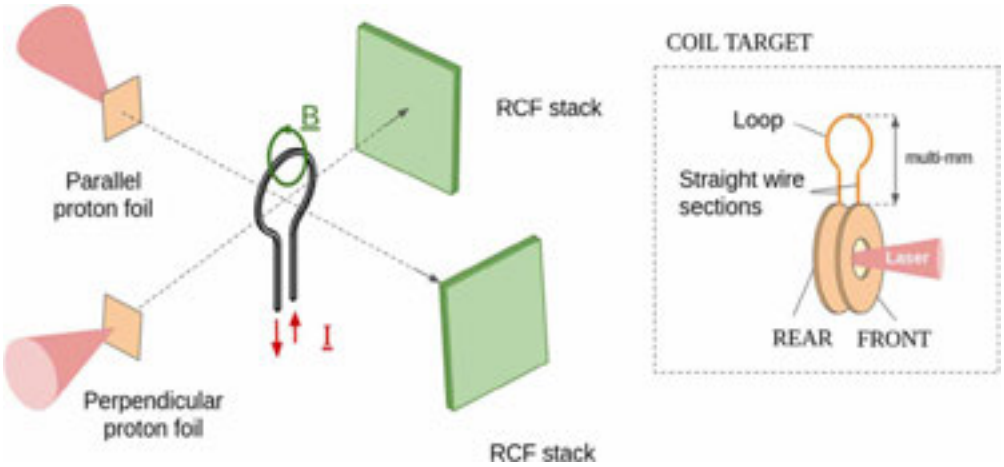

Schematic representation of the dual-axis experiment.

Measuring the principal Hugoniot of inertial-confinement-fusion-relevant TMPTA plastic foams

R.W. Paddock, M.W. von der Leyen, R. Aboushelbaya, P.A. Norreys *(Department of Physics, Clarendon Laboratory, University of Oxford, UK)*
M. Oliver, R.H.H. Scott, R. J. Clarke, M. Notley, C. D. Baird, N. Booth, C. Spindloe, D. Haddock, S. Irving *(Central Laser Facility, STFC Rutherford Appleton Laboratory, Harwell Campus, Didcot, UK)*
D.E. Eakins, D.J. Chapman *(Department of Engineering Science, University of Oxford, UK)*
J. Pasley (York Plasma Institute, Department of Physics, University of York, UK)
M. Cipriani, F. Consoli *(ENEA — C.R. Frascati, Fusion and Nuclear Safety Department, Italy)*
B. Albertazzi, M. Koenig *(LULI, CNRS, CEA, Ecole Polytechnique, UPMC, Univ Paris 06: Sorbonne Universités, France)*
A. S. Martynenko, L. Wegert, P. Neumayer *(GSI Helmholtzzentrum für Schwerionenforschung, Germany)*
P. Tchórz, P. Rączka *(Institute of Plasma Physics and Laser Microfusion, Poland)*
P. Mabey *(Freie Universität Berlin, Germany)*
W. Garbett *(AWE plc, Aldermaston, Reading, UK)*
R.M.N. Goshadze, V.V. Karasiev, S.X. Hu *(Laboratory for Laser Energetics, University of Rochester, Rochester, New York, USA)*

Simulations involving foam materials (such as those of ICF capsules with DT-wetted-foam layers) often describe the foam using EOS models for homogeneous materials. To test the accuracy of this approximation, an experiment was performed at the CLF to measure principal Hugoniot data of TMPTA foam at 0.26 g/cm^3 (the density of DT-wetted foams, and of the foam in recently proposed 'hydrodynamic-equivalent' capsules).

Vulcan was used to drive a shock through a multi-layer target containing an α-quartz reference and the TMPTA foam. VISAR was used to measure the average shock velocity in these two materials, and an impedance matching calculation performed to determine the foam shock state achieved in each shot. SOP was used to estimate the temperature of the shocked foam. The results suggest that, for the 20 – 120 GPa pressure range accessed, this material can be reasonably well described using existing EOS models for homogeneous plastics.

Reproduced from R. W. Paddock et al. Phys. Rev. E **107**, *025206 (2023), published by the American Physical Society, under the terms of a Creative Commons Attribution (CC BY) license (http://creativecommons.org/licenses/by/4.0/) doi: 10.1103/PhysRevE.107.025206*

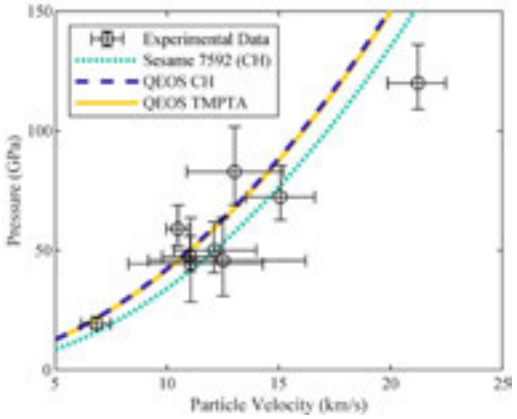

Experimentally determined principal Hugoniot states in the TMPTA foam, compared to a range of EOS models for homogenous plastics. These models well describe the data to within the accuracy of the experiment.

Contact:
R.W. Paddock
robert.paddock@physics.ox.ac.uk

Generation of photoionized plasmas in the laboratory of relevance to accretion-powered x-ray sources using keV line radiation

D. Riley, R.L. Singh, S. White, M. Charlwood, D. Bailie, C. Hyland, T. Audet, G. Sarri, G. Gribakin, F.P. Keenan *(School of Mathematics and Physics, Queen's University Belfast, UK)*

B. Kettle, S.J. Rose, E.G. Hill *(Plasma Physics Group, Imperial College London, UK)*
G.J. Ferland *(Department of Physics and Astronomy, University of Kentucky, USA)*

In this paper we describe an experiment to generate x-ray photoionized plasmas in the laboratory, of relevance to accretion-powered x-ray sources such as neutron star binaries and quasars, which includes significant improvements over similar previous work. One of the key astrophysical plasma properties of interest is the photoionization parameter, $\xi=4\pi F/n_e$ where F is the x-ray flux and n_e the electron density. We demonstrate that we can achieve values of ξ >100 erg-cm s^{-1} using laser-plasma x-ray sources, in the regime of interest for several astrophysical scenarios.

In particular, we show that our use of a keV line source, rather than the usual quasi-blackbody radiation fields normally employed in such experiments, has allowed us to generate the same ratio of inner-shell to outer-shell photoionization as that expected from a blackbody source with ~keV spectral temperature. This is also a key factor in allowing experiments to be compared to the predictions of codes employed to model astrophysical sources.

Contact:
D. Riley
d.riley@qub.ac.uk

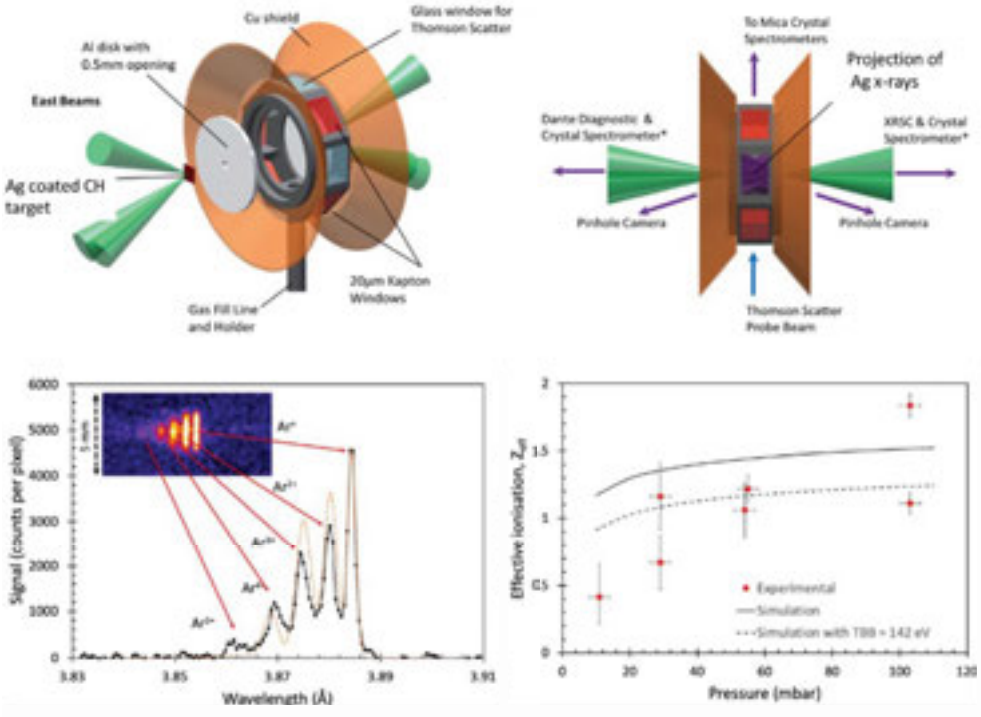

Top: Gas cell target for photoionisation experiment. The Ar gas fill varied from 10-500 mbar. The end windows were CH coated with Ag. L-shell x-rays from the Ag photoionised and heated the Ar plasma.

Below Left: A spherical crystal spectrometer was used to spatially resolve the K- β fluorescence.

Below right: The fluorescence was used to estimate an effective ionisation state that could be compared to simulation using an in-house time dependent code.

Triggering and probing electromagnetic stochasticity in a low-density magnetized plasma irradiated by a multi-speckled laser beam

W. Yao, R. Lelièvre, J. Fuchs *(LULI - CNRS; École Polytechnique, CEA; Université Paris-Saclay; UPMC Université Paris 06; Sorbonne Université, France)*
P. Antici *(INRS-EMT, Varennes, Quebec, Canada)*
J. Béard *(LNCMI-T, CNRS, Toulouse, France)*
M. Borghesi, C. Fegan, P. Martin, A. McIlvenny *(Centre for Plasma Physics, School of Mathematics and Physics, Queen's University Belfast, UK)*
A.F.A. Bott *(Department of Physics, University of Oxford, UK)*
D.C. Carroll *(Central Laser Facility, STFC Rutherford Appleton Laboratory, Harwell Campus, Didcot, UK)*
S.N. Chen *("Horia Hulubei" National Institute for Physics and Nuclear Engineering, Bucharest-Magurele, Romania)*
A. Ciardi *(Sorbonne Université, Observatoire de Paris, Université PSL, CNRS, LERMA, Paris, France)*
L. Gremillet *(CEA, DAM, DIF, Arpajon, France)*
E. d'Humières *(University of Bordeaux, Centre Lasers Intenses et Applications, CNRS, CEA, UMR 5107, Talence, France)*
B. Khiar *(Office National d'Etudes et de Recherches Aérospatiales (ONERA), France)*
R. Smets *(Laboratoire de Physique des Plasmas (LPP), CNRS, Observatoire de Paris, Sorbonne Université, Université Paris-Saclay, École Polytechnique, Institut Polytechnique de Paris, France)*

The triggering of electromagnetic stochasticity in magnetized plasmas via high-power lasers is investigated by sending a nanosecond-duration, multi-speckled laser pulse into a low-density gas, coupled with a strong, initially homogeneous, external magnetic field perpendicular to the laser pulse. Detailed characterization of the induced electromagnetic structures is realized through proton radiography, in addition to Thomson scattering measurements for the background plasma heating.

The experiment is performed using an intense short-pulse laser and several long-pulse lasers, at the Vulcan Target Area West laser facility at the Rutherford Appleton Laboratory. Additionally, the energy spectrum of MeV protons propagated through the plasma is registered with a Thomson parabola. This allows us to assess the impact of the stochastic EM structures in the plasma on the transport of the collisionless proton beam.

Contact:
J. Fuchs
julien.fuchs@polytechnique.edu

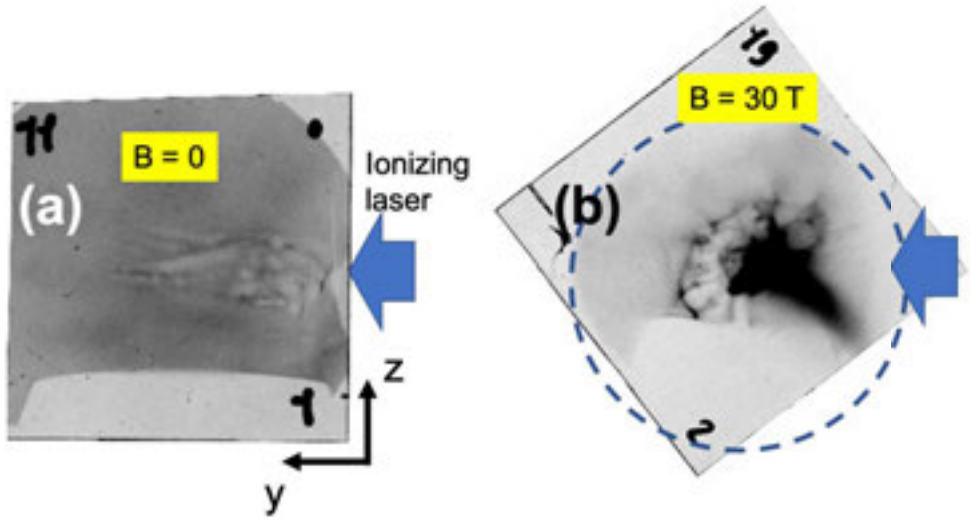

Proton radiography results (a) without and (b) with external applied magnetic field. In both cases the gas pressure is 25 bars, and the time delay (between the long, ionizing beam and the short pulse beam that drives the probing protons) is 0.7 ns.

Laser science and development

Laser shock peening of tungsten and its dependency on polarisation of light for induced compressive stresses

S. Banerjee, J. Spear *(Central Laser Facility, STFC Rutherford Appleton Laboratory, Harwell Campus, Didcot, UK)*

P.J. Dalton *(School of Maths and Physics, Queen's University Belfast, UK)*

We report on laser shock peening (LSP) of tungsten, a material used as a divertor in Tokamak machines for magnetic confinement fusion reactions such as the ITER facility (France) and JET facility (UK). Peak compressive stresses of -370 MPa and depths of up to 1.75 mm were recorded when 0.25 cm^2 area of tungsten (99.95% pure) was irradiated by a 1030 nm Yb:YAG laser operating at 10 J, 10 ns.

Furthermore, we demonstrate enhancement of compressive stresses in one direction, by application of circular polarised light in hard material like tungsten. However, no enhancement of compressive stresses with circular polarisation was observed in soft material like aluminium.

Contact:
J. Spear
jacob.spear@stfc.ac.uk

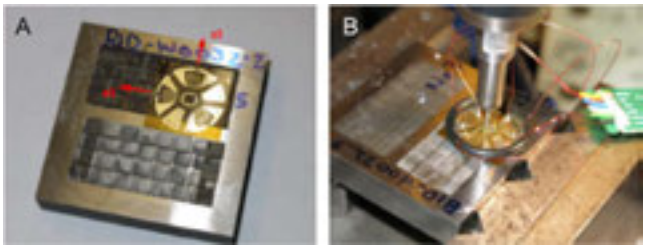

Figure 1: Incremental Central Hole Drilling (ICHD) on tungsten samples (A) Gauge attached to the tungsten sample (B) Hole drilling for residual stress measurements.

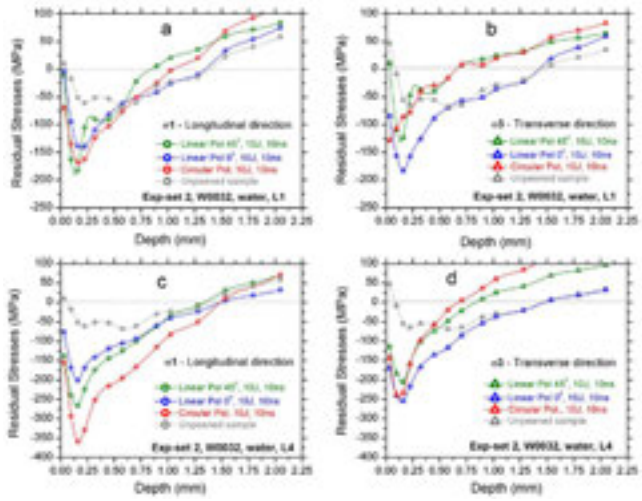

Figure 2: Residual stresses developed during laser shock peening of tungsten in experiments set 2 (repeat) for pulse energy (10 J), different polarisation (Linear and circular) and different shots (L1 and L4)
(a) Residual stresses in longitudinal direction (σ1) for one shot (L1)
(b) Residual stresses in transverse direction (σ3) for one shot (L1)
(c) Residual stresses in longitudinal direction (σ1) for four shots at same location with 100% overlap (L4) (d) Residual stresses in transverse direction (σ3) for four shots at same location with 100% overlap (L4).

Development of an automated null ellipsometer for characterising large-aperture, high-reflectance optical coatings used in DiPOLE systems

D.L. Clarke, M. De Vido *(Central Laser Facility, STFC Rutherford Appleton Laboratory, Harwell Campus, Didcot, UK)*
L. Dixon *(Department of Physics, University of Surrey, UK)*
M.J.D. Esser *(Centre for Doctoral Training in Applied Photonics, Heriot-Watt University, Edinburgh, UK)*

Characterising the properties of high-reflectance, optical coatings for high-power laser systems is important for improving optical-to-optical efficiency and extending system capabilities. In particular, removing the phase delay introduced by these optical coatings is important for reducing a large cause of loss in high-power laser systems, known as depolarisation.

To remove phase delay, it must first be quantified. Null ellipsometry is a method for measuring phase delay, hence, a partially-automated, null ellipsometer has been commissioned to characterise coatings over a wide range of angles. Automation of the null ellipsometer has both reduced measurement time and increased accuracy.

Contact:
D.L. Clarke
danielle.clarke@stfc.ac.uk

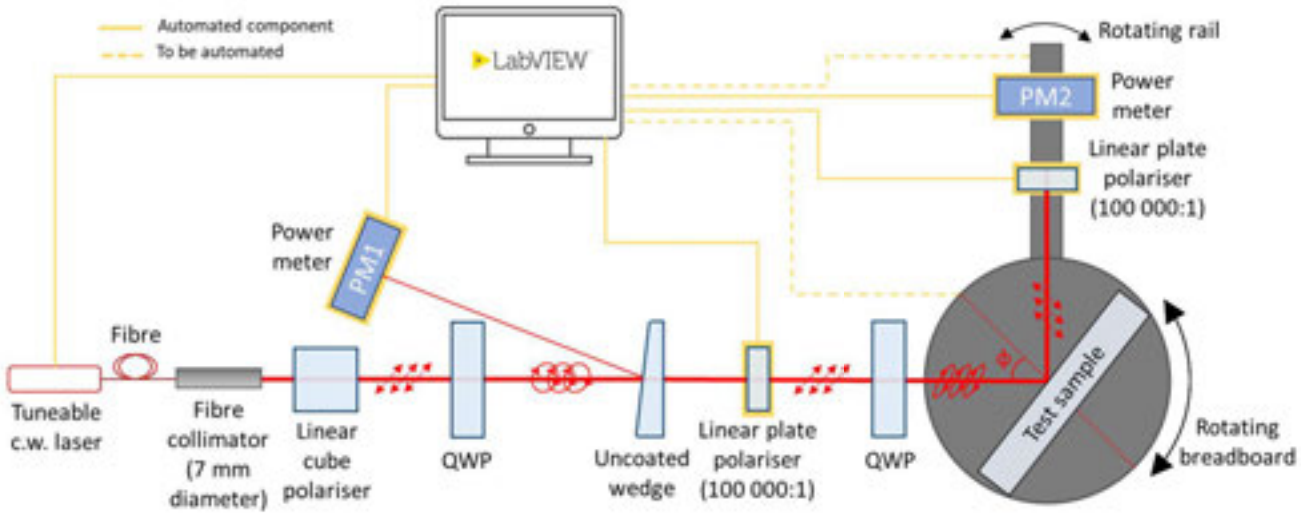

Experimental setup of the partially automated null ellipsometer for characterising phase delay introduced by the coating of the test sample over a range of angles.

Second and third harmonic conversion of a kilowatt average power, 100-J-level diode pumped Yb:YAG laser in large aperture LBO

P.J. Phillips, S. Banerjee, P.Mason, J. Smith, J. Spear, M. De Vido, K. Ertel, T. Butcher, C. Edwards, C. Hernandez-Gomez, J. Collier *(Central Laser Facility, STFC Rutherford Appleton Laboratory, Harwell Campus, Didcot, UK)*

G. Quinn, D. Clarke *(Central Laser facility, STFC Rutherford Appleton Laboratory, Harwell Campus, Didcot, UK; Institute of Photonic and Quantum Sciences, Heriot-Watt University, Edinburgh, UK)*

We report on the successful demonstration of second and third harmonic conversion of a high pulse energy, high average power 1030 nm diode pumped Yb-doped yttrium aluminium garnet (Yb:YAG) nanosecond pulsed laser in a large aperture lithium triborate (LBO) crystal. We demonstrated generation of 59.7 J at 10 Hz (597 W) at 515 nm (second harmonic) and of 65.0 J at 1 Hz (65 W) at 343 nm (third harmonic), with efficiencies of 66% and 68%, respectively. These results, to the best of our knowledge, represent the highest energy and power reported for frequency conversion to green and UV-A wavelengths.

Reproduced with permission from P.J. Phillips et al. Optics Letters Vol. **46**, *Issue 8, pp. 1808-1811 (2021) © 2021 Optical Society of America. doi: 10.1364/OL.419861*

Contact:
P.J. Phillips
jonathan.phillips@stfc.ac.uk

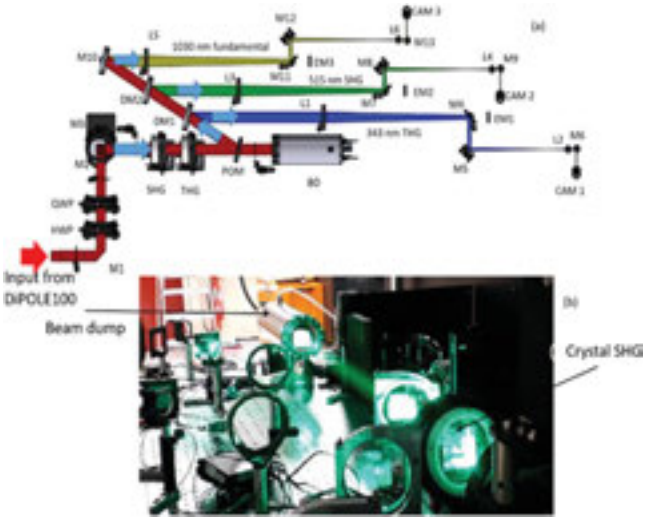

Figure 1: (a) Schematic of the experimental setup for SHG and THG of DiPOLE100. Arrows indicate beam travel. (b) Photograph showing the SHG crystal and the beam dump during the experiment with reflections showing the incident and generated beams.

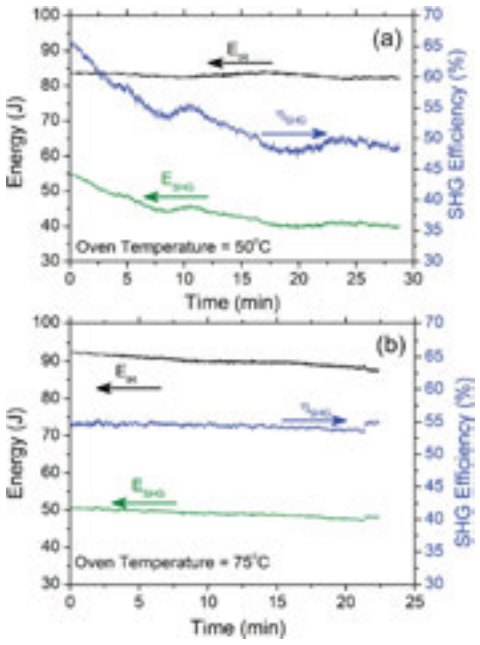

Figure 2: Long-term energy stability of SHG (a) LBO crystal oven temperature at 50°C and (b) oven temperature at 75°C. Green curve of 515 nm energy, black curve of 1030 nm input energy, and the blue curve is the efficiency, with the arrows indicating their respective axis.

Confinement and absorption layer free nanosecond laser shock peening of tungsten and its alloy

S. Banerjee, J. Spear *(Central Laser Facility, STFC Rutherford Appleton Laboratory, Harwell Campus, Didcot, UK)*

Traditionally, nanosecond laser shock peening (ns-LSP) of metals requires an additional application of an absorption layer (black paint) and more importantly a confinement layer (typically water or transparent material) on the workpiece for introduction of compressive stresses.

In this paper, we demonstrate for the first time, to the best of our knowledge, introduction of compressive stresses in pure tungsten and its alloy TAM7525 (75% tungsten and 25% copper) without any absorption and confinement layer for ns-LSP. Peak compressive stresses of −349 MPa and −357 MPa were measured in pure tungsten and TAM7525, respectively, when a 0.25 cm^2 area was irradiated by a Yb:YAG laser (1030 nm) operating at ~5 J, ~2 ns with circular polarization.

These peak compressive stresses (without confinement layer) compare well to those with tungsten ns-LSP done with water as confinement layer at twice the energy at 10-ns pulse duration. Furthermore, compared to femtosecond laser shock peening (fs-LSP) of aluminium at atmospheric pressure, the depth of compressive stresses recorded in tungsten and its alloy (~7 times denser than aluminium) is nearly four times more in the case of confinement layer free nanosecond laser shock peening (CLF-ns-LSP).

Contact:
J. Spear
jacob.spear@stfc.ac.uk

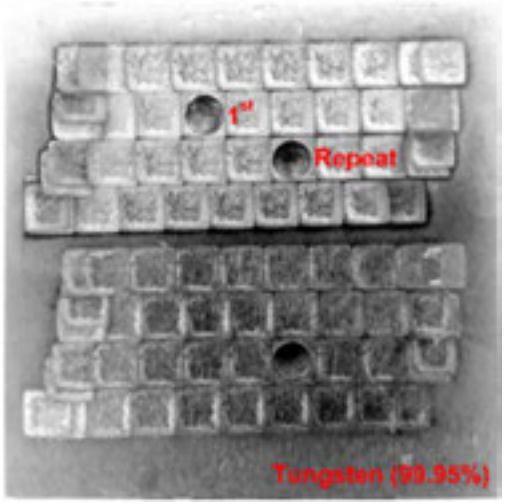

Figure 1: Laser shock peening locations (bottom 7.5 J, 2 ns, and top 5.2 J, 2 ns) without any absorption and confinement layer for pure tungsten.

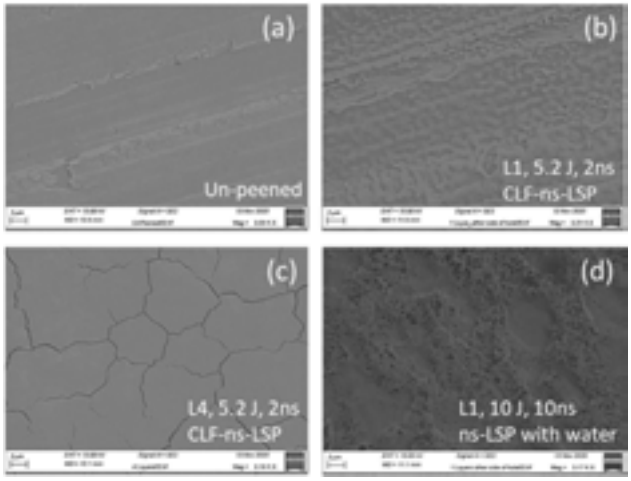

Figure 2: SEM image for tungsten at 2 μm resolution: (a) surface profile for an un-peened sample; (b) surface profile after CLF-ns-LSP with one shot (L1); (c) surface profile after CLF-ns-LSP with four 100% overlapping shots (L4); (d) surface profile after ns-LSP with water.

Modernisation of the Gemini TA2 vacuum control system

D. Bloemers, B. Morkot *(Central Laser Facility, STFC Rutherford Appleton Laboratory, Harwell Campus, Didcot, UK)*

The new Gemini Target Area 2 (TA2) Vacuum control has been built around the Siemens S7-1200 PLC with a Weintek HMI. Advancements in industrial controllers since the original development have enabled the implementation of several improvements, which provide increased machine safety through more robust monitoring and fault reporting, while maintaining a simple user experience.

The approach taken with the user interface was to provide operators a clear overview of the system, showing the status of important elements through text and iconography with particular attention paid to colour to ensure it remained readable while wearing laser safety glasses. Additionally the processor's increased resources offered the opportunity to incorporate the area's gas control system, which will provide a single point of interaction and simplify operations.

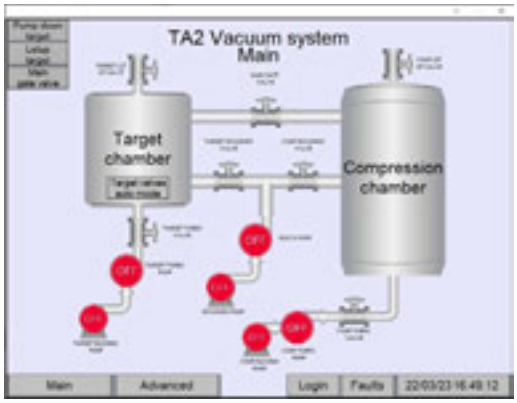

The new graphical user interface for the TA2 vacuum control system.

Contact:
D. Bloemers
desmond.bloemers@stfc.ac.uk

Full Automation of Thompson Chamber for Gemini Experiments

B. Morkot, M. Dominey, A. Thomas, H. Edwards, I. Hollingham *(Central Laser Facility, STFC Rutherford Appleton Laboratory, Harwell Campus, Didcot, UK)*

A new, fully automated vacuum chamber for Thompson plates has been constructed for experiments in Gemini, with an integrated automatic vacuum control system and interface. The system features an HMI giving users the ability to start and stop fully automated pump downs and let ups, as well as open the gate valve between the Thompson chamber and the main chamber to take shots. The gate valve is interlocked by measuring the pressure differential in both chambers, thus preventing users from opening the gate valve in conditions that could potentially cause damage to expensive vacuum equipment, such as the turbo pumps.

The system also features a chamber pressure evaluation in the pump down sequence, which can save time for users during pump downs if the chamber has not been fully let up. The chamber achieved an excellent vacuum of 7.72 x 10^{-7} mBar during testing and was recently used in a Gemini experiment, led by Queen's University Belfast, studying solid targets irradiated at grazing incidence. The experiment employed three Thomson parabolas at 0°, 5° and 10° incidence to the target as the main diagnostics.

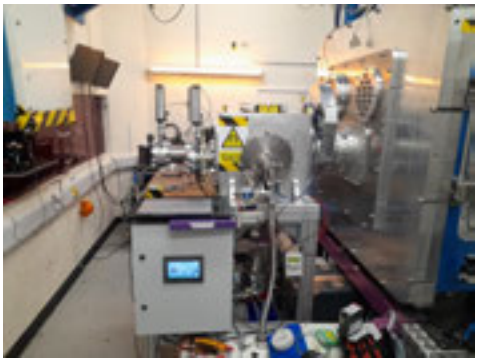

Contact:
B. Morkot
benjamin.morkot@stfc.ac.uk

EPICS Laser Control System GUI using Blazor

A. Muhammad, T. Zata *(Central Laser Facility, STFC Rutherford Appleton Laboratory, Harwell Campus, Didcot, UK)*

The software team at Central Laser Facility (CLF) is developing a modern, cross-platform Graphical User Interface (GUI) for the Extreme Photonics Applications Centre (EPAC). In contrast to the traditional control system GUI for EPICS, the team utilized Blazor, allowing for unified back-end and front-end code using C#.

Over the last couple of years, our team has built an ecosystem of libraries to facilitate C# to EPICS communication and GUI components development. The EPICS compliant Blazor components enable the real-time updates based on the Process Variable (PV) changes and do not need hidden scripts for complex logic. These libraries are easy to use, debug and test.

Overall, our new Blazor-based control system GUI provides users with a secure, accessible, and user-friendly control system which can be rolled out with any EPICS installations we support across the CLF.

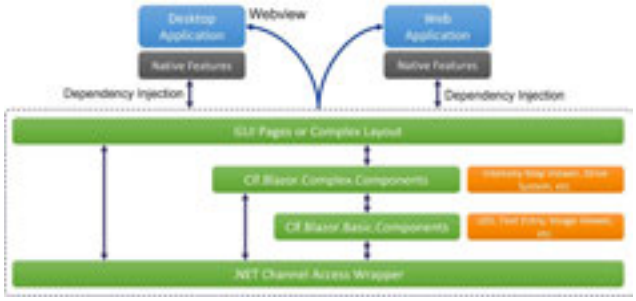

Figure 1: Architecture of the Control system user-interface application for EPAC.

Figure 2: The summary view of the Front end for the Pump Laser in EPAC.

Contact:
A. Muhammad
aoun.muhammad@stfc.ac.uk

VOPPEL Compression chamber grating stages fault finding, characterisation and testing

I. Symonds, R. Sarasola, A. Stallwood, N. Stuart *(Central Laser Facility, STFC Rutherford Appleton Laboratory, Harwell Campus, Didcot, UK)*

The new VOPPEL project for Vulcan Target Area Petawatt (TAP) includes the design and development of two ultra-high vacuum, five axis, precision stages used as grating mounts for laser alignment and manipulation. The stages were designed by Andy Stallwood of the CLF's Mechanical Engineering Design Group, and assembled in-house by the Mechanical Technician Group. The Controls Team was involved in the testing and development of these stages, to ensure that the motors, encoders and drive system could deliver linear and rotational movement to a high degree of accuracy, repeatedly and reliably.

These stages were developed and characterised ready to be integrated with the existing Parker drive system employed in TAP, as well as the ACS drive system. Work carried out included replacing motors that were unable to deliver enough torque, aligning optical encoders to achieve the best read-back signals, and setting limit ranges to prevent collision.

The results of testing these stages demonstrated capabilities of repeatable and accurate incremental linear motion as low as 2 nanometres and minimal angular movement to 0.2 microradians.

Contact:
I. Symonds
isaac.symonds@stfc.ac.uk

Software developments in Gemini

V.A. Marshall *(Central Laser Facility, STFC Rutherford Appleton Laboratory, Harwell Campus, Didcot, UK)*

The Gemini laser system software consists of a network of distributed applications used to control sections of the laser and monitor parameters both on-shot and continuously.

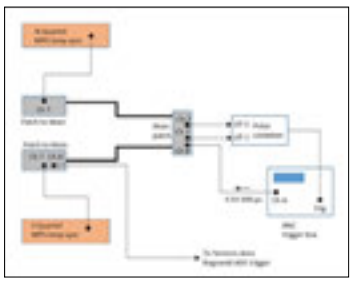

Figure 1: Circuit logic of pulse-combiner box, designed to give a TTL-level pulse of 300 µs duration which is fed to the new data acquisition device.

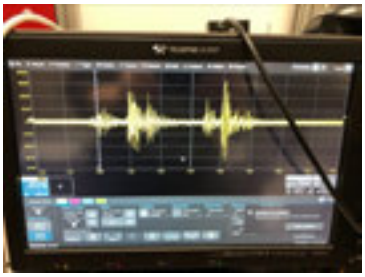

Figure 2: EMP noise generated by the two capacitor banks in the area in which the data acquisition device operates can interfere with the trigger.

Over the last year we have consolidated work on Gemini diagnostics, including an investigation into the effects of EMP on the ACQ2106 data acquisition device and the installation of a back-reflection prevention flipper.

Contact:
V.A. Marshall
victoria.marshall@stfc.ac.uk

Figure 3: Flipper control interface configured to move a flipper into the alignment section of the beamline on-shot, to block back-reflections from the full power section.

Proposed Target Area 2 work-plan in preparation for EPAC

D.R. Symes, C. Armstrong, N. Bourgeois, S.J.D Dann, T. Dzelzainis, K. Fedorov, O. Finlay
(Central Laser Facility, STFC Rutherford Appleton Laboratory, Harwell Campus, Didcot, UK)

The Extreme Photonics Applications Centre (EPAC) will provide a major upgrade of high-power laser capability in the UK with a laser energy and repetition rate higher than Gemini. Many new systems are being developed such as control software, high frame rate detectors, targets, and electron beam components. It is important that iterative design and prototyping takes place before EPAC commissioning in 2025.

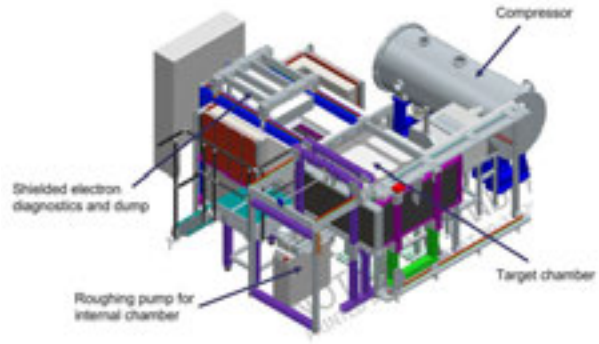

Experimental arrangement in TA2 for producing high repetition rate 100 MeV electron beams.

We describe our proposed work-plan to use Target Area 2 to address technical challenges and confirm that our design is robust and suitable. We will install active stabilization systems in the TA2 beam and improve our gas targets to produce more consistent laser-wakefield accelerated electron beams. The use of machine learning algorithms will be explored to find stable operating parameters and offer flexible, tunable secondary sources. High repetition rate solid target technology based on tape drives and liquid sheets will also be developed.

Contact:
D R Symes
dan.symes@stfc.ac.uk

Contrast enhancement by the transmission grating in the stretcher

Y. Tang, C. Hooker, S. Hawkes, P.P. Rajeev *(Central Laser Facility, STFC Rutherford Appleton Laboratory, Harwell Campus, Didcot, UK)*

D. Egan *(The Orion Laser Facility, AWE plc, Aldermaston, UK)*

Ultra-high intensity lasers based on the chirped pulse amplification technique (CPA) have proven to be a very powerful drive source to accelerate electrons and protons, producing ultrafast coherent X-ray pulses and high quality bright proton beams.[1,2]

The temporal contrast of such lasers plays a crucial role in these experiments. The contrast pedestal (CP) is a well-known common feature of such lasers. The CP appears in the temporal profile in a triangular shape, extending a few tens of picoseconds, typically at a level of 10^{-5} to 10^{-4} of the peak intensity close to the main peak.

This feature has a very detrimental effect on laser-matter interactions with solid state targets due to the pre-plasma formation prior to the main peak that alters the subsequent interaction, or destroys the target. In this report, we demonstrate the contrast enhancement by using transmissions gratings (TGs) in the stretcher. We also report a novel method to accurately evaluate the CP induced by the stretcher and impact of individual components in the stretcher on the CP by precise quantitative characterisation of the surface roughness of large optics. This way, we are able to predict the CP of the high power laser pulses even before the actual laser system is constructed.

1. S.-W. Bahk, P. Rousseau, T. Planchon, V. Chvykov, G. Kalintchenko, A. Maksimchuk, G. A. Mourou, and V. Yanovsky, Opt. Lett. 29, 2837 (2004)
2. D. Umstadter, Phys. Plasma 4, 1774 (2001)

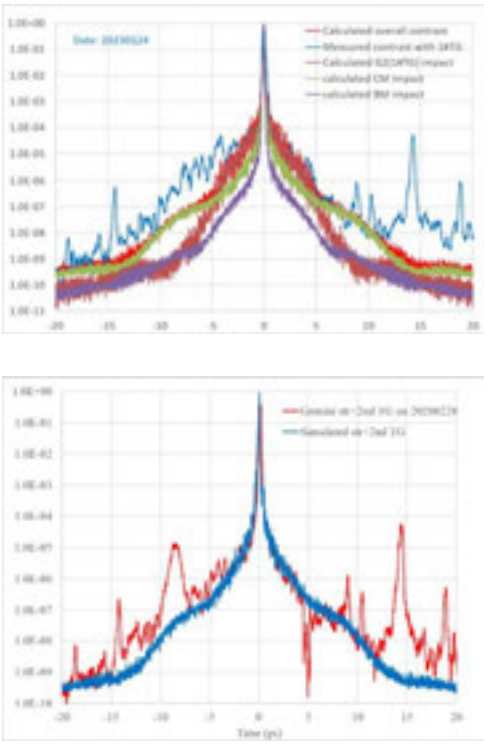

(a) Measured and calculated contrast with 1#TG and contribution of individual optics; (b) measured and calculated contrast with 2#TG.

Contact:
Y. Tang
yunxin.tang@stfc.ac.uk

Vertically aligned nanowire arrays as laser targets

S.T. Bamforth *(Central Laser Facility, STFC Rutherford Appleton Laboratory, Harwell Campus, Didcot, UK; University of Southampton, University Road, Southampton, UK)*
S. Irving *(Central Laser Facility, STFC Rutherford Appleton Laboratory, Harwell Campus, Didcot, UK)*
K. Lancaster *(School of Physics, Engineering and Technology, University of York, UK)*
S. Vinko, A. Miscampbell *(Department of Physics, University of Oxford, UK)*

Vertically aligned nanowire arrays have become a more prevalent type of target for high-powered laser experiments in recent years and have garnered interest due to their applicability to various fields. In this paper, nanowire arrays were formed by electrodepositing nickel from its sulphate into nano-porous anodized aluminium templates. The dimensions of the arrays were tuned by altering reaction conditions. Arrays were shot in Pisa in collaboration with Dr Kate Lancaster at the University of York to obtain Optical Transition Radiation (OTR), ion, x-ray and reflectivity data. This could allow the Target Fabrication department to provide tuneable nanowire arrays as targets for high power laser experiments. The benefits of nanowire arrays are their high absorbance of incident light and their ability to form a high-density plasma on laser ablation.

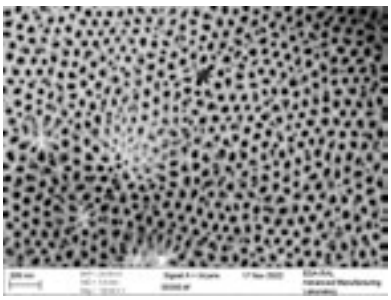

Figure 1: Nano-porous template made by two-step anodization.

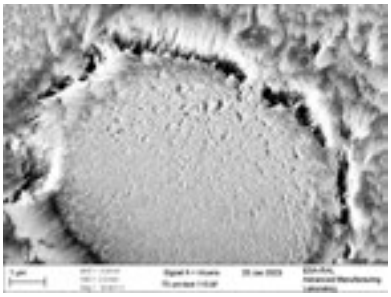

Figure 2: Nanowire array from two-step anodized template.

Contact:
S.T. Bamforth
scott.bamforth@stfc.ac.uk

S. Irving
samuel.irving@stfc.ac.uk

MATLAB-based Analysis of Micro-target Surfaces for Evaluation and Optimal Laser Shot Positioning

C. Gardner, S. Astbury, C. Spindloe, M. Tolley *(Target Fabrication Group, Central Laser Facility, STFC Rutherford Appleton Laboratory, Harwell Campus, Didcot UK)*
A. McIlvenny, M. Borghesi *(Centre for Light-Matter Interactions, School of Mathematics and Physics, Queen's University Belfast, UK)*

The purpose of this project was to assist an experiment aiming to shoot a laser along the surface of a metal target ranging in thickness from 1-25 µm. The assembly of such targets is a significant challenge, and, as a result, the target foil is never fabricated completely to specification. Thus, it is important to evaluate each target to maximise its value to the experiment and to account for its imperfections. This project involved mapping the surface of each foil using a white light interferometer and analysing the data using MATLAB scripts. The result was an estimate of the best location for a laser shot for each target foil. This quasi-automated evaluation of individual targets proved to be very useful for the experiment, and the approach could be adapted to be effective in typical high-power laser experiments shooting at target-normal incidence.

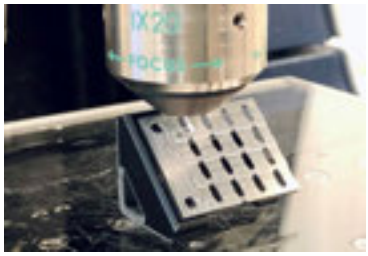

Figure 1: The target array for the Borghesi experiment under an interferometer lens. It is positioned at a 45° angle so that the foil sits quasi-normal to the interferometer's optical axis.

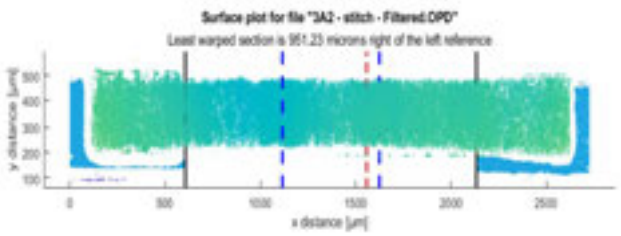

Figure 2: The output plot from the MATLAB script. The red dotted line indicates the best location for the laser shot; the blue dotted lines mark the searched area; the black lines are reference markers, chosen as the edges of the foil mount.

Contact:
C. Gardner
cg1g20@soton.ac.uk

S. Astbury
sam.astbury@stfc.ac.uk

Particle Functionalisation for Dispersion of inorganic 'Dust' within Low Density Polymeric Targets

S. Irving *(Central Laser Facility, STFC Rutherford Appleton Laboratory, Harwell Campus, Didcot, UK)*

Low density materials are often desired for high power laser targets, because the length of laser-matter interaction can be increased without increasing the mass of material relative to solid targets.

Dispersion of nano and micro particulate within the 'foams' provides routes to generating x-rays which are often desired for high power laser experiments, as well as simulating astrophysical phenomena.[1]

Dispersion of the particles can prove to be difficult due to aggregation caused by unfavoured interactions between the chemical phases. Methods of improving particle dispersion in the low density phase have clear benefits for the quality of laser targets available to users. This paper reports on experiments carried out on the use of silanization to improve particle dispersion in foams.

[1] M. Manuel, et al. (2018). Conceptual design of an experiment to study dust destruction by astrophysical shock waves. High Power Laser Science and Engineering, 6, e39

Contact:
S. Irving
samuel.irving@stfc.ac.uk

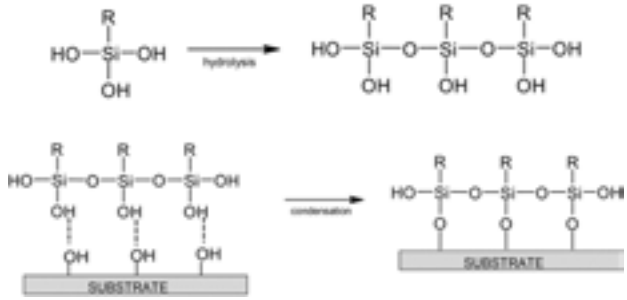

Figure 1: Schematic of the silanization process.

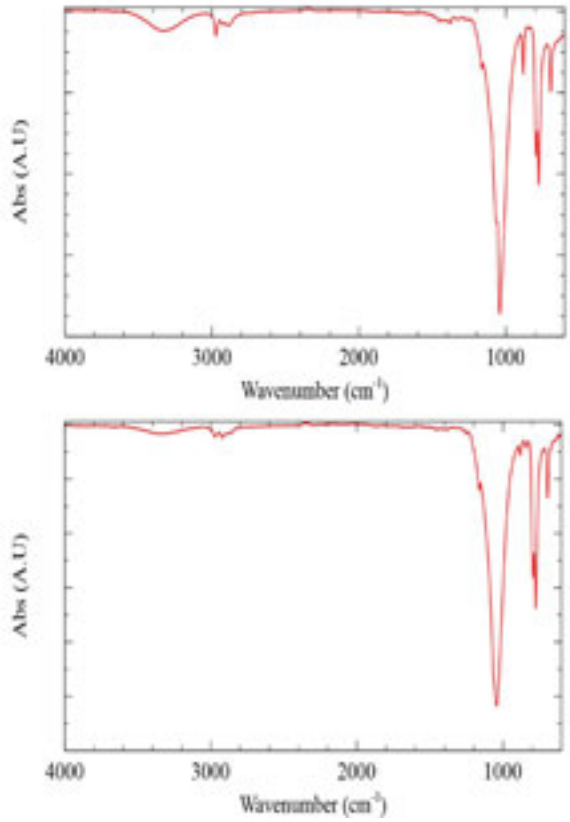

Figure 2: FTIR spectra of silica powders before (top) and after coating (bottom).

Advances in Tape Target Technologies towards 1 Hz Operation for EPAC and other High Repetition Rate Facilities

W. Robins, S. Astbury, M. Tolley, C. Spindloe *(Target Fabrication Group, Central Laser Facility, STFC Rutherford Appleton Laboratory, Harwell Campus, Didcot, UK)*
R. Sarasola, K. Rodgers *(Electrical and Controls Group, Central Laser Facility, RAL Space, STFC Rutherford Appleton Laboratory, Harwell Campus, Didcot, UK)*
G. Hull, D. Symes *(Central Laser Facility, STFC Rutherford Appleton Laboratory, Harwell Campus, Didcot, UK)*
R. Gray, R. Wilson *(Department of Physics, SUPA, University of Strathclyde, Glasgow, UK)*

To meet the demand for the number of shots required for higher repetition rate, higher power experiments, a stream of targets is required, at rates far above any that have previously been supplied for intense laser interactions. In response to this demand, the Target Fabrication Group has continued the developments of a tape target delivery system [1,2], which has applications across a broad range of experimental platforms from use as an interaction target to use as a plasma mirror or a beam block. We discuss the development of a range of these systems in the CLF based on a standard architecture, and share the results of a range of test experiments across different facilities.

1. S. Astbury et al, Development of patterned tape-drive targets for high rep-rate HPL experiments, CLF Annual Reports 2017-2018
2. S. Astbury et al, Progression of a tape-drive targetry solution for high rep-rate HPL experiments within the CLF, CLF Annual Reports 2018-2019

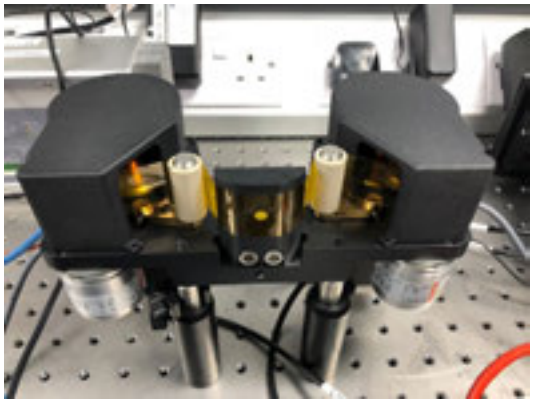

The latest version of the CLF tape drive with 2μm stability in the laser direction and a range of debris mitigation shields in place, to ensure repeatability and reliability over long runs at high rep rate.

Contact:
W. Robins
wayne.robins@stfc.ac.uk

Time-resolved multiple probe UV-vis transient absorption spectroscopy at 100 kHz

I.P. Clark, G.M. Greetham, M. Towrie, I.V. Sazanovich, A.E. Edmeades *(Central Laser Facility, Research Complex at Harwell, STFC Rutherford Appleton Laboratory, Harwell Campus, Didcot, UK)*
G.F. Karras *(Diamond Light Source Ltd, Harwell Science & Innovation Campus, Didcot, UK)*

Transient-absorption spectroscopy, whether in the UV-visible or mid-infrared, is a powerful tool for studying transient species, enabling a wide breadth of research, from DNA photo-oxidation, to catalysis, and protein folding. The Ultra facility has introduced new UV-visible transient absorption capabilities. The development enables, for the first time, 100 kHz time-resolved multiple probe UV-visible transient absorption spectroscopy (TRMPS). As well as high signal to noise, the system is capable of measuring femtosecond to millisecond dynamics in a single experiment.

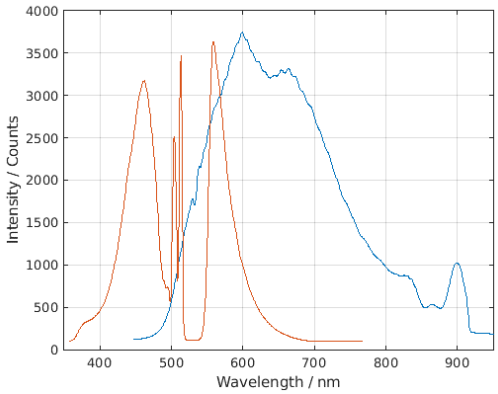

Spectra of continuum generated using both 515 nm driven (red) and 1030 nm driven (blue) calcium fluoride.

Contact:
I.P Clark
ian.clark@stfc.ac.uk

Kerr-gated Raman experiment driven by 100 kHz Ytterbium based OPCPA laser system

I.V. Sazanovich *(Central Laser Facility, Research Complex at Harwell, STFC Rutherford Appleton Laboratory, Harwell Campus, Didcot, UK)*

G. Chaterjee *(SLAC National Accelerator Laboratory, California, USA)*
G.F. Karras *(Diamond Light Source Ltd, Harwell Science & Innovation Campus, Didcot, UK)*

Optical Kerr gating is the most efficient approach so far to suppress the strong fluorescence background when detecting weak Raman signals. Here we report the first implementation of the Kerr gated Raman setup driven by a 100 kHz Ytterbium laser source.

The driving laser Dira 200-100 from Trumpf Scientific delivers 200 W average power at 1030 nm and provides a sufficient pulse energy to expand the beam spot size at the Kerr medium, whilst maintaining efficient Kerr effect.

This enables an increase in the probe spot size and a reduction in the probe beam fluence to collect Raman signal from photosensitive and/or degradable samples of interest. In this setup, we have achieved efficient Kerr gating, reaching 70% for 0.75 mm diameter gating spot and demonstrated 12 cm^{-1} spectral resolution (see figure). We have also confirmed that Kerr gated Raman can be done efficiently with 3 mm diameter gating spot.

Contact:
I.V. Sazanovich
igor.sazanovich@stfc.ac.uk

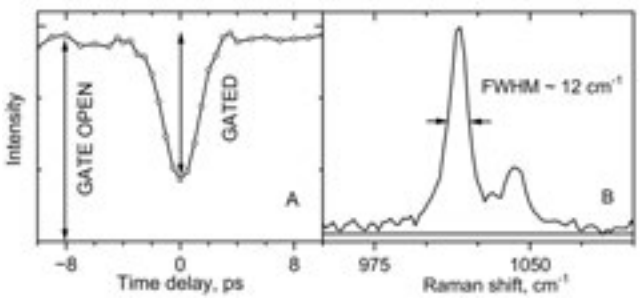

(A) The time profile of the Kerr-gated Raman signal of toluene at 1006 cm^{-1} obtained in the "inverted gating" approach with the gating beam spot size of 0.75 mm x 0.75 mm. The Kerr gate efficiency is estimated as the ratio of the negative "GATED" peak intensity to the "GATE OPEN" intensity. (B) The illustration of the spectral resolution achieved in the Kerr-gated Raman experiment, toluene used as a sample.

Dispersion management in the Vulcan OPCPA petawatt laser using a grating-prism compressor

V. Aleksandrov, M. Galimberti, I. Musgrave, N. Stuart, C. Hernandez-Gomez *(Central Laser Facility, STFC Rutherford Appleton Laboratory, Harwell Campus, Didcot, UK)*

The residual dispersion of femtosecond petawatt lasers can limit their output pulse duration and temporal contrast. We have designed a pulse stretcher and a grating-prism compressor based on transmission gratings to control the residual dispersion in the VOPPEL (Vulcan OPcpa PEtawatt Laser) CPA system up to the fifth order.

Contact:
V. Aleksandrov
veselin.aleksandrov@stfc.ac.uk

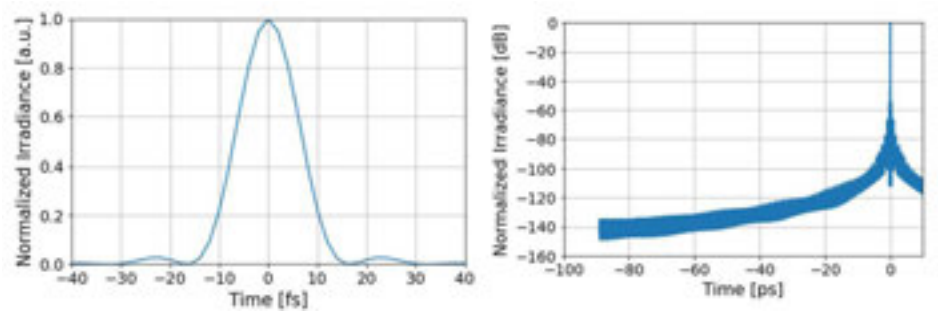

The calculated temporal contrast and pulse duration of the CPA output is not affected by the residual dispersion.

Progress on improving stability of the short picosecond pulse by fast stabilisation in Vulcan

L.E. Bradley, M. Galimberti, A. Kidd, P. Oliveira, A. Aiken, C. Suciu, J. Patel, I.O. Musgrave *(Central Laser Facility, STFC Rutherford Appleton Laboratory, Harwell Campus, Didcot, UK)*

Energy stability of the short picosecond CPA pulse in Vulcan can vary over time. This creates operationally dynamic conditions as the energies between shots can deviate from user requested energies. We present progress in stabilising the beams near-field while identifying future interventions to improve stability.

Contact:
P. Oliveira
pedro.oliveira@stfc.ac.uk

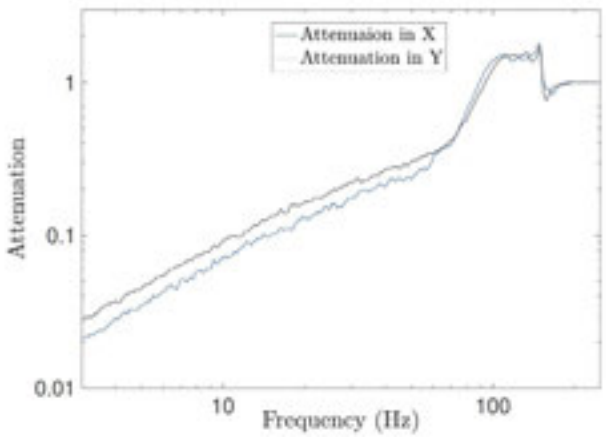

Log-log plot showing the closed loop attenuation as a function of frequency for the lock-in amplifier

Novel active near-field and far-field fast beam stabilisation of a picosecond short pulse

L.E. Bradley, P. Oliveira, M. Galimberti *(Central Laser Facility, STFC Rutherford Appleton Laboratory, Harwell Campus, Didcot, UK)*

We describe the use of an active fast beam stabilisation to achieve spatial locking of the beam in the near-field and far-field references. The beam stabilisation scheme comprises a PID feedback loop between two position sensitive detectors (PSD) and two fast piezo mirrors, improving on previous work that locked one reference.

Our stabilisation scheme is operational in user experiments demonstrating that this proof of concept may be extended to other beamlines within the Central Laser Facility and other high-power laser facilities.

Contact:
P. Oliveira
pedro.oliveira@stfc.ac.uk

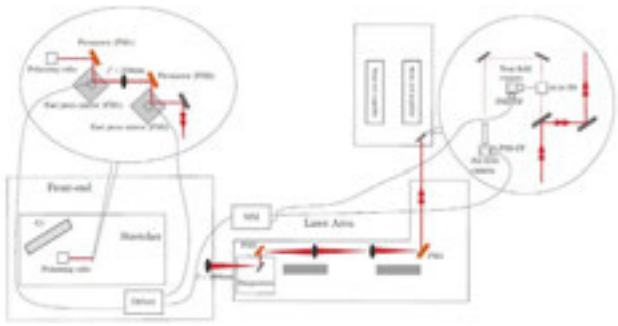

Figure 1: Operational set up showing the optical beam path. The beam propagates from the front-end stretcher with two output fast mirrors (FM1 and FM2) to the two position sensitive detectors (PSD) in the Vulcan laser area before amplification.

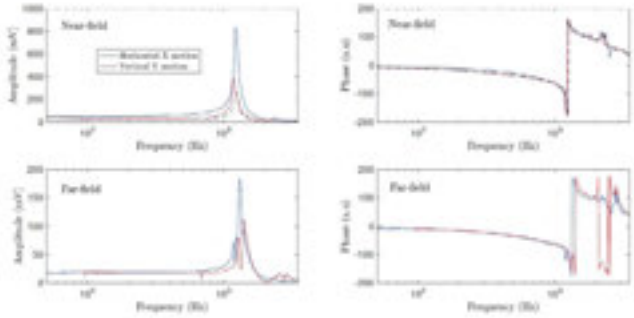

Figure 2: Stability characterisation: performing the frequency sweep between 30 Hz to 4.0 kHz with the near-field and far-field piezo mirrors. Black line shows the sweep after sufficient damping to the horizontal motion in the near-field.

Plasma diagnostics

Development of an Imaging Spectrometer for High-Repetition Rate Proton Measurement

M. Alderton, R. Wilson, T.P. Frazer, E.J. Dolier, J. Patel, M. Peat, E.F.J. Bacon, R.J. Gray, P. McKenna *(Department of Physics, University of Strathclyde, Glasgow, UK)*

S. Astbury, C. Armstrong, T. Dzelzainis, O. Finlay, C. Spindloe *(Central Laser Facility, STFC Rutherford Appleton Laboratory, Harwell Campus, Didcot, UK)*

As laser-driven proton sources increase in repetition-rate to match upcoming laser facilities, new and improved diagnostics will be required to measure the spatial and spectral profiles of laser-driven proton beams.

Current proton measurements are incompatible with high-repetition rate operation, or are unable to capture spatial and spectral information simultaneously. In this report we present development of an imaging spectrometer using Lanex as an active detector, to simultaneously measure the spatial and spectral profile of laser-driven proton beams.

In collaboration with the CLF's Target Fabrication group, we have utilised 3D printed step filters to uniformly sample the spatial profile of proton beams at fixed proton energies, using automated analysis to interpolate the full profile of the proton beam.

Contact:
M. Alderton
matthew.alderton@strath.ac.uk

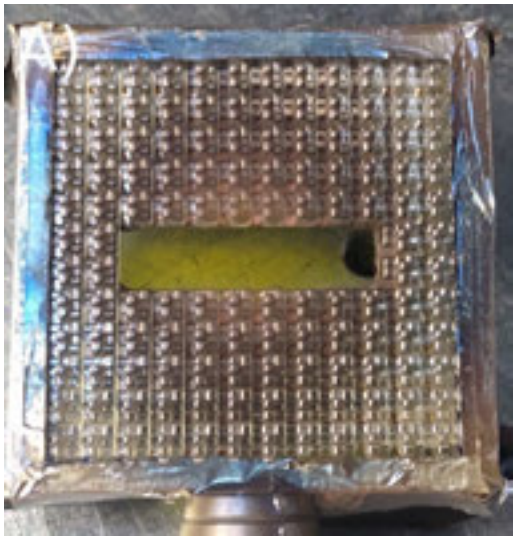

Figure 1: The 3D printed PROBIES mask front surface. The device contains an active surface of 36 mm, with the Lanex scintillator attached to the rear of the mask.

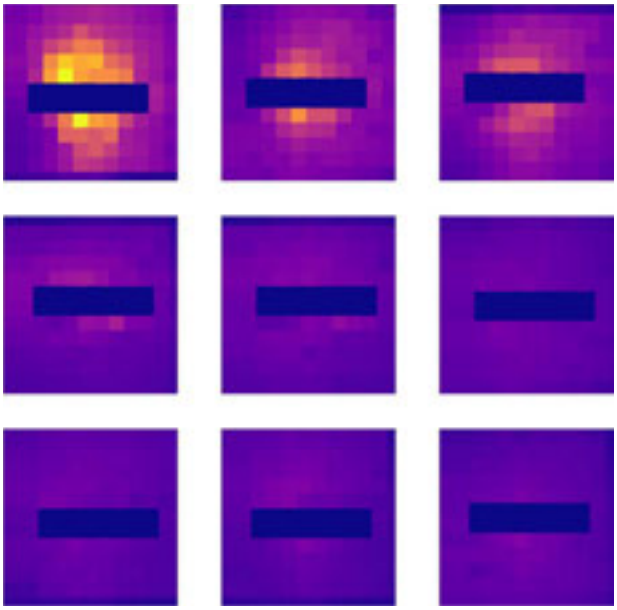

Figure 2: Interpolation of the spatial profiles of each peak in the mask design. Peak breakthrough energy increases from left to right.

Ultrafast and XUV science

Photoelectron spectroscopy measurements of roaming reactions in acetaldehyde

G.L. Abma, D.A. Horke *(Radboud University, Institute for Molecules and Materials, Nijmegen, The Netherlands)*
M.A. Parkes *(Department of Chemistry, University College London, UK)*
W.O. Razmus, R.S. Minns *(School of Chemistry, University of Southampton, UK)*
Y. Zhang, A.S. Wyatt, E. Springate, R.T. Chapman *(Central Laser Facility, Research Complex at Harwell, STFC Rutherford Appleton Laboratory, Harwell Campus, Didcot, UK)*

The dissociation reaction of acetaldehyde is mediated by a roaming reaction, where the CH_3 and HCO fragments are seen to roam around each other at intermediate distances between that associated with the bound molecule and the dissociated fragments. We have performed time-resolved photoelectron spectroscopy measurement of the roaming reaction where we observe the formation and collapse of the roaming intermediate.

Contact:
R.S. Minns
r.s.minns@soton.ac.uk

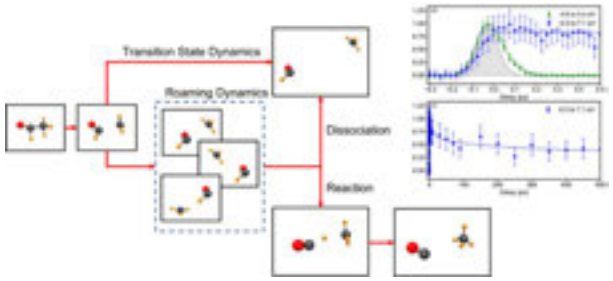

Cartoon representation of the photochemical reaction of acetaldehyde following either a transition state or roaming reaction pathway. The inset shows the temporal changes in photoelectron signal for the peaks associated with the initially excited state (green) and the roaming intermediate (blue).

Photoelectron Imaging in the Molecular Frame

J.O.F. Thompson *(School of Chemistry, University of Nottingham, UK; Central Laser Facility, STFC, Rutherford Appleton Laboratory, Harwell Campus, Didcot, UK)*
J. Woodhouse, R.S. Minns *(School of Chemistry, University of Southampton, UK)*
K.L. Reid *(School of Chemistry, University of Nottingham, UK)*
R.T. Chapman, A.S. Wyatt, Y. Zhang, E.L. Springate *(Central Laser Facility, Research Complex at Harwell, STFC Rutherford Appleton Laboratory, Harwell Campus, Didcot, UK)*

The internal conversion of energy in photoexcited molecules is extremely important in the chemistry of several biological processes, such as vision. Developing new tools to monitor these processes is crucial to gain new insights into these complex dynamics. One such tool is photoelectron angular distributions (PADs), which can provide detailed information regarding the electronic character of the states involved in these processes. Traditional methods of obtaining these PADs can, however, provide only a partial and obscured measurement of this character. This report details experiments performed at the CLF's Artemis facility using strong field alignment and HHG photoelectron spectroscopy to overcome these limitations, and measure PADs approaching the molecular frame limit. We highlight the success of the experiments and implications for this new methodology

Contact:
J.O.F. Thompson
james.thompson@stfc.ac.uk

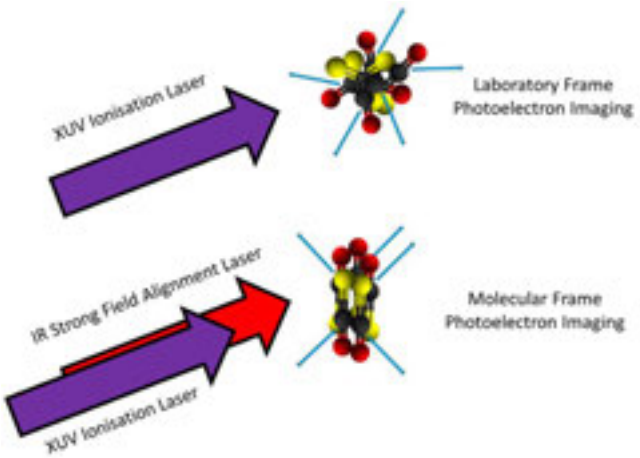

Imaging and dynamics for physical and life sciences

Resolving the Effect of Oxygen Vacancies on Co Nanostructures Using Soft XAS/X-PEEM

A.M. Beale, C. Qiu, Y. Odarchenko, I. Lezcano-Gonzalez *(Department of Chemistry, University College London, UK; Research Complex at Harwell, Rutherford Appleton Laboratory, Harwell, Didcot, UK)*
Q. Meng *(School of Chemical Engineering and Light Industry, Guangdong University of Technology, Guangzhou, China)*
S. Xu *(Research Complex at Harwell, Rutherford Appleton Laboratory, Harwell, Didcot, UK; Cardiff Catalysis Institute, School of Chemistry, Cardiff University, UK)*
P. Olalde-Velasco, F. Maccherozzi *(Diamond Light Source, Harwell Science and Innovation Campus, Didcot, UK)*
L. Zanetti-Domingues, M. Martin-Fernandez *(Central Laser Facility, Research Complex at Harwell, STFC Rutherford Appleton Laboratory, Harwell Campus, Didcot, UK)*

Improving both the extent of metallic Co nanoparticle (Co NP) formation and their stability is necessary to ensure good catalytic performance, particularly for Fischer–Tropsch synthesis (FTS). Here, we observe how the presence of surface oxygen vacancies (O_{vac}) on TiO_2 can readily reduce individual Co_3O_4 NPs directly into CoO/Co^0 in the freshly prepared sample by using a combination of X-ray photoemission electron microscopy (X-PEEM) coupled with soft X-ray absorption spectroscopy. The O_{vac} are particularly good at reducing the edge of the NPs as opposed to their centre, leading to smaller particles being more reduced than larger ones.

We then show how further reduction (and O_{vac} consumption) is achieved during heating in H_2/syngas (H_2 + CO) and reveal that O_{vac} also prevents total reoxidation of Co NPs in syngas, particularly the smallest (~8 nm) particles, thus maintaining the presence of metallic Co, potentially improving catalyst performance.

Reproduced from ACS Catal. 2022, **12**, *9125–9134, published by Americal Chemical Society, under the terms of a Creative Commons Attribution (CC BY) license (http://creativecommons.org/licenses/by/4.0/) doi: 10.1021/acscatal.2c00611*

Contact:
A.M. Beale
andrew.beale@ucl.ac.uk

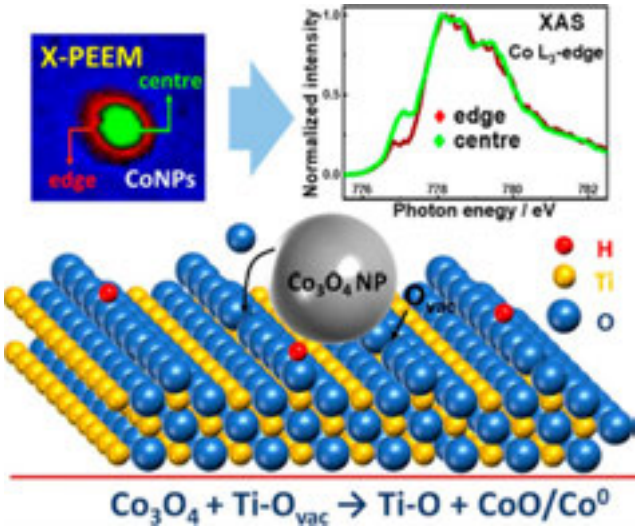

Multi-dimensional and spatiotemporal correlative imaging at the plasma membrane of live cells to determine the continuum nano-to-micro scale lipid adaptation and collective motion

M. Bernabé-Rubio *(Department of Cell Biology and Immunology, Centro de Biología Molecular Severo Ochoa, Consejo Superior de Investigaciones Científicas and Universidad Autónoma de Madrid, Spain; King's College London Centre for Stem Cells and Regenerative Medicine, Guy's Campus, London, UK)*
M. Bosch-Fortea *(Department of Cell Biology and Immunology, Centro de Biología Molecular Severo Ochoa, Consejo Superior de Investigaciones Científicas and Universidad Autónoma de Madrid, Spain; Institute of Bioengineering and School of Engineering and Materials Science, Queen Mary, University of London, UK)*
M.A. Alonso *(Department of Cell Biology and Immunology, Centro de Biología Molecular Severo Ochoa, Consejo Superior de Investigaciones Científicas and Universidad Autónoma de Madrid, Spain)*
J. Bernardino de la Serna *(Central Laser Facility, Research Complex at Harwell, STFC Rutherford Appleton Laboratory, Harwell Campus, Didcot, UK; National Heart and Lung Institute, Imperial College London, UK; NIHR Imperial Biomedical Research Centre, London, UK)*

The primary cilium is a specialized plasma membrane protrusion with important receptors for signalling pathways. In polarized epithelial cells, the primary cilium assembles after the midbody remnant (MBR) encounters the centrosome at the apical surface. The membrane surrounding the MBR, namely remnant-associated membrane patch (RAMP), once situated next to the centrosome, releases some of its lipid components to form a centrosome-associated membrane patch (CAMP) from which the ciliary membrane stems.

The RAMP undergoes a spatiotemporal membrane refinement during the formation of the CAMP, which becomes highly enriched in condensed membranes with low lateral mobility. To better understand this process, we have developed a correlative imaging approach that yields quantitative information about the lipid lateral packing, its mobility and collective assembly at the plasma membrane at different spatial scales over time. Our work paves the way towards a quantitative understanding of the spatiotemporal lipid collective assembly at the plasma membrane as a functional determinant in cell biology and its direct correlation with the membrane physicochemical state.

These findings allowed us to gain a deeper insight into the mechanisms behind the biogenesis of the ciliary membrane of polarized epithelial cells.

Reproduced from the bioRxiv preprint version (which was not certified by peer review), doi: https://doi.org/10.1101/2021.03.02.433589; this version posted March 2, 2021. It is made available under a CC-BY-NC-ND 4.0 International license. A definitive version was subsequently published in Methods, Volume **193**, *September 2021, Pages 136-147 © Elsevier 2021 doi: 10.1016/j.ymeth.2021.06.007*

Contact:
J. Bernardino de la Serna
j.bernardino-de-la-serna@imperial.ac.uk

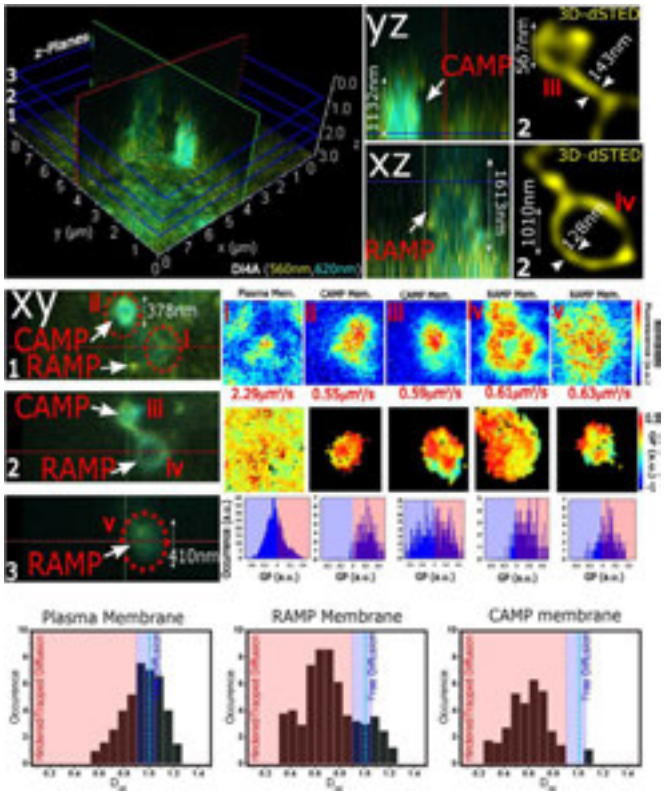

The RAMP has domains with condensed membrane and slow-moving constituents

MDCK cells showing a RAMP/CAMP labelled with Di4A. Top row panel, to the left-hand-side: large orthogonal axial reconstitution of raw micrograph view showing below at the central panel (left-hand-side) the XY section at 3 z-planes (z1: proximal, z2: middle and z3: distal); central images: YZ and XZ projections; right-hand-side images: zoomed-in deconvolved super-resolution STED image of the z2 middle plane. Central row panel to the right-hand-side from top to bottom row: diffusion coefficient values, intensity map and GP map of each of the cross sections z1-z3 and a plasma membrane region and occurrence histograms of GP values for cross sections z1– z3 and a plasma membrane region. Bottom row panel: frequency histograms obtained from LICSR showing the Drat at the plasma membrane, RAMP and CAMP (>15 regions of interest from >7 cells). Red-shadowed region indicates hindered or trapped diffusion; blue-shadowed region indicates free diffusion.

Real-time imaging and analysis of cell-hydrogel interplay within an extrusion-bioprinting capillary

G. Poologasundarampillai, S. Nagi Jayash *(School of Dentistry, Institute of Clinical Sciences, University of Birmingham, UK)*
A. Haweet *(School of Dentistry, Institute of Clinical Sciences, University of Birmingham, UK; Central Laser Facility, Research Complex at Harwell, STFC Rutherford Appleton Laboratory, Harwell Campus, Didcot, UK)*
G. Morgan, J.E. Moore Jr *(Department of Bioengineering, Imperial College London)*
A. Candeo *(Central Laser Facility, Research Complex at Harwell, STFC Rutherford Appleton Laboratory, Harwell Campus, Didcot, UK; Dipartimento di Fisica, Politecnico di Milano, Italy)*

Additive manufacturing platforms are transforming research and industrial sectors worldwide. In regenerative medicine and pharmaceutical applications, they facilitate the development of patient-specific devices for implantation, as well as in vitro models of tissues and organs for disease modelling and drug screening. A key example is extrusion-based bioprinting, where a bioink that contains cells, biomolecules and a support matrix (often hydrogel), is extruded through a narrow capillary onto a platform forming the desired structure. The printing parameters and hydrogel flow behavior likely determine the extent to which cells are damaged mechanically as they pass through the capillary. Here, we present direct observations of the hydrogels and suspended cells during the printing process to help elucidate conditions potentially leading to mechanical damage and cell death. Light-sheet fluorescence microscopy was applied to observe the real-time flow of bioinks through a capillary mimicking the conditions found in bioprinting.

Bioink formulations exhibiting constant and shear thinning viscosities, along with UV-crosslinked gelatin methacrylol (GelMA) were studied, and cell viability of post-printed gels were measured via fluorescent imaging. Cell tracking enabled flow profiles of bioinks to be deduced. In agreement with current flow simulations, the constant and shear thinning formulations displayed a Poiseuille flow profile although with a plug velocity profile for the latter.

The UV-crosslinked GelMA formulation exhibited a two-phase annular flow with gel morphologies depicting gross-melt fractures attributed to over-gelled hydrogels. Cell viability was higher in UV-crosslinked GelMA at high flow rates compared to uncrosslinked GelMA. The findings presented here will improve modeling cell-material flow during bioprinting through accurate estimation of flow conditions, in particular for complex materials. The novel imaging approach could be further exploited to provide process monitoring and feedback to improve the outcomes of 3D bioprinting.

Contact:
A. Candeo
alessia.candeo@polimi.it

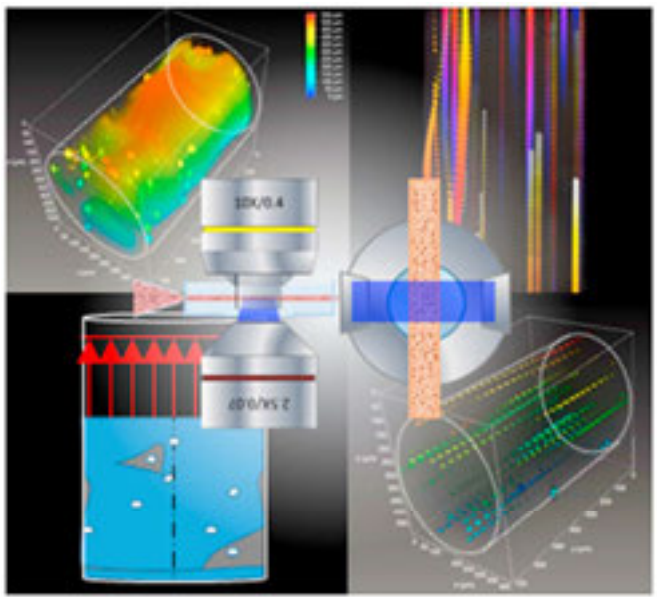

Super-Resolution Microscopy Using a Bioorthogonal-Based Cholesterol Probe Provides Unprecedented Capabilities for Imaging Nanoscale Lipid Heterogeneity in Living Cells

M. Lorizate, M. Calleja-Felipe *(Department of Biochemistry and Molecular Biology, University of the Basque Country (UPV/EHU) and Instituto Biofisika (UPV/EHU, CSIC), Spain)*
F-X. Contreras *(Department of Biochemistry and Molecular Biology, University of the Basque Country (UPV/EHU) and Instituto Biofisika (UPV/EHU, CSIC), Spain; IKERBASQUE, Basque Foundation for Science, Bilbao, Spain)*
O. Terrones, J. Olazar-Intxausti *(Department of Biochemistry and Molecular Biology, University of the Basque Country (UPV/EHU), Spain)*
J.A. Nieto-Garai, I. Rojo-Bartolomé, O. Morana, A. Arboleya *(Department of Biochemistry and Molecular Biology, University of the Basque Country (UPV/EHU) and Instituto Biofisika (UPV/EHU, CSIC), Spain; Fundación Biofísica Bizkaia/Biofisika Bizkaia Fundazioa (FBB), Spain)*
D. Ciceri *(Fundación Biofísica Bizkaia/Biofisika Bizkaia Fundazioa (FBB), Spain)*
A. Martin *(National Heart and Lung Institute, Imperial College London, UK)*
M. Szynkiewicz *(Central Laser Facility, Research Complex at Harwell, STFC Rutherford Appleton Laboratory, Harwell Campus, Didcot, UK)*
J. Bernardino de la Serna *(National Heart and Lung Institute, Imperial College London, UK; Central Laser Facility, Research Complex at Harwell, STFC Rutherford Appleton Laboratory, Harwell Campus, Didcot, UK; NIHR Imperial Biomedical Research Centre, London, UK)*

Despite more than 20 years of work since the lipid raft concept was proposed, the existence of these nanostructures remains highly controversial due to the lack of noninvasive methods to investigate their native nanorganization in living unperturbed cells. There is an unmet need for probes for direct imaging of nanoscale membrane dynamics with high spatial and temporal resolution in living cells. In this paper, a bioorthogonal-based cholesterol probe (chol-N_3) is developed that, combined with nanoscopy, becomes a new powerful method for direct visualization and characterization of lipid raft at unprecedented resolution in living cells.

The chol-N_3 probe mimics cholesterol in synthetic and cellular membranes without perturbation. When combined with live-cell super-resolution microscopy, chol-N_3 demonstrates the existence of cholesterol-rich nanodomains of <50 nm at the plasma membrane of resting living cells. Using this tool, the lipid membrane structure of such subdiffraction limit domains is identified, and the nanoscale spatiotemporal organization of cholesterol in the plasma membrane of living cells reveals multiple cholesterol diffusion modes at different spatial localizations. Finally, imaging across thick organ samples outlines the potential of this new method to address essential biological questions that were previously beyond reach.

Reproduced from Lorizate, Maier et al. "Super-Resolution Microscopy Using a Bioorthogonal-Based Cholesterol Probe Provides Unprecedented Capabilities for Imaging Nanoscale Lipid Heterogeneity in Living Cells." Small methods vol. **5**,*9 (2021): e2100430, under of a Creative Commons Attribution (CC BY) license (http://creativecommons.org/licenses/by/4.0/). doi:10.1002/smtd.202100430*

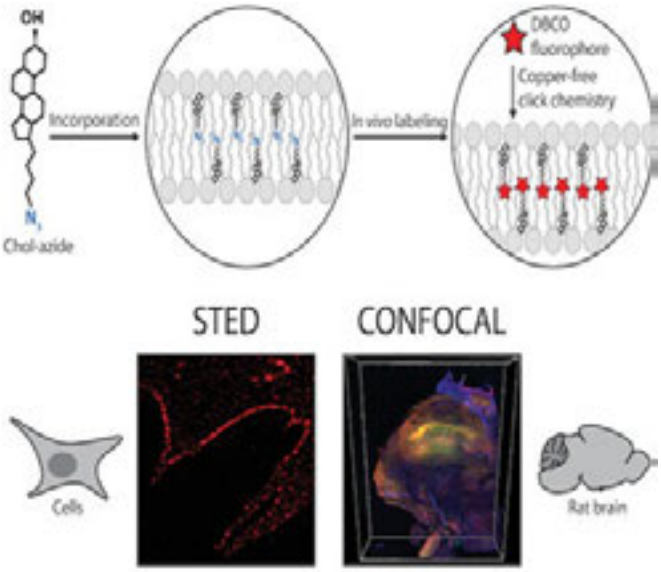

Direct imaging and characterization of nanoscale lipid heterogeneity in living cells with high temporal and spatial resolution using developed bioorthogonal cholesterol probe and nanoscopy are introduced. This probe enables tackling biological questions that were previously beyond reach. Visualization of cholesterol distribution through thick tissues outlines the tool's potential to investigate the role of cholesterol in health and disease.

Contact:
F-X. Contreras
xabier.contreras@ehu.eus

J. Bernardino de la Serna
j.bernardino-de-la-serna@imperial.ac.uk

Identification of a New Cholesterol-Binding Site within the IFN-γ Receptor that is Required for Signal Transduction

O. Morana, J.A. Nieto-Garai, A. Arboleya, D. Ciceri, I. Rojo-Bartolomé *(Instituto Biofisika (UPV/EHU, CSIC), University of the Basque Country (UPV/EHU), Spain; Fundación Biofísica Bizkaia/Biofisika Bizkaia Fundazioa (FBB), University of the Basque Country (UPV/EHU), Spain; Department of Biochemistry and Molecular Biology, Faculty of Science and Technology, University of the Basque Country (UPV/EHU), Spain)*
P. Björkholm *(Center for Biomembrane Research, Department of Biochemistry and Biophysics, Stockholm University, Sweden; Science for Life Laboratory, Stockholm University, Sweden)*
O. Terrones *(Department of Biochemistry and Molecular Biology, Faculty of Science and Technology, University of the Basque Country (UPV/EHU), Spain)*
C.M. Blouin, C. Lamaze *(Institut Curie - Centre de Recherche, PSL Research University, Membrane Mechanics and Dynamics of Intracellular Signaling Laboratory, Paris, France; Institut National de la Santé et de la Recherche Médicale (INSERM), Paris, France; Centre National de la Recherche Scientifique (CNRS), Paris, France)*
M. Lorizate *(Instituto Biofisika (UPV/EHU, CSIC), University of the Basque Country (UPV/EHU), Spain; Department of Biochemistry and Molecular Biology, Faculty of Science and Technology, University of the Basque Country (UPV/EHU), Spain)*
F.-X. Contreras *(Instituto Biofisika (UPV/EHU, CSIC), University of the Basque Country (UPV/EHU), Spain; Department of Biochemistry and Molecular Biology, Faculty of Science and Technology, University of the Basque Country (UPV/EHU), Spain; IKERBASQUE, Basque Foundation for Science, Bilbao, Spain)*
J. Bernardino de la Serna *(National Heart and Lung Institute, Imperial College London, UK; Central Laser Facility, Research Complex at Harwell, STFC Rutherford Appleton Laboratory, Harwell Campus, Didcot, UK; NIHR Imperial Biomedical Research Centre, London, UK)*

The cytokine interferon-gamma (IFN-γ) is a master regulator of innate and adaptive immunity involved in a broad array of human diseases that range from atherosclerosis to cancer. IFN-γ exerts its signalling action by binding to a specific cell surface receptor, the IFN-γ receptor (IFN-γR), whose activation critically depends on its partition into lipid nanodomains. However, little is known about the impact of specific lipids on IFN-γR signal transduction activity. Here, a new conserved cholesterol (chol) binding motif localized within its single transmembrane domain is identified.

Through direct binding, chol drives the partition of IFN-γR2 chains into plasma membrane lipid nanodomains, orchestrating IFN-γR oligomerization and transmembrane signalling. Bioinformatics studies show that the signature sequence stands for a conserved chol-binding motif presented in many mammalian membrane proteins.

The discovery of chol as the molecular switch governing IFN-γR transmembrane signalling represents a significant advance for understanding the mechanism of lipid selectivity by membrane proteins, but also for figuring out the role of lipids in modulating cell surface receptor function. Finally, this study suggests that inhibition of the chol-IFNγR2 interaction may represent a potential therapeutic strategy for various IFN-γ-dependent diseases.

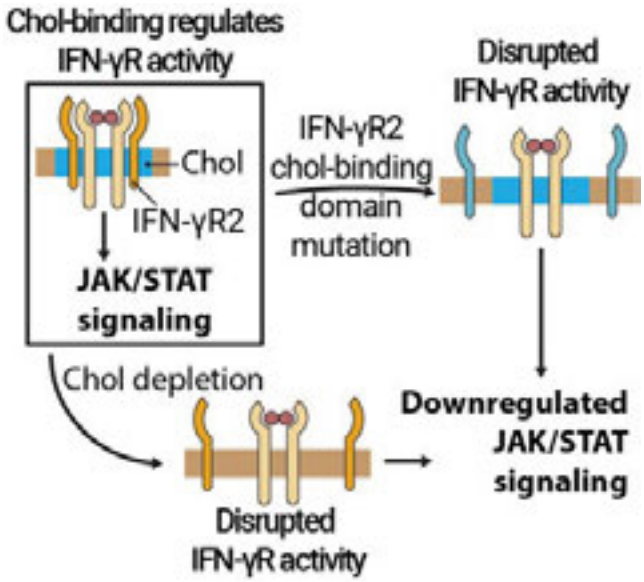

This work uncovers the role of cholesterol as the molecular determinant controlling interferon-gamma receptor (IFN-γR) activity. Through a multidisciplinary approach the structural signature within the IFN-γR required for cholesterol binding is identified. Binding of cholesterol is critical for receptor plasma membrane compartmentalization, heterodimerization, and signal transduction. This work identifies a therapeutic target for prevention and treatment of IFN-γ dependent diseases.

Contact:
F.-X. Contreras
xabier.contreras@ehu.eus

Measurement of gas-phase OH radical oxidation and film thickness of organic films at the air–water interface using material extracted from urban, remote and wood smoke aerosol

R.H. Shepherd *(Central Laser Facility, Research Complex at Harwell, STFC Rutherford Appleton Laboratory, Harwell Campus, Didcot, UK; Department of Earth Sciences, Royal Holloway, University of London, UK)*
M.D. King *(Department of Earth Sciences, Royal Holloway, University of London, UK)*
A.R. Rennie *(Department of Chemistry – Ångström Laboratory, Uppsala University, Sweden)*
A.D. Ward *(Central Laser Facility, Research Complex at Harwell, STFC Rutherford Appleton Laboratory, Harwell Campus, Didcot, UK)*
M.M. Frey, N. Brough, J. Eveson, S. Del Vento *(British Antarctic Survey, Natural Environment Research Council, Cambridge, UK)*
A. Milsom, C. Pfrang *(School of Geography, Earth and Environmental Sciences, University of Birmingham, UK)*
M.W.A. Skoda, R.J.L. Welbourn *(ISIS Pulsed Neutron and Muon Source, STFC Rutherford Appleton Laboratory, Harwell Campus, Didcot, UK)*

The presence of an organic film on a cloud droplet or aqueous aerosol particle has the potential to alter the chemical, optical and physical properties of the droplet or particle. In the study presented, water insoluble organic materials extracted from urban, remote (Antarctica) and wood burning atmospheric aerosol were found to have stable, compressible, films at the air–water interface that were typically ~6–18 Å thick. These films are reactive towards gas-phase OH radicals and decay exponentially, with bimolecular rate constants for reaction with gas-phase OH radicals of typically 0.08–1.5 × 10^{-10} cm^3 $molecule^{-1}$ s^{-1}. These bimolecular rate constants equate to initial OH radical uptake coefficients estimated to be ~0.6–1 except woodsmoke (~0.05).

The film thickness and the neutron scattering length density of the extracted atmosphere aerosol material (from urban, remote and wood burning) were measured by neutron reflection as they were exposed to OH radicals. For the first time neutron reflection has been demonstrated as an excellent technique for studying the thin films formed at air–water interfaces from materials extracted from atmospheric aerosol samples.

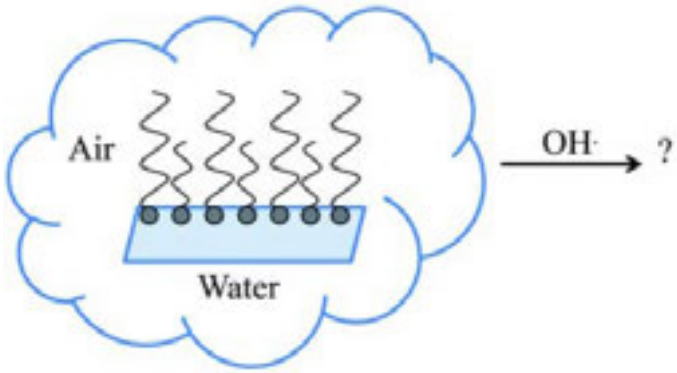

Additionally, the kinetics of gas-phase OH radicals with a proxy compound, the lipid 1,2-distearoyl-*sn*-glycero-3-phosphocholine (DSPC) was studied displaying significantly different behaviour, thus demonstrating it is not a good proxy for atmospheric materials that may form films at the air–water interface. The atmospheric lifetimes, with respect to OH radical oxidation, of the insoluble organic materials extracted from atmospheric aerosol at the air–water interface were a few hours. Relative to a possible physical atmospheric lifetime of 4 days, the oxidation of these films is important and needs inclusion in atmospheric models. The optical properties of these films were previously reported *[Shepherd et al., Atmos. Chem. Phys.*, 2018, **18**, 5235–5252] and there is a significant change in top of the atmosphere albedo for these thin films on core–shell atmospheric aerosol using the film thickness data and confirmation of stable film formation at the air–water interface presented here.

Contact:
M.D. King
m.king@rhul.ac.uk

Mie scattering from optically levitated mixed sulfuric acid–silica core–shell aerosols: observation of core–shell morphology for atmospheric science

M.R. McGrory, R.H. Shepherd *(Central Laser Facility, Research Complex at Harwell, STFC Rutherford Appleton Laboratory, Harwell Campus, Didcot, UK; Department of Earth Sciences, Royal Holloway, University of London, UK)*
M.D. King *(Department of Earth Sciences, Royal Holloway, University of London, UK)*
N. Davidson, F.D. Pope *(School of Geography, Earth and Environmental Sciences, University of Birmingham, UK)*
I.M. Watson *(School of Earth Science, University of Bristol, UK)*
R.G. Grainger *(National Centre for Earth Observation, Atmospheric, Oceanic and Planetary Physics, University of Oxford, UK)*
A.C. Jones *(Met Office, Exeter, UK; College of Engineering Maths and Physical Sciences, University of Exeter, UK)*
A.D. Ward *(Central Laser Facility, Research Complex at Harwell, STFC Rutherford Appleton Laboratory, Harwell Campus, Didcot, UK)*

Sulfuric acid is shown to form a core–shell particle on a micron-sized, optically-trapped spherical silica bead. The refractive indices of the silica and sulfuric acid, along with the shell thickness and bead radius were determined by reproducing Mie scattered optical white light as a function of wavelength in Mie spectroscopy. Micron-sized silica aerosols (silica beads were used as a proxy for atmospheric silica minerals) were levitated in a mist of sulfuric acid particles; continuous collection of Mie spectra throughout the collision of sulfuric acid aerosols with the optically trapped silica aerosol demonstrated that the resulting aerosol particle had a core–shell morphology.

Contrastingly, the collision of aqueous sulfuric acid aerosols with optically trapped polystyrene aerosol resulted in a partially coated system. The light scattering from the optically levitated aerosols was successfully modelled to determine the diameter of the core aerosol (±0.003 μm), the shell thickness (±0.0003 μm) and the refractive index (±0.007). The experiment demonstrated that the presence of a thin film rapidly changed the light scattering of the original aerosol.

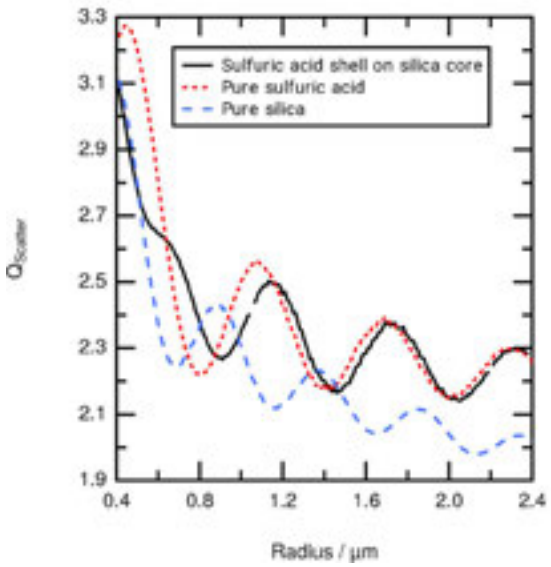

When a 1.964 μm diameter silica aerosol was covered with a film of sulfuric acid 0.287 μm thick, the wavelength dependent Mie peak positions resembled sulfuric acid. Thus mineral aerosol advected into the stratosphere would likely be coated with sulfuric acid, with a core–shell morphology, and its light scattering properties would be effectively indistinguishable from a homogenous sulfuric acid aerosol if the film thickness was greater than a few 100s of nm for UV-visible wavelengths.

Reproduced from Phys. Chem. Chem. Phys., 2022, ***24****, 5813, published by the Royal Society of Chemistry, under the terms of a Creative Commons Attribution (CC BY) license (http://creativecommons.org/licenses/by/3.0/). doi: 10.1039/d1cp04068e*

Contact:
A.D. Ward
andy.ward@stfc.ac.uk

A Dinuclear Osmium(II) Complex Near-Infrared Nanoscopy Probe for Nuclear DNA

A.J.H.M. Meijer, J.A. Thomas, S.A. Archer, C.C. Robertson, S. Sreedharan, H. Carson *(Department of Chemistry, University of Sheffield, UK)*
B. Dietzek-Ivanšić, F. Dröge *(Institute of Physical Chemistry, Friedrich Schiller University Jena, Germany; Leibniz Institute for Photonic Technology Jena e.V., Germany)*
F.F. Noakes *(Department of Chemistry and Department of Biomedical Science, University of Sheffield, UK)*
A. Raza, S. MacNeil, J.W. Haycock *(Materials Science & Engineering, University of Sheffield, UK)*
C.G.W. Smythe *(Department of Biomedical Science, University of Sheffield, UK)*
J. Bernardino de la Serna *(Central Laser Facility, Research Complex at Harwell, STFC Rutherford Appleton Laboratory, Harwell Campus, Didcot, UK; National Heart and Lung Institute, Faculty of Medicine, Imperial College London, UK)*

With the aim of developing photostable nearinfrared cell imaging probes, a convenient route to the synthesis of heteroleptic Os^{II} complexes containing the $Os(TAP)_2$ fragment is reported. This method was used to synthesize the dinuclear Os^{II} complex, $[\{Os(TAP)_2\}_2tpphz]^{4+}$ (where tpphz = tetrapyrido[3,2-a:2',3'-c:3",2''-h:2''',3'''-j]phenazine and TAP = 1,4,5,8-tetraazaphenanthrene). Using a combination of resonance Raman and time-resolved absorption spectroscopy, as well as computational studies, the excited state dynamics of the new complex were dissected. These studies revealed that, although the complex has several close lying excited states, its near-infrared, NIR, emission (λ_{max} = 780 nm) is due to a low-lying Os → TAP based ^{3}MCLT state. Cell-based studies revealed that unlike its Ru^{II} analogue, the new complex is neither cytotoxic nor photocytotoxic. However, as it is highly photostable as well as live-cell permeant and displays NIR luminescence within the biological optical window, its properties make it an ideal probe for optical microscopy, demonstrated by its use as a super-resolution NIR STED probe for nuclear DNA.

Reproduced with permission from J. Am. Chem. Soc. 2021, 143, 48, 20442–20453, © 2021 American Chemical Society. doi: 10.1021/jacs.1c10325

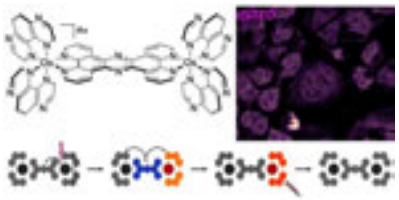

Contact:
A.J.H.M. Meijer
a.meijer@sheffield.ac.uk

B. Dietzek-Ivanšić
benjamin.dietzek@uni-jena.de

J.A. Thomas
james.thomas@sheffield.ac.uk

The impact of molecular self-organisation on the atmospheric fate of a cooking aerosol proxy

A. Milsom *(School of Geography, Earth and Environmental Sciences, University of Birmingham, UK)*
A.M. Squires *(Department of Chemistry, University of Bath, UK)*
A.D. Ward *(Central Laser Facility, Research Complex at Harwell, STFC Rutherford Appleton Laboratory, Harwell Campus, Didcot, UK)*
C. Pfrang *(School of Geography, Earth and Environmental Sciences, University of Birmingham, UK; Department of Meteorology, University of Reading, UK)*

Atmospheric aerosols influence the climate via cloud droplet nucleation and can facilitate the long-range transport of harmful pollutants. The lifetime of such aerosols can therefore determine their environmental impact. Fatty acids are found in organic aerosol emissions with oleic acid, an unsaturated fatty acid, being a large contributor to cooking emissions. As a surfactant, oleic acid can self-organise into nanostructured lamellar bilayers with its sodium salt, and this self-organisation can influence reaction kinetics. We developed a kinetic multi-layer model-based description of decay data we obtained from laboratory experiments of the ozonolysis of coated films of this self-organised system, demonstrating a decreased diffusivity for both oleic acid and ozone due to lamellar bilayer formation. Diffusivity was further inhibited by a viscous oligomer product forming in the surface layers of the film. Our results indicate that nanostructure formation can increase the reactive half-life of oleic acid by an order of days at typical indoor and outdoor atmospheric ozone concentrations. We are now able to place nanostructure formation in an atmospherically meaningful and quantifiable context. These results have implications for the transport of harmful pollutants and the climate.

*Reproduced from Milsom, A., Squires, A. M., Ward, A. D., and Pfrang, C.: The impact of molecular self-organisation on the atmospheric fate of a cooking aerosol proxy, Atmos. Chem. Phys., **22**, 4895–4907, 2022, under the terms of a Creative Commons Attribution (CC BY) license (http://creativecommons.org/licenses/by/4.0/) doi:10.5194/acp-22-4895-2022*

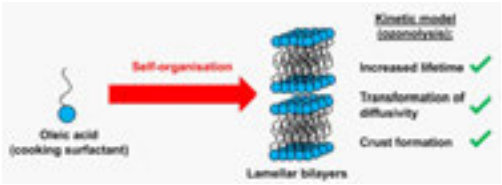

Contact:
C. Pfrang
c.pfrang@bham.ac.uk

Sphingomyelin Depletion Inhibits CXCR4 Dynamics and CXCL12-Mediated Directed Cell Migration in Human T Cells

S.R. Gardeta, E.M. García-Cuesta, G. D'Agostino, B. Soler Palacios, A. Quijada-Freire, P. Lucas, J.M. Rodríguez-Frade, M. Mellado *(Chemokine Signaling Group, Department of Immunology and Oncology, National Center for Biotechnology/Consejo Superior de Investigaciones Científicas, Madrid, Spain)*

J. Bernardino de la Serna *(National Heart and Lung Institute, Imperial College London, UK; Central Laser Facility, Research Complex at Harwell, STFC Rutherford Appleton Laboratory, Harwell Campus, Didcot, UK; NIHR Imperial Biomedical Research Centre, London, UK)*

C. Gonzalez-Riano, C. Barbas *(Metabolomic and Bioanalysis Center (CEMBIO), Pharmacy Faculty, Centro de Estudios Universitarios, Madrid, Spain)*

Sphingolipids, ceramides and cholesterol are integral components of cellular membranes, and they also play important roles in signal transduction by regulating the dynamics of membrane receptors through their effects on membrane fluidity. Here, we combined biochemical and functional assays with single-particle tracking analysis of diffusion in the plasma membrane to demonstrate that the local lipid environment regulates CXCR4 organization and function and modulates chemokine-triggered directed cell migration.

Prolonged treatment of T cells with bacterial sphingomyelinase promoted the complete and sustained breakdown of sphingomyelins and the accumulation of the corresponding ceramides, which altered both membrane fluidity and CXCR4 nanoclustering and dynamics.

Under these conditions CXCR4 retained some CXCL12-mediated signaling activity but failed to promote efficient directed cell migration. Our data underscore a critical role for the local lipid composition at the cell membrane in regulating the lateral mobility of chemokine receptors, and their ability to dynamically increase receptor density at the leading edge to promote efficient cell migration.

Palacios B, Quijada-Freire A, Lucas P, Bernardino de la Serna J, Gonzalez-Riano C, Barbas C, Rodríguez-Frade JM and Mellado M (2022) Sphingomyelin Depletion Inhibits CXCR4 Dynamics and CXCL12-Mediated Directed Cell Migration in Human T Cells. Front. Immunol. **13**:*925559, under the terms of a Creative Commons Attribution (CC BY) license (http://creativecommons.org/licenses/by/4.0/) doi: 10.3389/fimmu.2022.925559*

Contact:
M. Mellado
mmellado@cnb.csic.es

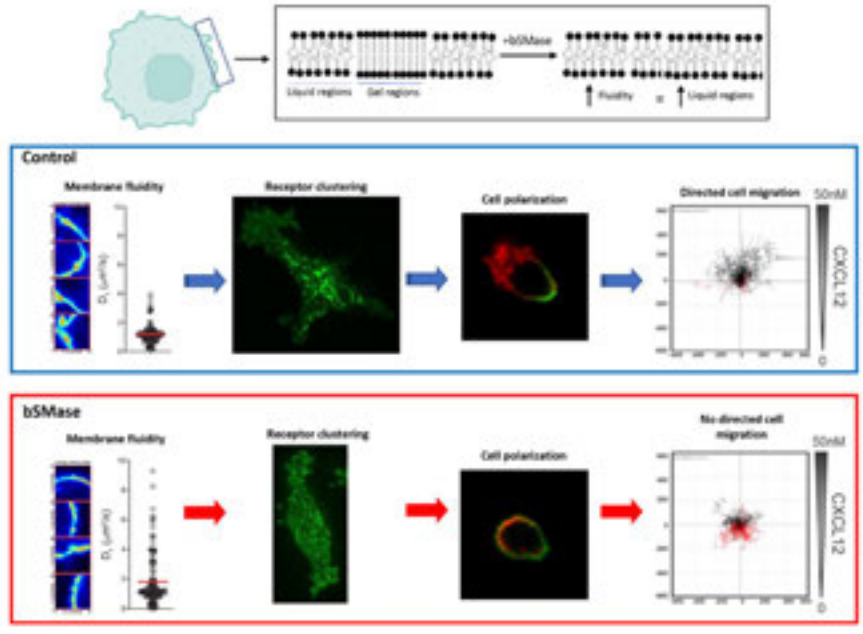

By increasing membrane fluidity, bSMase treatment alters receptor clustering, cell polarization and the ability of cells to sense chemotactic gradients.

AR cooperates with SMAD4 to maintain skeletal muscle homeostasis

M. Forouhan, W.F. Lim, T.C. Roberts, A.A. Speciale, R. Ellerington, A. Garcia-Guerra *(Department of Paediatrics, University of Oxford, UK)*
L.C. Zanetti-Domingues, C.J. Tynan *(Central Laser Facility, Research Complex at Harwell, STFC Rutherford Appleton Laboratory, Harwell Campus, Didcot, UK)*
B. Malik, P. Fratta, L. Greensmith *(Department of Neuromuscular Diseases, UCL Queen Square Institute of Neurology, London, UK)*
R. Manzano *(Department of Physiology, Anatomy and Genetics, University of Oxford, UK)*
G. Sorarú *(Department of Neurosciences, Neurology Unit, University of Padova, Italy; Venetian Institute of Molecular Medicine (VIMM), Padova, Italy)*
M. Pennuto *(Venetian Institute of Molecular Medicine (VIMM), Padova, Italy; Department of Biomedical Sciences, University of Padova, Italy)*
M.A. Wood, C. Rinaldi *(Department of Paediatrics, University of Oxford, UK; MDUK Oxford Neuromuscular Centre, University of Oxford, UK)*

Androgens and androgen-related molecules exert a plethora of functions across different tissues, mainly through binding to the transcription factor androgen receptor (AR). Despite widespread therapeutic use and misuse of androgens as potent anabolic agents, the molecular mechanisms of this effect on skeletal muscle are currently unknown. Muscle mass in adulthood is mainly regulated by the bone morphogenetic protein (BMP) axis of the transforming growth factor (TGF)-β pathway via recruitment of mothers against decapentaplegic homolog 4 (SMAD4) protein. Here we show that, upon activation, AR forms a transcriptional complex with SMAD4 to orchestrate a muscle hypertrophy programme by modulating SMAD4 chromatin binding dynamics and enhancing its transactivation activity.

We challenged this mechanism of action using spinal and bulbar muscular atrophy (SBMA) as a model of study. This adult-onset neuromuscular disease is caused by a polyglutamine expansion (polyQ) in AR and is characterized by progressive muscle weakness and atrophy secondary to a combination of lower motor neuron degeneration and primary muscle atrophy. Here we found that the presence of an elongated polyQ tract impairs AR cooperativity with SMAD4, leading to an inability to mount an effective anti-atrophy gene expression programme in skeletal muscle in response to denervation. Furthermore, adeno-associated virus, serotype 9 (AAV9)-mediated muscle-restricted delivery of BMP7 is able to rescue the muscle atrophy in SBMA mice, supporting the development of treatments able to fne-tune AR-SMAD4 transcriptional cooperativity as a promising target for SBMA and other conditions associated with muscle loss.

Reproduced from Forouhan, M., Lim, W.F., Zanetti-Domingues, L.C. et al. AR cooperates with SMAD4 to maintain skeletal muscle homeostasis. Acta Neuropathol **143**, *713–731 (2022)., under the terms of a Creative Commons Attribution (CC BY) license (http://creativecommons.org/licenses/by/4.0/) doi: 10.1007/s00401-022-02428-1*

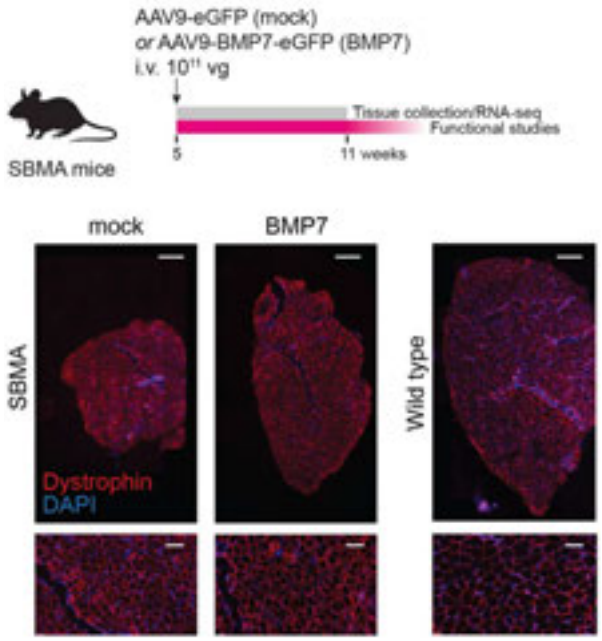

AAV9-mediated delivery of BMP7 in skeletal muscle counteracts muscle atrophy in spinal and bulbar muscular atrophy (SBMA).
(Top) Experimental design; arrow indicates the timing of the intravenous (i.v.) injection. Dose is expressed as vector genome (vg).
(Bottom) Whole-muscle cross section of TA muscle stained with dystrophin (red) and DAPI (blue) showing partial restoration of muscle atrophy in SBMA muscle upon treatment with BMP7. Scale bar, 1 mm (top) and 100 µm (below).

Contact:
C. Rinaldi
carlo.rinaldi@paediatrics.ox.ac.uk

Myosin VI regulates the spatial organisation of mammalian transcription initiation

Y. Hari-Gupta, H.C.W. Reed *(School of Biosciences, University of Kent, UK)*
N. Fili, Á. dos Santos A.W. Cook, R.E. Gough, C.P. Toseland *(Department of Oncology and Metabolism, University of Sheffield, UK)*
L. Wang, M. Martin-Fernandez *(Central Laser Facility, Research Complex at Harwell, STFC Rutherford Appleton Laboratory, Harwell Campus, Didcot, UK)*
J. Aaron, E. Wait, T-L. Chew *(Advanced Imaging Center, HHMI Janelia Research Campus, Ashburn, VA, USA)*
T. Venit *(Science Division, Biology Program, New York University Abu Dhabi (NYUAD), Abu Dhabi, United Arab Emirates)*
A. Grosse-Berkenbusch, J.C.M. Gebhardt *(Institute of Biophysics, Ulm University, Germany)*
P. Percipalle *(Science Division, Biology Program, New York University Abu Dhabi (NYUAD), Abu Dhabi, United Arab Emirates; Department of Molecular Bioscience, The Wenner Gren Institute, Stockholm University, Sweden)*

During transcription, RNA Polymerase II (RNAPII) is spatially organised within the nucleus into clusters that correlate with transcription activity. While this is a hallmark of genome regulation in mammalian cells, the mechanisms concerning the assembly, organisation and stability remain unknown. Here, we have used combination of single molecule imaging and genomic approaches to explore the role of nuclear myosin VI (MVI) in the nanoscale organisation of RNAPII. We reveal that MVI in the nucleus acts as the molecular anchor that holds RNAPII in high density clusters. Perturbation of MVI leads to the disruption of RNAPII localisation, chromatin organisation and subsequently a decrease in gene expression. Overall, we uncover the fundamental role of MVI in the spatial regulation of gene expression.

Contact:
C.P. Toseland
c.toseland@sheffield.ac.uk

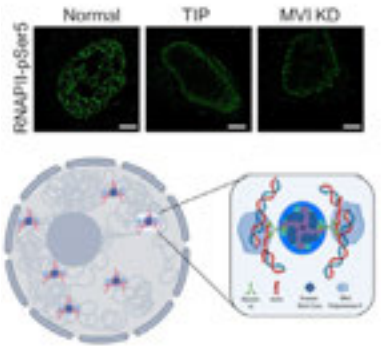

Top: Cartoon depiction of the MVI key features including the cargo-binding domain (CBD).

Bottom: Schematic of myosin VI anchoring RNAPII at transcription factories.

In Situ Sol–Gel Synthesis of Unique Silica Structures Using Airborne Assembly: Implications for In-Air Reactive Manufacturing

C.R. Barker *(Department of Earth Sciences, Royal Holloway University of London, UK; Central Laser Facility, Research Complex at Harwell, STFC Rutherford Appleton Laboratory, Harwell Campus, Didcot, UK)*
F.K. Lewns, G. Poologasundarampillai *(School of Dentistry, University of Birmingham, UK)*
A.D. Ward *(Central Laser Facility, Research Complex at Harwell, STFC Rutherford Appleton Laboratory, Harwell Campus, Didcot, UK)*

Optical trapping enables the real-time manipulation and observation of morphological evolution of individual particles during reaction chemistry. Here, optical trapping was used in combination with Raman spectroscopy to conduct airborne assembly and kinetic experiments. Micro-droplets of alkoxysilane were levitated in air prior to undergoing either acid- or base-catalyzed sol–gel reaction chemistry to form silica particles. The evolution of the reaction was monitored in real-time; Raman and Mie spectroscopies confirmed the in situ formation of silica particles from alkoxysilane droplets as the product of successive hydrolysis and condensation reactions, with faster reaction kinetics in acid catalysis. Hydrolysis and condensation were accompanied by a reduction in droplet volume and silica formation. Two airborne particles undergoing solidification could be assembled into unique 3D structures such as dumb-bell shapes by manipulating a controlled collision.

Our results provide a pipeline combining spectroscopy with optical microscopy and nanoscale FIB–SEM imaging to enable chemical and structural insights, with the opportunity to apply this methodology to probe structure formation during reactive inkjet printing.

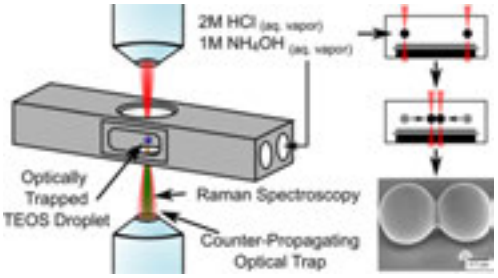

Contact:
G. Poologasundarampillai
g.poologasundarampillai@bham.ac.uk

A.D. Ward
andy.ward@stfc.ac.uk

Correlative multi-scale cryo-imaging unveils SARS-CoV-2 assembly and egress

L. Mendonça, A-S. Krebs, L. Chen, T. Ni *(Division of Structural Biology, Wellcome Trust Centre for Human Genetics, University of Oxford, UK)*
P. Zhang *(Division of Structural Biology, Wellcome Trust Centre for Human Genetics, University of Oxford, UK; Diamond Light Source, Harwell Science and Innovation Campus, Didcot, UK; Department of Structural Biology, University of Pittsburgh, Pennsylvania, USA)*
A. Howe, J.B. Gilchrist, Y. Sheng, J. Radecke, I. Kounatidis, M.A. Koronfel. M. Harkiolaki *(Diamond Light Source, Harwell Science and Innovation Campus, Didcot, UK)*
D. Sun *(Department of Structural Biology, University of Pittsburgh, Pennsylvania, USA)*
M.L. Knight, W. James *(Sir William Dunn School of Pathology, University of Oxford, UK)*
L.C. Zanetti-Domingues, B. Bateman, M. Szynkiewicz, M.L. Martin-Fernandez *(Central Laser Facility, Research Complex at Harwell, STFC Rutherford Appleton Laboratory, Harwell Campus, Didcot, UK)*
V.D. Li *(Murray Edwards College, University of Cambridge, UK)*

Since the outbreak of the SARS-CoV-2 pandemic, there have been intense structural studies on purified viral components and inactivated viruses. However, structural and ultrastructural evidence on how the SARS-CoV-2 infection progresses in the native cellular context is scarce, and there is a lack of comprehensive knowledge on the SARS-CoV-2 replicative cycle. To correlate cytopathic events induced by SARS-CoV-2 with virus replication processes in frozen-hydrated cells, we established a unique multi-modal, multi-scale cryo-correlative platform to image SARS-CoV-2 infection in Vero cells.

This platform combines serial cryoFIB/ SEM volume imaging and soft X-ray cryo-tomography with cell lamellae-based cryo-electron tomography (cryoET) and subtomogram averaging. Here we report critical SARS-CoV-2 structural events – e.g. viral RNA transport portals, virus assembly intermediates, virus egress pathway, and native virus spike structures, in the context of whole-cell volumes revealing drastic cytppathic changes. This integrated approach allows a holistic view of SARS-CoV-2 infection, from the whole cell to individual molecules.

Contact:
P. Zhang
peijun.zhang@strubi.ox.ac.uk

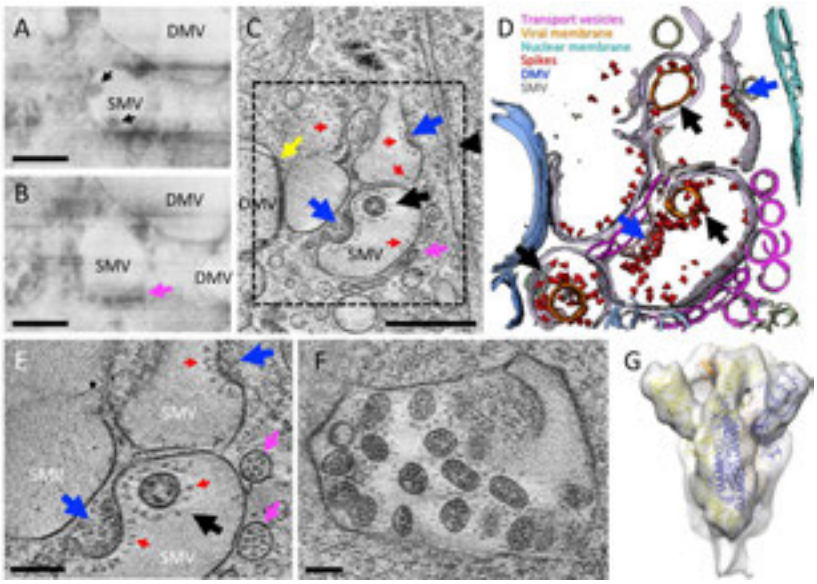

SARS-CoV-2 cytoplasmic viral assembly. *(A-B) CryoFIB/SEM images of two sequential slices separated by 80 nm. Black arrows point to virus particles in single membrane vesicle (SMV). Pink arrow points to small dense vesicles lining the outside of virus-containing SMV. (C) Tomographic slice of cryoFIB lamella depicting SARS-CoV-2 assembly, with DMV portals (yellow arrow), assembling viruses (blue arrow), assembled virus (black arrow), viral spikes on SMV membranes (red arrows), dense vesicles around the assembly site (pink arrow, as in B) and a nucleopore (black arrowhead). (D) Density segmentation of C, displaying three virus particles (black arrows) and two assembly sites (blue arrows). (E) An enlarged view (at a different angle) of boxed area in C, showing assembled virus (black arrow), assembling viruses (blue arrows), spikes (red arrows) and spike-containing vesicles (pink arrows). (F) Large intracellular virus-containing vesicle (LVCV) full of readily assembled viruses. (G) Subtomogram average of viral spikes of intracellular viruses from cell lamellae at 11 Å resolution, fitted with an atomic model of spike trimer (PDB 6ZB5) (Toelzer et al., 2020). Scale bar is 300 nm in A, B and C; and 100 nm in E and F.*

Shining Light on Metalloenzyme Catalysis

P.A. Ash, R. Frew *(School of Chemistry, University of Leicester, UK; Leicester Institute of Structural & Chemical Biology, University of Leicester, UK)*
R.M. Evans, P. Rodríguez Maciá *(Department of Chemistry, University of Oxford, Inorganic Chemistry Laboratory, UK)*
S.B. Carr *(Research Complex at Harwell, STFC Rutherford Appleton Laboratory, Harwell Campus, Didcot, UK)*
G. Greetham, I. Sazanovich *(Central Laser Facility, Research Complex at Harwell, STFC Rutherford Appleton Laboratory, Harwell Campus, Didcot, UK)*

In this study we demonstrate the potential of time-resolved multiple probe spectroscopy (TRMPS) at Ultra to provide unique insight into proton-coupled electron transfer reactions in biology. By exploiting an intrinsically photosensitive step during the [NiFe] hydrogenase catalytic cycle, we are able to track the movement of a proton (H^+) relative to electron transfer on mechanistically-relevant timescales. The TRMPS method is sufficiently sensitive to allow detection of low-intensity transient intermediates in dilute (*ca* mM) biological samples. Here we have established proof-of-concept methodologies that will allow detailed interrogation of biological proton-coupled electron transfer via photodissociation of intrinsic or extrinsic ligands at metalloenzyme active sites. Proton-coupled electron transfer is ubiquitous in nature, and underpins the efficiency of metalloenzymes that catalyse thermodynamically 'difficult' reactions under ambient conditions using earth-abundant metals.

A deep understanding of metalloenzyme mechanisms is needed in order to inspire a new generation of catalysts for sustainable, 'green' energy-conversion processes.

Contact:
P.A. Ash
philip.ash@leicester.ac.uk

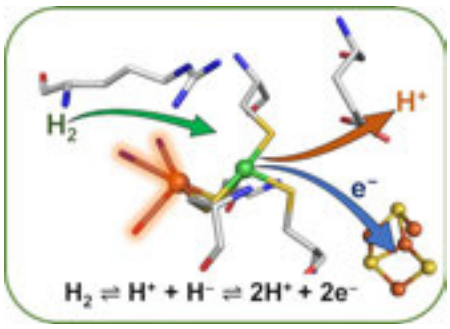

Activation of H_2 by [NiFe] hydrogenase enzymes is reliant upon the highly coordinated movement of protons (H^+) and electrons (e^-), and serves as a paradigm for studying biological proton-coupled electron transfer.

A flexible mid-IR laser with high power for temperature-jump spectroscopy

A.E. Edmeades, M. Towrie, P.M. Donaldson *(Central Laser Facility, Research Complex at Harwell, STFC Rutherford Appleton Laboratory, Harwell Campus, Didcot, UK)*

Time resolved temperature-jump (T-jump) infrared (IR) spectroscopy using pulsed laser techniques is a promising method for studying thermally activated processes in catalysis. The current T-jump setup in Ultra-B delivers 70 µJ pulses of 1 ns duration at 1 kHz. Up to 2 mJ of total laser energy can be delivered by using 30 successive laser pulses, achieving higher, more sustained T-jumps. We present a new mid-IR wavelength tunable laser based on a nanosecond pulsed fibre pumping a signal resonant periodically poled lithium niobate (PPLN) optical parametric oscillator (OPO).

Pulse energies of up to 100 µJ at 84 kHz have been observed. This new laser is capable of inducing greater heating on a µs timescale than the existing 1 kHz system. Flexibility in the fibre laser parameters combined with the IR wavelength tunability provides the opportunity to design pulse sequences to control heating and cooling times for a wide range of samples.

Contact:
A.E. Edmeades
amy.edmeades@stfc.ac.uk

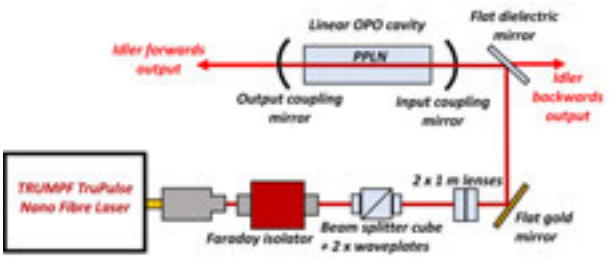

A T-jump laser setup based on a Nd fibre laser and PPLN OPO.

Kerr gated Raman spectroscopy as a diagnostic for high states of electrochemical lithium intercalation into graphite electrodes for Li-ion cells

L.J. Hardwick, A.R. Neale, D.C. Milan, T. Samarakoon F. Braga *(Stephenson Institute for Renewable Energy, Department of Chemistry, University of Liverpool, UK)*

I.V. Sazanovich *(Central Laser Facility, Research Complex at Harwell, STFC Rutherford Appleton Laboratory, Harwell Campus, Didcot, UK)*

The general applicability of Kerr gated Raman spectroscopy as a strong diagnostic tool for tracking high states of charge in graphitic electrodes has been expanded through combinations of ex situ and operando spectroelectrochemical experiments.

The approximate sensitivity of the graphitic G-band towards lithiation at high states from $Li_{0.5}C_6$ to LiC_6 was found to be a general observation; consistent across different graphite materials and electrolyte formulations (Figure 1), and experimental conditions, and was retained in subsequent cycles (Figure 2).

While this information is often lost underneath emission baselines in conventional Raman investigations of electrochemical intercalation into graphite, these findings further strengthen the potential of Kerr gated Raman spectroscopy as a powerful tool to track the high states of charge in graphite-based electrodes in Li-ion cells.

Contact:
L. J. Hardwick
hardwick@liverpool.ac.uk

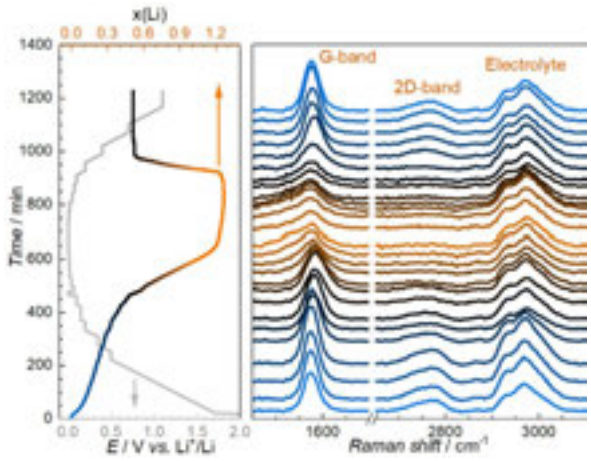

Figure 1: (a) Potential sweep/hold potential and changes in cell capacity (x in Li_xC_6) of the graphite electrode and (b) the operando Kerr gated Raman spectra showing the primary G and 2D graphite bands at 1580 and 2780 cm^{-1}, respectively (electrolyte bands at ca. 2980 cm^{-1}).

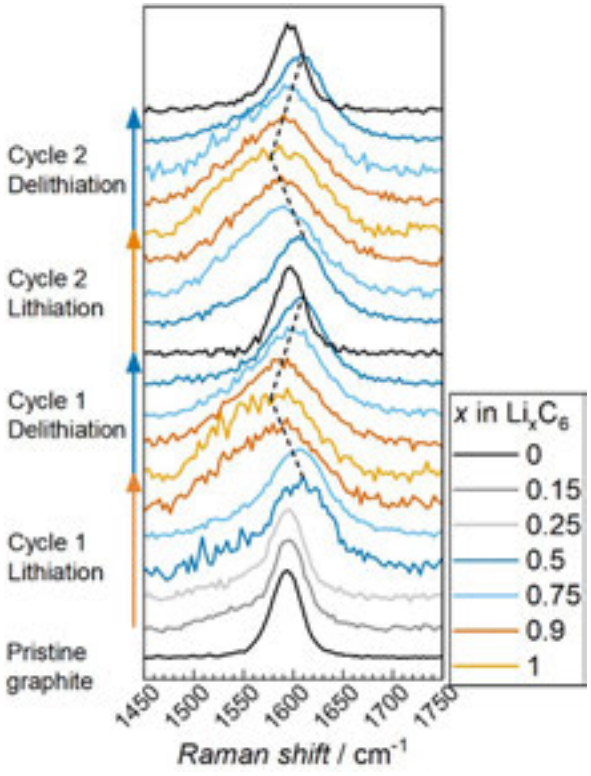

Figure 2: Ex situ Kerr gated Raman spectra (normalised) of SFG-6 graphite electrodes cycled to various states of intercalation (x in Li_xC_6). The dashed lines show an approximation of the band shift for each cycle.

2D-IR Spectroscopy Reveals Structural and Dynamical Details of [NiFe] Hydrogenases

C.C.M. Bernitzky, M. Horch, Y. Rippers *(Department of Physics, Freie Universität Berlin, Germany)*
G.M. Greetham *(Central Laser Facility, Research Complex at Harwell, STFC Rutherford Appleton Laboratory, Harwell Campus, Didcot, UK)*
O. Lenz, C. Lorent, J. Schoknecht, C. Schulz, I. Zebger *(Department of Chemistry, Technische Universität Berlin, Germany)*
N.T. Hunt, A. Parkin, B. Procacci, J. Walton, S.L.D. Wrathall *(Department of Chemistry and York Biomedical Research Institute, University of York, UK)*

Utilising active-site CO/CN^- ligands as vibrational reporter groups (A), we have studied hydrogen-transforming enzymes, so-called hydrogenases, by pump-probe and two-dimensional (2D) infrared (IR) techniques. 2D-IR spectroscopy verified unusual vibrational features of a unique [NiFe] hydrogenase (B) and allowed insights into the constrained structure of its oxygen-protected state (doi:10.1021/jacs.2c06400). Moreover, detailed information on CO bond properties of multiple redox-structural states of the active site were obtained.

The data indicate that the CO bond dissociation energy does not follow the trend of the CO-stretch fundamental frequency (C) but is significantly affected by the shape of the bond potential.

This finding was supported by a study on another hydrogenase (doi:10.1039/D2CP04188J), which additionally revealed differences between the protein-embedded active site and a bioinspired model complex in different solvents (A).

This work also resolved a complex signal pattern related to the CN^- ligands, which could be explained and structurally interpreted by quantum chemical calculations (D)(doi:10.3390/catal12090988).

Contact:
M. Horch
marius.horch@fu-berlin.de

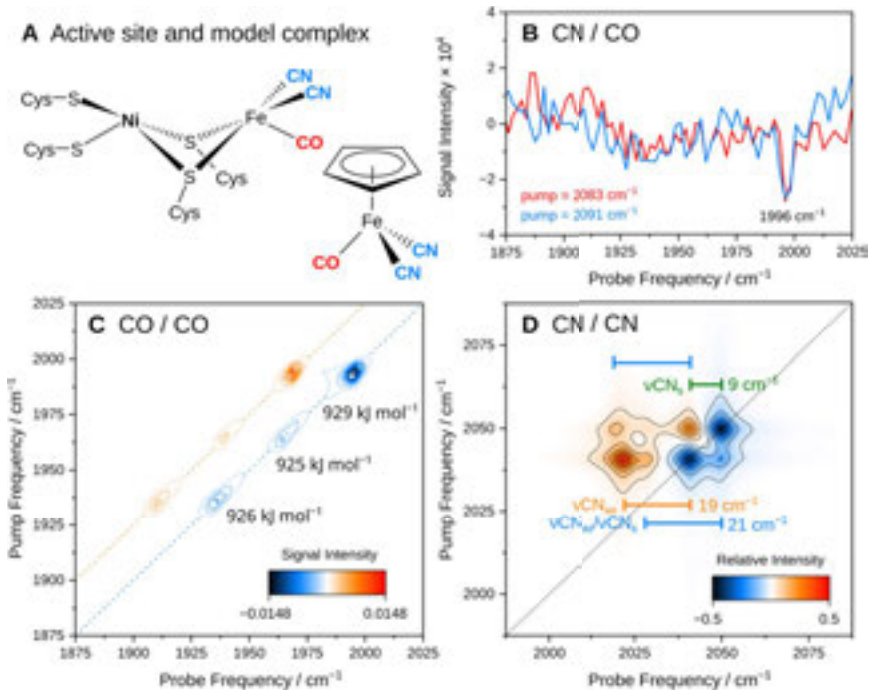

(A) Structures of the active site of [NiFe] hydrogenase and a biomimetic model complex. Diatomic ligands used as IR reporter groups are highlighted. (B) Pump slice through the 2D-IR spectrum, revealing coupling between CN stretch modes and a high-frequency CO stretch mode, confirming that the latter reflects an active-site ligand. (C) CO stretch signals of three redox-structural states of the [NiFe] active site, resolved by 2D-IR spectroscopy. Indicated bond dissociation energies do not correlate with CO stretch fundamental frequencies. (D) Simulated 2D-IR spectrum reproducing the experimental CN-stretch signature by including resonant interactions in the underlying calculations.

Temperature-Jump/Drop Infrared Spectroscopy Reveals RNA Tetraloop Refolding Dynamics

C.P. Howe, B. Procacci, N.T. Hunt *(Department of Chemistry and York Biomedical Research Institute, University of York, UK)*

G.M. Greetham, A.W. Parker *(Central Laser Facility, Research Complex at Harwell, STFC Rutherford Appleton Laboratory, Harwell Campus, Didcot, UK)*

The structural dynamics of RNA and DNA are essential to cellular function, but direct measurement of folding is challenging. We present a temperature-jump/drop method able to measure both melting and refolding dynamics, and apply it to a series of 12-nucleotide R/DNA sequences featuring the UNCG tetraloop commonly found in biological RNAs.

Stem-loop melting occurred an order of magnitude slower in RNA than DNA, while the refolding dynamics of both sequences required similar timescales. Both melting and refolding followed Arrhenius behaviour, though refolding was characterised by a negative activation energy, consistent with the complex energy landscape of folding initiation.

Placing a single AU pair at key points in the stem showed that RNA sequences begin melting from the loop while DNA hairpins begin melting from the terminal end of the stem. We thus conclude that conformational changes of analogous pairs of RNA and DNA tetraloops proceed by different mechanisms.

References:
J. Phys. Chem. Lett. 2022, 13, 39, 9171–9176
https://doi.org/10.1021/acs.jpclett.2c02338
J. Phys. Chem. B 2023, 127, 7, 1586–1597
https://doi.org/10.1021/acs.jpcb.2c08709

Contact:
N.T. Hunt
neil.hunt@york.ac.uk

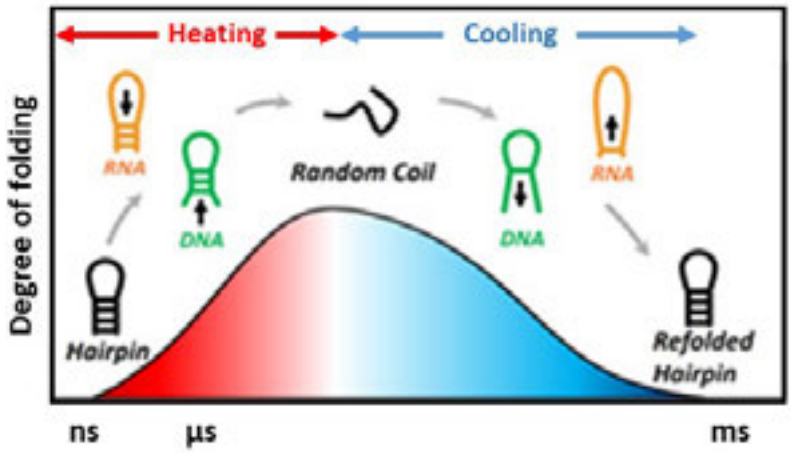

Schematic diagram of the T jump/drop experiment. A ns-duration laser-induced rise in temperature causes hairpin melting followed by fast sample cooling which enables measurement of refolding dynamics.

A comprehensive understanding of carbon–carbon bond formation by alkyne migratory insertion into manganacycles

L.A. Hammarback, J.B. Eastwood, T.J. Burden, C.J. Pearce, I.J.S. Fairlamb, J.M. Lynam *(Department of Chemistry, University of York, UK)*

I.P. Clark, M. Towrie *(Central Laser Facility, Research Complex at Harwell, STFC Rutherford Appleton Laboratory, Harwell Campus, Didcot, UK)*
A. Robinson *(Syngenta Crop Protection AG, Münchwilen, Switzerland)*

Migratory insertion (MI) is one of the most important processes underpinning the transition metal-catalysed formation of C–C and C–X bonds. In this work, a comprehensive model of MI is presented, based on the direct observation of the states involved in the coupling of alkynes with cyclometallated ligands, augmented with insight from computational chemistry.

Time-resolved spectroscopy demonstrates that photolysis of complexes $[Mn(C^N)(CO)_4]$ (C^N = cyclometalated ligand) results in ultra-fast dissociation of a CO ligand. Performing the experiment in a toluene solution of an alkyne results in the initial formation of a solvent complex *fac*-$[Mn(C^N)(toluene)(CO)_3]$. Solvent substitution gives an η^2-alkyne complex fac-$[Mn(C^N)(\eta^2\text{-}R^1C_2R^2)(CO)_3]$ which undergoes MI of the unsaturated ligand into the Mn–C bond. These data allowed for the dependence of second order rate constants for solvent substitution and first order rate constants for C–C bond formation to be determined.

A systematic investigation into the influence of the alkyne and C^N ligand on this process is reported.

The experimental data enabled the development of a computational model for the MI reaction which demonstrated that a synergic interaction between the metal and the nascent C–C bond controls both the rate and regiochemical outcome of the reaction. The time-resolved spectroscopic method enabled the observation of a multistep reaction occurring over 8 orders of magnitude in time, including the formation of solvent complexes, ligand substitution and two sequential C–C bond formation steps.

Contact:
I.J.S. Fairlamb
ian.fairlamb@york.ac.uk

J.M. Lynam
jason.lynam@york.ac.uk

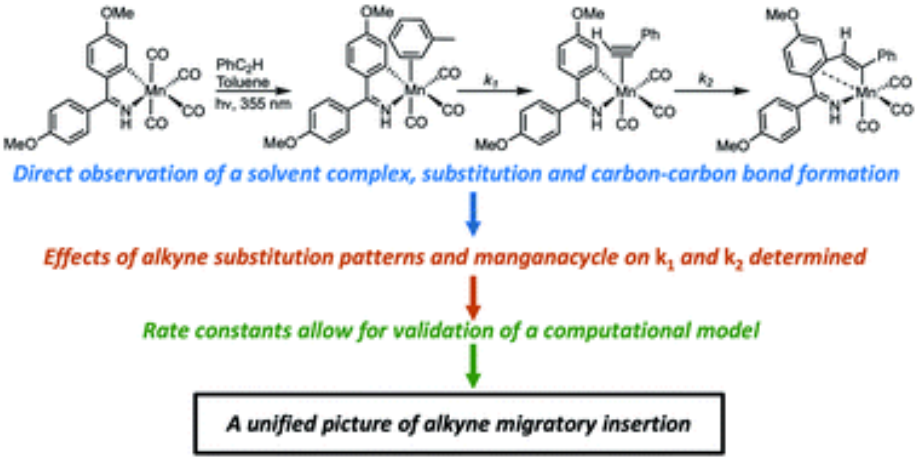

The Influence of the Epigenetic Base 5-methly-cytosine on DNA Excited State Dynamics

M. Stitch, S.J. Quinn *(School of Chemistry, University College Dublin, Ireland)*

M. Towrie, A.W. Parker *(Central Laser Facility, Research Complex at Harwell, STFC Rutherford Appleton Laboratory, Harwell Campus, Didcot, UK)*

The photochemistry of DNA has been exhaustively studied due to its importance in skin cancer, the most common form of cancer (40% of cases globally). However, photochemical studies on sequences containing epigenetic bases[1] have yet to be fully explored. This is remarkable as, for example, modified cytosine in the form of methylated-cytosine (5mC) may be called the fifth base of human DNA, constituting approximately 1% of the bases in mammalian genomes. We apply ultrafast time-resolved infrared spectroscopy to investigate photochemical differences between cytosine and its epigenetic form 5-methyl cytosine, as well as within a model DNA duplex sequence. We identify both similarities and subtle differences between the two bases in terms of their photochemistry.

1 Bases that have slightly different chemical structure but remain biologically competent and able to perturb cell function, for example leading to the onset of cancer.

Contact:
A.W. Parker
tony.parker@stfc.ac.uk

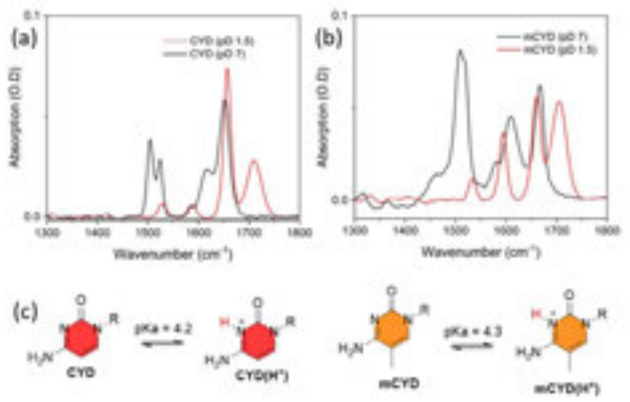

Figure 1: FTIR absorbance spectra of (a) cytidine, b) 5-methyl-cytidine (mCYD) recorded in D_2O buffer, c) structures of epigenetic derivatives and reported pKa values.

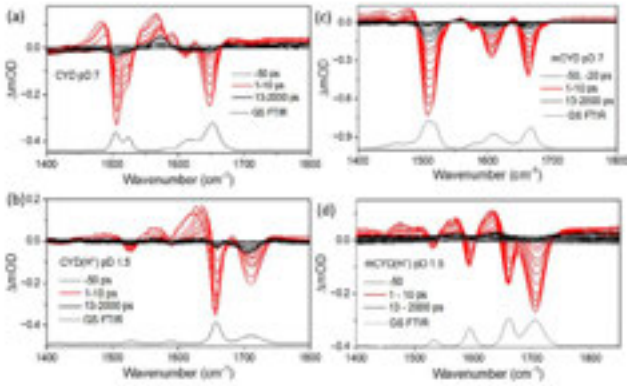

Figure 2: TRIR difference spectra of 10 mM of CYD (a) and (b) and mCYD (c) & (d) in 100 mM K phosphate in D_2O at pD 7 and pD 1.5 (λ_{ex}= 265 nm, 2 kHz,150 fs). Removal of 2000 ps delay subtracted, to remove baseline drift associated with hot D_2O.

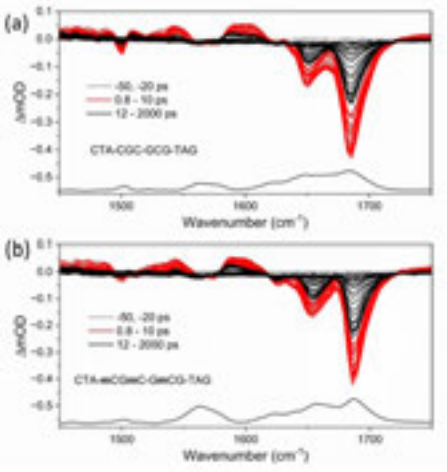

Figure 3: TRIR difference spectra of 10 mM of (a) CTACGCGCGTAG and (b): CTAmCGmCGmCGTAG in 50 mM K phosphate, pD 7, in D_2O (λ_{ex}= 285 nm, 2 kHz,150 fs).

G-Quadruplex Binding of an enantiomeric Osmium Polypyridyl Probe Revealed by Time-Resolved Infrared and NMR Solution Studies

M. Stitch, S.J. Quinn *(School of Chemistry, University College Dublin, Ireland)*
M. Towrie *(Central Laser Facility, Research Complex at Harwell, STFC Rutherford Appleton Laboratory, Harwell Campus, Didcot, UK)*

K. Peterková, P. Podbevšek, J. Plavec *(Slovenian NMR Center, National Institute of Chemistry, Ljubljana, Slovenia)*
R.Z. Boota, P.A. Scattergood, P.I.P. Elliott *(Department of Chemical Sciences, University of Huddersfield, UK)*

Quadruplex DNA structures are important diagnostic and therapeutic targets due to their role in gene regulation, epigenetic processes and their overexpression in oncogenes. These structures adopt various folded topologies that present multiple binding sites. This study reports on the ability of time-resolved infrared spectroscopy (TRIR) to provide information on the binding environment of a NIR emitting polypyridyl osmium complex when bound to two biologically relevant quadruplex structures, human telomere (hTel) and cMYC form.

Visible excitation of the probe reveals the identity of nucleobases in the binding site. In the case of the cMYC structure binding is exclusively through stacking to guanines whose bleach carbonyl bands appear in the TRIR, while in the case of the hTel form the contributions of the thymine and adenine bleaches indicate additional loop interactions. These results are supported by complementary NMR studies and indicates the role that TRIR can play in developing new DNA probes.

Contact:
S.J. Quinn
susan.quinn@ucd.ie

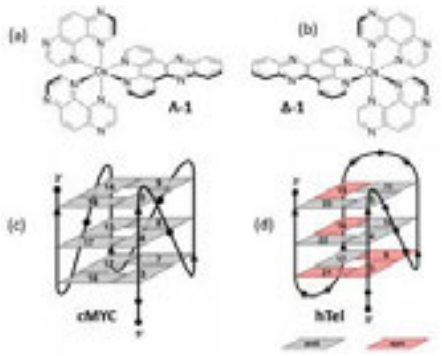

*Figure 1: Molecular structures of probe **1** and schematic representation of (a) **cMYC** and (b) **hTel G4** structures.*

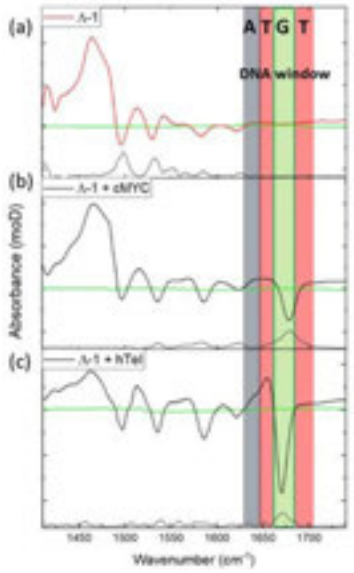

*Figure 2: TRIR difference spectra recorded at 50 ps of (a) 0.4 mM of **1** and (b) in the presence of 0.4 mM of **cMYC**, (c) in the presence of 0.4 mM of **hTel** in 25 mM K phosphate and 70 mM KCl, pH 7, 50 ps after ex l_{ex} = 400 nm, 2 kHz,150 fs).*

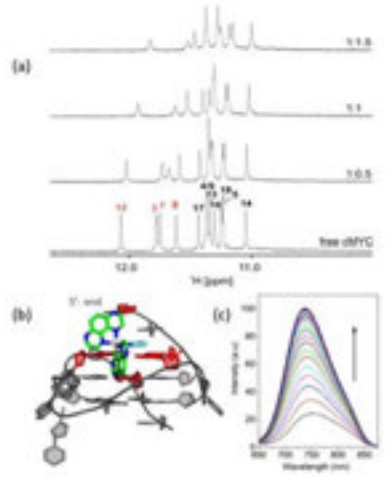

*Figure 3: (a) ^{1}H NMR spectra of the **cMYC**, with increasing [Λ-**1**] molar equivalents with 70 mM KCl, 25 mM K-phosphate buffer, pH 7, 298 K, in 90% H_2O and 10% D_2O. (b) Modelling of Λ-**1** with the **cMYC** structure (PDB ID: 2LBY), nucleotides interaction highlighted in red. (c) Change in the emission of Λ-**1** in the presence of increasing [**cMYC**].*

Artemis Operations Report

R.T. Chapman and E. Springate Central Laser Facility, Research Complex at Harwell, STFC Rutherford Appleton Laboratory, Harwell Campus, Didcot, UK

Introduction

This was the first year of Artemis returning to operations, although the effects of the COVID pandemic meant that the upgrade project was continuing in parallel.

The year started with alignment and testing of the high harmonic generation (HHG) beamline for the 1 kHz laser system. Changes made to the beamline during the upgrade project meant that the conditions for HHG had to be optimised for the new geometry. The mirror used for alignment after the monochromator was motorised, along with the pump-probe alignment mirror in the toroidal mirror chamber. The design changes, coupled with the replacement of the optics in the monochromator, improved the throughput of the beamline by a factor of ten.

The engineering work for the upgrade project was completed at the end of the summer, and the lab was officially opened by Professor John Collier, Director of the CLF, in September.

The first experiment of the year was a novel type of experiment for Artemis: molecular-frame photo-angular distributions. This was a challenging experiment that required the laser system to be running with high stability to get three beams on target.

The autumn provided the first opportunity to welcome back laser service engineers. This meant an extended period of both installing the new 100 kHz system, making it ready for site acceptance tests, as well as servicing the 1 kHz system to optimise its performance. The site acceptance tests were completed successfully at the end of November.

Three further experiments were carried out at the end of 2021, including a commissioning experiment using the AMO chamber to look at roaming dynamics in acetaldehyde, a materials experiment on the 1 kHz beamline, and a collaborative experiment with Ultra using the 100 kHz system for a Kerr Gated Raman proof-of-principle experiment. In the New Year, Artemis undertook another novel experiment, using the hollow fibre compressor for generating high harmonics in solids.

A safety shutdown followed, where improvements were made to the gas handling systems in the lab, along with some procedural changes. The year concluded with the 1 kHz lab open for user experiments, commissioning of the XUV beamline in the 100 kHz lab in preparation for upcoming materials science experiments, and the two laser systems running at specification.

Table 1: Artemis operations by week in 2021/22.

Week beginning	Activity
05/04/2021	1 kHz beamline installation and testing
12/04/2021	
19/04/2021	
26/04/2021	
03/05/2021	
10/05/2021	
17/05/2021	
24/05/2021	Thompson - 20120006
31/05/2021	
07/06/2021	
14/06/2021	
21/06/2021	
28/06/2021	
05/07/2021	Laser Maintenance
12/07/2021	
19/07/2021	Thompson - 20120006
26/07/2021	Interlock Upgrade
02/08/2021	
09/08/2021	
16/08/2021	Laser Maintenance
23/08/2021	
30/08/2021	Thompson - 20120006
06/09/2021	
13/09/2021	Flatfield Spectrometer Installation
20/09/2021	Laser Install & Servicing
27/09/2021	
04/10/2021	
11/10/2021	
18/10/2021	
25/10/2021	
01/11/2021	Da Como - 20120002
08/11/2021	
15/11/2021	
22/11/2021	Laser Site Acceptance Tests
29/11/2021	Laser Site Acceptance Tests / AMO Commissioning
06/12/2021	AMO Commissioning
13/12/2021	
20/12/2021	Maintenance Week
27/12/2021	Christmas Shutdown
03/01/2022	Maintenance Week
10/01/2022	Laser Service
17/01/2022	Matthews - 20120009
24/01/2022	
31/01/2022	
07/02/2022	Safety System Upgrades
14/02/2022	
21/02/2022	
28/02/2022	
07/03/2022	
14/03/2022	
21/03/2022	Chamber Changeover and setup
28/03/2022	

Contact:
R. Chapman
richard.chapman@stfc.ac.uk

Gemini Operational Statistics

S. Hawkes

Central Laser Facility, STFC Rutherford Appleton Laboratory, Harwell Campus, Didcot, UK

During the reporting year, April 21 – April 22, a total of six complete experiments were delivered in the Astra-Gemini Target Area and three experiments in TA2. In total 33 high power laser experimental weeks were delivered to the Gemini Target Area and 23 weeks to TA2. The delivered Gemini schedule is presented in Figure 1.

The availability of the Gemini laser system (delivery to the Gemini Target Area) was 82% during normal working hours, rising to 146% with time made up from running outside of normal working hours. The reliability of the Gemini laser was 88%. An individual breakdown of the availability and reliability for these TA3 experiments conducted is presented in Figure 2.

TA2 availability was 89% during normal working hours, rising to 125% with time made up outside of normal working hours. The reliability of the laser delivery to TA2 was 92%. An individual breakdown of the availability and reliability for these TA2 experiments conducted is presented in Figure 3.

The high levels of total availability were made possible by the continued unique operational model employed on Gemini, which involves running the laser late into the evening. In addition, frequent weekend operational days were made available.

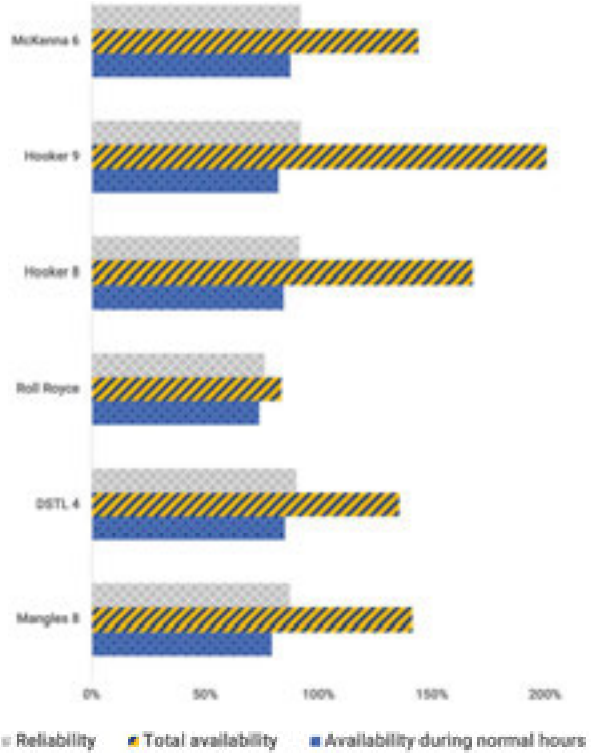

Figure 2: Gemini TA3 2021/22 operational statistics.

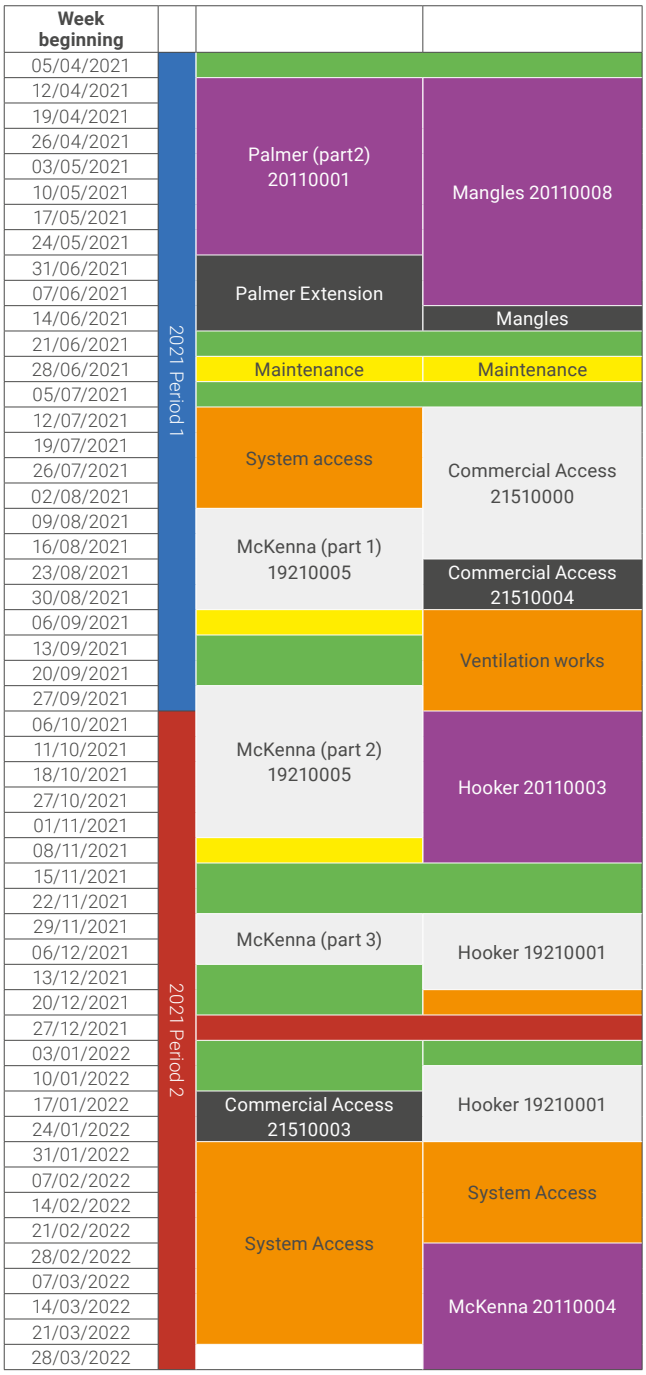

Figure 1: Gemini 2021/22 operational schedule.

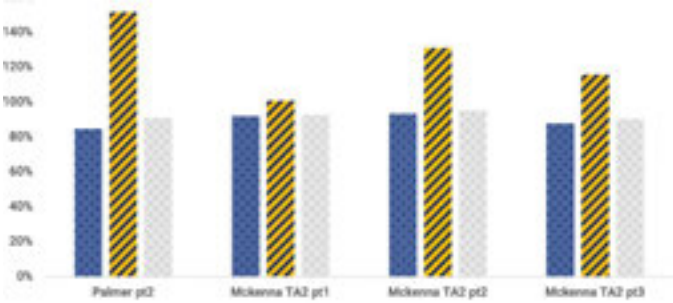

Figure 3: 2021/22 TA2 operational statistics.

Contact: S. Hawkes steve.hawkes@stfc.ac.uk

Octopus and Ultra Operational Statistics

B.C. Bateman, M. Szynkiewicz, S.K. Roberts and D.T. Clarke Central Laser Facility, Research Complex at Harwell, STFC Rutherford Appleton Laboratory, Harwell Campus, Didcot, UK

During the reporting period (April 2021 to March 2022), there were not any calls for applications to access Octopus and Ultra facilities due to the uncertainty surrounding the global Coronavirus pandemic. The statistics reported on this page represent experiments awarded access time in previous calls for access but re-scheduled to take place during the reporting period.

Octopus facility

17 unique User groups performed re-scheduled experiments at the Octopus facility during the reporting period. 21 experiments comprising 58 weeks of access time were delivered to the UK User community throughout the year. In addition, a total of five weeks proof of concept experiments and 2.4 weeks of commercial access were scheduled. Figure 1 shows that Biology and Bio-materials was the most popular experiment subject conducted.

There were a total of 14 formal reviewed publications recorded throughout the year.

Ultra facility

11 unique User groups performed re-scheduled experiments at the Ultra facility during the reporting period. 12 experiments comprising 38 weeks of access time were delivered to the UK User community throughout the year. In addition, three days of proof-of-concept experiments and two weeks of commercial access were scheduled. Figure 2 shows that Chemistry was the most popular experiment subject conducted.

There were a total of 17 formal reviewed publications recorded throughout the year.

Octopus and Ultra availability and user satisfaction feedback

A total of 27 hours downtime was reported over the combined 96 weeks of delivered access during this reporting period. Figure 3 shows an average user satisfaction rating of 93.4% over the five surveyed categories.

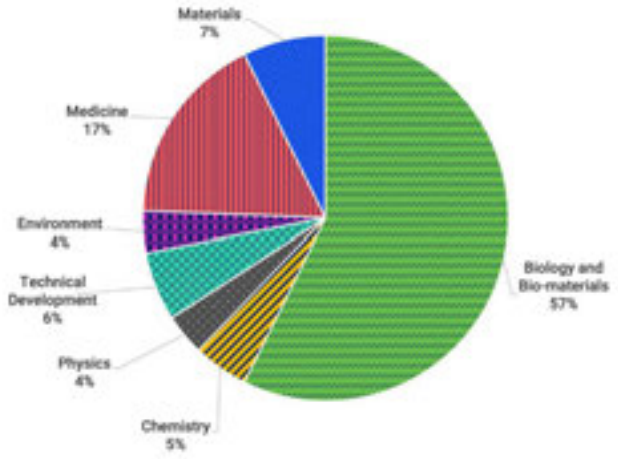

Figure 1: Octopus experiments by subject.

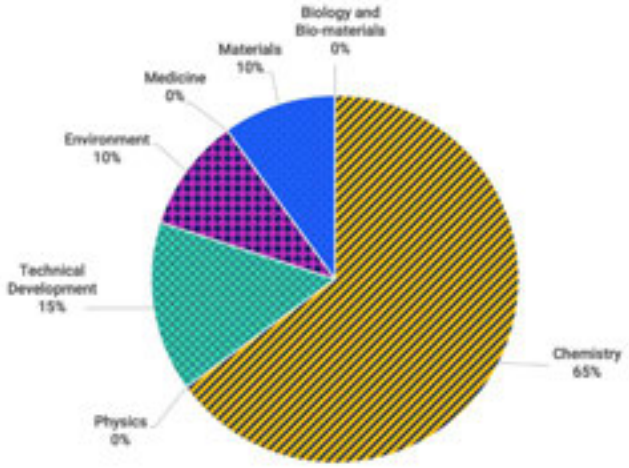

Figure 2: Ultra experiments by subject.

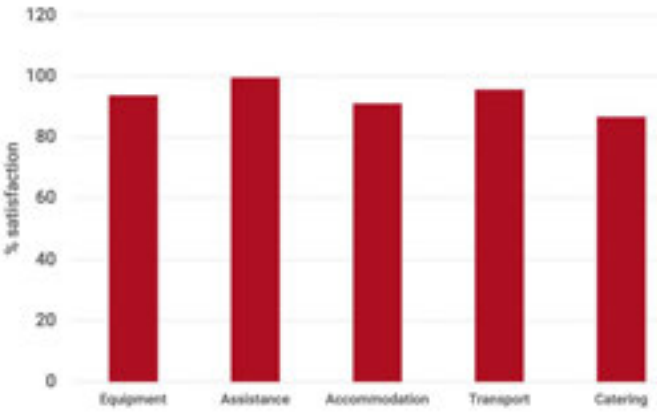

Figure 3: Octopus and Ultra average user satisfaction.

Contact:
D.T. Clarke
dave.clarke@stfc.ac.uk

Target Fabrication Operational Statistics

S. Astbury, D. Haddock, C. Spindloe & M. K. Tolley
Target Fabrication Group, Central Laser Facility, STFC Rutherford Appleton Laboratory, Harwell Campus, Didcot, UK

Introduction

The following report details the operational statistics for the Target Fabrication Group of the Central Laser Facility (CLF) over the reporting period of April 2021 – April 2022. Target supply to the four high-power laser (HPL) experimental areas in the CLF is covered (Gemini TA2, TA3 and Vulcan TAP, TAW).

Over the reporting period a total of 11 HPL experiments were supported, six in Vulcan and five in Gemini. In comparison to the previous reporting period (January 2020 to April 2021), the number of experiment-weeks that the Target Fabrication Group supported was 210% higher (82 weeks compared with 38 weeks in 2020-2021). This increase was primarily due to the removal of restrictions imposed by the government in response to the SARS-CoV-2 pandemic and the return to normal user operations that this allowed. Support is back to the level that was seen in 2018-2019.

The vast majority of the targets captured in this report were used for laser-matter interactions; however, some targets (for example filter packs) are used for diagnostic purposes and often returned post-experiment. Over the last few years, the development of the CLF tape drive systems [1,2] has facilitated the delivery of large numbers of high-repetition rate (HRR) targets, as well as acting as a beam diversion system for imaging experiments. Thus far, the tape drive system has only been employed on the Gemini facility and while the target delivery figures for these areas seem low, it is typical that an entire spool of tape will be captured as a single target on the issue list. Cross-referencing with the eCAT shot data for every experiment in each target area would be necessary to get a true value of target shots on this media. While this is a considerable endeavour to carry out for every experiment that uses HRR media for this report, this data is captured in the section 'High-Repetition Rate Targetry' at the end of this paper. This data skews the reporting numbers and, in the future, for EPAC, the Group will likely have to report on effort/time rather than shot numbers.

Supported Experiments

As documented in previous statistical reports, each target design varies in complexity depending on the area of physics it is designed to investigate, and thus differs from area to area and in some cases shot to shot. Vulcan experiments are typically set up in a single-target shot mode and so tend to comprise single targets on stalks, possibly as part of a cluster of experimental packages and backlighters, and are often more complex in design. Targets for Gemini experiments are more HRR-focused and usually comprise simple foil arrays mounted on a target wheel or, more recently, tape-drive. Many Gemini experiments are gas target led and although the group does not facilitate gas targets directly (they are an engineering group led component), we are involved in characterisation and advanced machining if required.

Table 1 details the supported experiments over the reporting period and their duration, including extension weeks. It is worth noting that two extensive TA2 experiments are covered in this report, which differs from previous years, totalling 23 support weeks, although the level of required support for TA2 experiments from the Target Fabrication Group is usually limited.

Table 1: Experiments supported by the Target Fabrication Group through the 2021/22 reporting period.

Proposal Number	Date/Area/PI	Supported Weeks
20110008	0421 GTA3 Mangles	9
20110001	0521 GTA2 Palmer	12
21510000	0721 GTA3 DSTL	7
19210005	0821 GTA2 Pirozkhov	11
20110003/ 19210001	1021 GTA3 Hooker	8
19210010	0421 TAP McKenna	6
20110006	0421 TAW Armstrong	
18210011	0721 TAP Hicks	6
21210001	1021 TAW Ridgers	5
21210003	0122 TAW Norreys	5
21210004	0322 TAW Kar	5
Total		**82**

Target Complexity and Classification

The varying target types provided by the Target Fabrication Group are categorised as Class 1, 2 and 3 targets, and this offers a method of classifying the complexity and research/planning necessary for experimental delivery. These definitions are somewhat subjective in nature, but are typically classified as follows:

- Class 1: Targets that require fewer specialist resources to manufacture. Materials are typically procured 'off-the-shelf' and minimal specialist equipment is required for assembly. Typical targets include micron-thick foils or alignment wires glued to posts.
- Class 2: Targets that require the use of specialist manufacturing equipment and knowledge, which would be a very involved process for a non-Target Fabrication entity to replicate. Examples include nanometre thin-film and multilayer coatings.
- Class 3: Targets that require long-term R&D projects to establish and perfect, often referred to as "high-specification targets". Such targets include complex 3D assemblies, MEMS-coatings, reduced-density/ foams and multi-step tape targets.

Target Supply

(Note – not including individual tape target shots, where one target can be 1000s of shots)

The 2021-22 supporting period saw a total of 982 targets supplied to the 11 experiments in the CLF, 93% of which to the Vulcan target areas and the remaining 7% to the Gemini areas. There are a few caveats here however in that typically an entire target array (common for Gemini experiments) with anything between 9 and 60 shots worth of targets is captured as a single target in the records register.

Figure 1 right shows the breakdown of target complexity by target area over the 2021-22 reporting period, excluding Gemini TA2 data, which will be discussed later in this report.

It can be seen that, on average, 25-30% of all targets are Class 2 or 3, which require significant development and research time to complete.

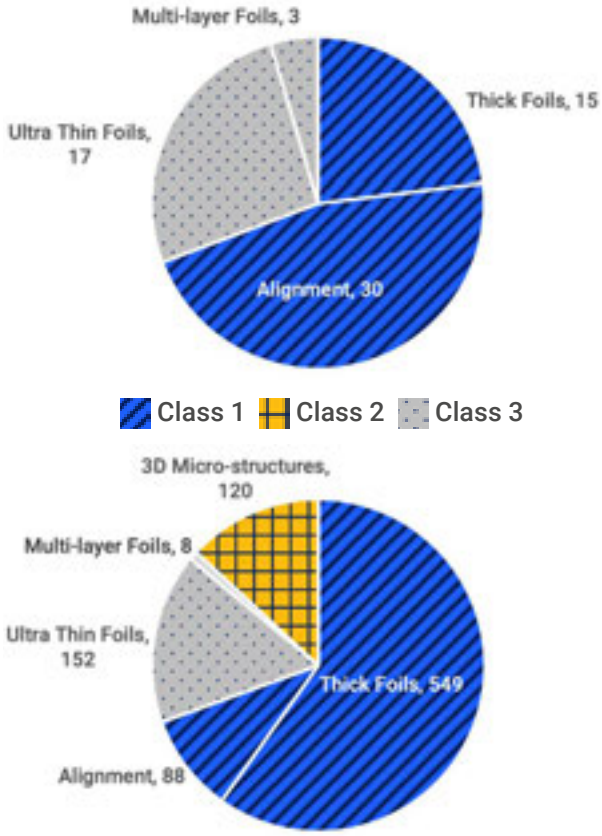

Figure 1: A breakdown of target number and classification in the Gemini (above) and Vulcan (below) target areas over the 2021/22 reporting period.

Target Supply Trends

The Target Fabrication Group keep a record of all targets which have been issued to each experiment in the CLF for referencing and QA purposes and as such are wishing to reinstate ISO9001 quality management system which will be especially important when shot numbers inevitably increase when EPAC is in full operation in the coming years.

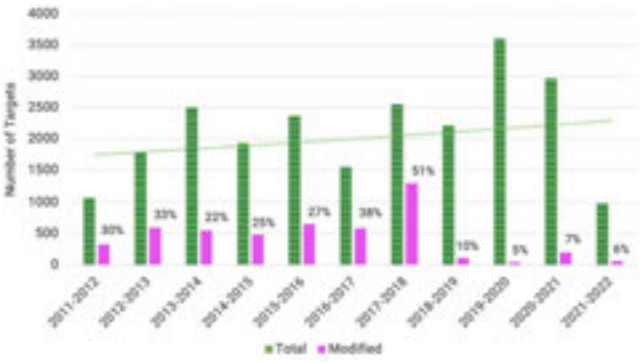

Figure 2: Total targets delivered by reporting periods from 2011 onwards showing the percentage of targets that had to be modified from the initial request.

Figure 2 shows the trend of target delivery over the past 11 reporting periods. This seems to indicate that there has been a significant reduction in target supply over the last year, with a total of 982, compared to 2959 targets supplied in the 2020-2021 period. However, this total omits those that comprised tape targets, highlighted later in this report. In the two previous reporting periods, complex tape targets were counted as individual shots and therefore the numbers are approximately 1500 higher than would have been reported if the tape were taken as a single target (as in this year's case).

Also shown in Figure 2 is the percentage of targets requested that were not on the target list initially requested by the user groups during an experiment. This typically means that the experimental aim during the campaign was re-aligned, or the on-shot data did not agree with the data from the simulations and the target requests were adjusted mid-experiment to achieve the physics results. This demonstrates the key benefit to the users of having an embedded target fabrication facility on site, where technicians can quickly adapt to a change in demand. There has been a significant improvement in reducing this figure over the past few years, which could be attributed to: better simulations and modelling; an increase in target complexity (and thus lack of adaptability mid-experiment); or the experience of the user groups. In total over the 2021-22 operating period, 60 of the 982 targets supplied were modified.

Figure 3 below shows the number of targets which were returned due to being out of specification or surplus to requirements over the reporting periods from 2011-22.

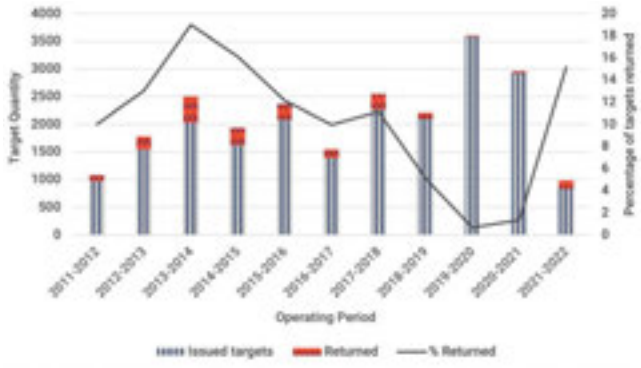

Figure 3: Returned targets vs total targets supplied over the last eleven reporting periods.

As can be seen in Figure 3, a more targets were returned than in the previous few years of experiments. This increase is attributed to the increase in targets delivered to the Vulcan facility which are more complex in nature, as well as the fact that there were comparatively fewer Gemini targets recorded for reasons previously discussed. The HRR nature of Gemini target areas tends to lead to fewer target returns causing a significant skew to the returns figures by area.

High-Repetition Rate Targetry

The Target Fabrication Group has been developing a tape driven target capability over the past few years, which has started to see some use in experimental campaigns in Gemini GTA2 and GTA3 [1,2]. While the Target Fabrication Group does have the technology available to produce multi-layer tape targets, the experiments that used tape targets during 2021-22 comprised simple off-the-shelf tapes and have been captured separately so as to not significantly skew the data. Figure 4 below shows the target output including simple tape media.

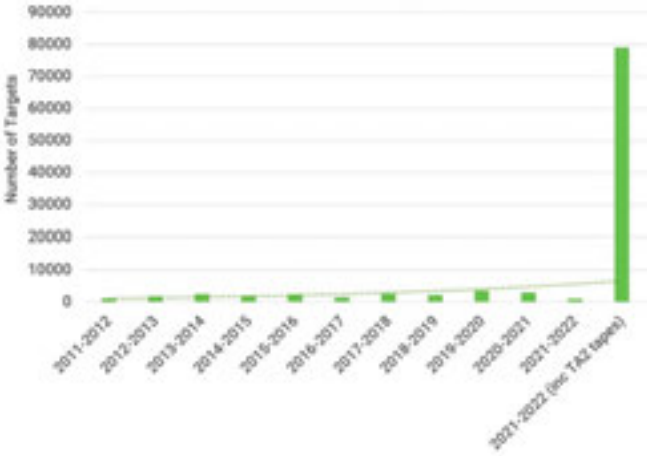

Figure 4: Total targets supplied to each area, including shots on tape media in GTA2 experiments.

As visible in Figure 4, including shots on simple tape media, a total of 79,064 targets were delivered across the CLF in the 2021-22 period. As EPAC will ultimately operate at a similar repetition rate to TA2, this provides a useful metric as to how many targets can be expected on a single experiment (the vast contribution of tape shots came from the 0521 GTA2 Palmer campaign on polyimide, stainless steel and copper).

It is likely that, due to the expected significant rise in target demand, data on HRR systems will be captured separately to that for lower repetition, more complex target types. This data will include tapes and shots on liquid target systems, a further capability which the Target Fabrication Group are developing.

External Contracts

In the reporting period 2021-2022 the operations of Scitech Precision Limited (SPL), Target Fabrication Group's commercial spin out to support the user community on external facilities, recovered for reasons the same as noted above that led to the increase in support for the CLF. The COVID-19 pandemic relaxation allowed many more user facilities to open and start experiments and therefore target requests increased. A total of 32 institutions engaged with SPL over this period for 98 individual contracts to a total value of £267k, which is a significant increase in turnover from the previous COVID-affected years and back to a pre-COVID level. In the reporting period, SPL continued to upgrade its capabilities in laser machining and also developed capabilities to deliver high repetition rate targets by integrating CLF tape systems with its Excimer laser tool.

Summary

Over the 2021-2022 reporting period, the Target Fabrication Group has delivered nearly 1000 targets of varying complexity to the CLF, spread across operational weeks in Vulcan and Gemini that totalled 82 weeks of user support. The majority of these targets were spread across Class 1 targets (approx. 70-75%) and Class 2 and 3 complex targets (approx. 25-30%). It is noted, however, that new target types, such as tape targets, are not now included in the total numbers: with these included, the shot numbers would have been nearly two orders of magnitude higher.

It is also noted that the target trends are moving towards large numbers of tape-produced or thin foil array targets for Gemini, and this trend will continue as EPAC-related experiments come online. The Group is investing significantly in development of technologies and capabilities to meet this demand.

References

1. *S. Astbury, W. Robins, C. Spindloe & M. Tolley, "Progression of a tape-drive targetry solution for high rep-rate HPL experiments within the CLF", CLF Annual Report 2018-2019*
2. *W. Robins, S. Astbury, C. Spindloe & M. Tolley, "Experimental Testing and Fielding of the CLF Precision Tape Drive in the Gemini Target Area", CLF Annual Report 2020-2021*

Contact:
S. Astbury
sam.astbury@stfc.ac.uk

Vulcan Operational Statistics

S.E.J. Chapman, J. Morse, P. Oliveira

Central Laser Facility, STFC Rutherford Appleton Laboratory, Harwell Campus, Didcot, UK

Introduction

Vulcan has completed another active experimental year (April 2021 - March 2022), with 35 full experimental weeks allocated between Target Areas West (TAW) and Petawatt (TAP). Overall the laser statistics show an improved operational standard, with an overall reliability of 88%.

Table 1 shows the operational schedule and statistics for this period. Information on the number of shots, energy-on-target success rate and availability hours are also provided in the table.

PERIOD	TAW	TAP
2021		
26 April – 11 Jun		P McKenna *Optimisation of a hybrid ion acceleration mechanism towards a stable, high-energy ion source* (Shots 71, Failed 11, Reliability 84.5%) (Availability 53.2%, w extra hours 92.9%) (5 weeks + extra 1 week) 19210010
17 May – 09 Jul	C Armstrong *Monoenergetic and micron-scale source size neutron beam generation* (Shots 95, Failed 28, Reliability 70.5%) (Availability 75.8%, w extra hours 148.0%) (5 weeks + extra 3 weeks) 20110006	
05 Jul – 13 Aug		G Hicks *Ion acceleration from optically shaped gas-jets* (Shots 70, Failed 8, Reliability 88.6%) (Availability 77%, w extra hours 97.1%) (5 weeks + extra 1 week) 18210011
01 Nov – 15 Dec	C Ridgers *Observing kinetic effects on the Biermann battery* (Shots 72, Failed 17, Reliability 76.4%) (Availability 81.6%, w extra hours 119.4%) (5 weeks) 21210001	
2022		
17 Jan – 23 Feb	P Norreys *Measuring the equation of state of CH foam using VISAR and SOP for low convergence ratio ICF capsule studies* (Shots 86, Failed 3, Reliability 96.5%) (Availability 87.9%, w extra hours 107.9%) (5 weeks) 21210003	
03 Mar – 10 Apr	S Kar *Ultra-short, beamed source of keV-MeV neutrons* (Shots 210, Failed 6, Reliability 97.1%) (Availability 88.1%, w extra hours 112.1%) (5 weeks) 21210004	

(Total shots fired, failed shots, reliability)
(Availability normal, additional hours)

Table 1: Experimental schedule for the period April 2021 – March 2021.

Some points to note are that TAW operations had to be interrupted for beam stability and defocus investigations between August and October. TAP saw similar disruption between August and March due to floor work and chamber installation.

In Table 1, the first set of numbers in parentheses indicates the total number of full energy laser shots delivered to target, followed by the number of these that failed and the percentage of successful shots. The second set of numbers shows the availability of the laser to target areas during normal operating hours, along with operations outside these hours.

The total number of full disc amplifier shots that have been fired to target this year is 604. Table 2 shows how this figure compares with that for the five previous years. 73 shots failed to meet user requirements. The overall shot success rate to target for the year is 88%, compared to 90%, 86%, 81%, 84% and 80% in the previous five years. Figure 1 shows the reliability of the Vulcan laser to all target areas over the past six years.

Year	No of shots	Failed shots	Reliability
16 – 17	948	93	90%
17 – 18	934	132	86%
18 – 19	607	113	81%
19 – 20	653	102	84%
20 – 21	325	64	80%
21 – 22	604	73	88%

Table 2: Shot totals and proportion of failed shots for the past six years.

Compared with 2020-21, the shot reliability to TAW is up 16% to 88%, while the shot reliability to TAP is down 7% to 87%.

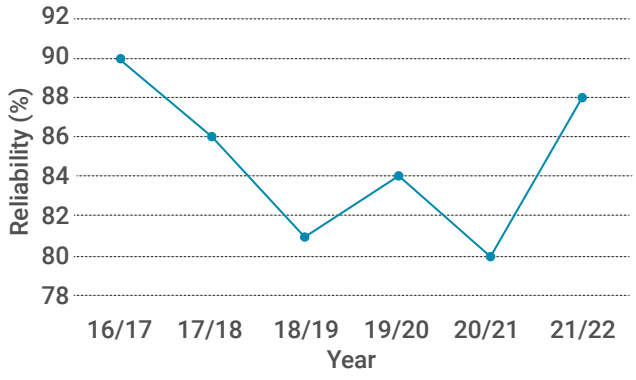

Figure 1: All areas shot reliability for each year 2016/17 to 2021/22.

Analysis of the failure modes reveals that the overriding causes of failed shots are beam alignment, high voltage related issues (especially its interference in the trigger system), and optical damage in the OPCPA system (TAP only). In order to mitigate the first two causes, several measures were implemented during the shutdown between the Armstrong and Ridgers experiments. The oscillator was moved in order to decrease the beam paths and get rid of the high voltage influence on the trigger system, and enclosures and imaging were introduced where possible. New diagnostics were added for the timing system and astigmatism correctors were introduced. These measures collectively resulted in an increase in the reliability of Vulcan TAW from 70.5% to 97.1%.

These modifications were carried out in conjunction with defocus evaluations, some of which will be published, and a realignment of the entire CPA system, stretchers and compressors. This work added to the time gap between the experiments.

There is a requirement which was originally instigated for the EPSRC FAA that the laser system be available from 09:00 to 17:00 hours, Monday to Thursday, and from 09:00 to 16:00 hours on Fridays, during the five week periods of experimental data collection (a total of 195 hours over the five week experimental period). The laser has not always met the start-up target of 9:00 am but it has been common practice to operate the laser well beyond the standard contracted finish time on several days during the week. In addition, the introduction of early start times on some experiments continues to lead to improvements in availability.

On average, Vulcan has been available for each experiment to target areas for 77.3% of the time during contracted hours, compared with 71.2% for the previous year. The overall availability to all target areas has decreased slightly to 112.9% compared with 124.1% in 2020-21. The time that the laser is unavailable to users is primarily the time taken for beam alignment at the start of the day.

Contact:
S.E.J. Chapman
sonya.chapman@stfc.ac.uk

Publications

Journal Papers

ARTEMIS

R Krause, M Chávez-Cervantes, S Aeschlimann, S Forti, F Fabbri, A Rossi, C Coletti, C Cacho, Y Zhang, PE Majchrzak, RT Chapman, E Springate, I Gierz

Ultrafast Charge Separation in Bilayer WS_2/Graphene Heterostructure Revealed by Time- and Angle-Resolved Photoemission Spectroscopy

FRONTIERS IN PHYSICS, 9, 668149 (2021)

P Majchrzak, K Volckaert, AG Čabo, D Biswas, M Bianchi, SK Mahatha, M Dendzik, F Andreatta, SS Grønborg, I Marković, JM Riley, JC Johannsen, D Lizzit, L Bignardi, S Lizzit, C Cacho, O Alexander, D Matselyukh, AS Wyatt, RT Chapman, E Springate, JV Lauritsen, PD King, CE Sanders, JA Miwa, P Hofmann, S Ulstrup

Spectroscopic view of ultrafast charge carrier dynamics in single- and bilayer transition metal dichalcogenide semiconductors

JOURNAL OF ELECTRON SPECTROSCOPY AND RELATED PHENOMENA, 250, 147093 (2021)

B Downes-Ward, EM Warne, J Woodhouse, MA Parkes, E Springate, PAJ Pearcy, Y Zhang, G Karras, AS Wyatt, RT Chapman, RS Minns

Photodissociation dynamics of methyl iodide across the A-band probed by femtosecond extreme ultraviolet photoelectron spectroscopy

JOURNAL OF PHYSICS B: ATOMIC, MOLECULAR AND OPTICAL PHYSICS, 54, 134003 (2021)

P Majchrzak, S Pakdel, D Biswas, AJH Jones, K Volckaert, I Marković, F Andreatta, R Sankar, C Jozwiak, E Rotenberg, A Bostwick, CE Sanders, Y Zhang, G Karras, RT Chapman, A Wyatt, E Springate, JA Miwa, P Hofmann, PDC King, N Lanatà, YJ Chang, S Ulstrup

Switching of the electron-phonon interaction in 1T-VSe_2 assisted by hot carriers

PHYSICAL REVIEW B, 103, L241108 (2021)

CALTA

P Shukla, X Shen, R Allott, K Ertel, S Robertson, R Crookes, H Wu, A Zammit, P Swanson, M Fitzpatrick

Response of silicon nitride ceramics subject to laser shock treatment

CERAMICS INTERNATIONAL, 47, 34538-34553 (2021)

K Kato, S Banerjee, N Umemura

Phase-matching properties of $AgGa_{0.86}In_{0.14}S_2$ for three-wave interactions in the 0.615-10.5910 μm spectral range

OPTICAL MATERIALS EXPRESS, 11, 2800-2805 (2021)

JP Phillips, S Banerjee, P Mason, J Smith, J Spear, M De Vido, K Ertel, T Butcher, G Quinn, D Clarke, C Edwards, C Hernandez-Gomez, J Collier

Second and third harmonic conversion of a kilowatt average power, 100-J-level diode pumped Yb:YAG laser in large aperture LBO

OPTICS LETTERS, 46, 1808-1811 (2021)

M Divoky, J Pilar, M Hanus, P Navratil, O Denk, P Severova, P Mason, T Butcher, S Banerjee, M De Vido, C Edwards, J Collier, M Smrz, T Mocek

150 J DPSSL operating at 1.5 kW level

OPTICS LETTERS, 46, 5771-5773 (2021)

GEMINI

A McIlvenny, D Doria, L Romagnani, H Ahmed, N Booth, E Ditter, O Ettlinger, G Hicks, P Martin, G Scott, S Williamson, A Macchi, P McKenna, Z Najmudin, D Neely, S Kar, M Borghesi

Selective Ion Acceleration by Intense Radiation Pressure

PHYSICAL REVIEW LETTERS, 127, 194801 (2021)

W Sun, DR Symes, CM Brenner, M Böhnel, S Brown, MN Mavrogordato, I Sinclair, M Salamon

Review of high energy x-ray computed tomography for non-destructive dimensional metrology of large metallic advanced manufactured components

REPORTS ON PROGRESS IN PHYSICS, 85, 16102 (2022)

B Kettle, D Hollatz, E Gerstmayr, GM Samarin, A Alejo, S Astbury, CD Baird, S Bohlen, M Campbell, C Colgan, D Dannheim, C Gregory, H Harsh, P Hatfield, J Hinojosa, Y Katzir, J Morton, C Murphy, A Nurnberg, J Osterhoff, G Perez, K Poder, PP Rajeev, C Roedel, F Roeder, FC Salgado, G Sarri, A Seidel, S Spannagel, C Spindloe, S Steinke, M Streeter, AGR Thomas, C Underwood, R Watt, M Zepf, SJ Rose, S Mangles

A laser-plasma platform for photon-photon physics: the two photon Breit-Wheeler process

NEW JOURNAL OF PHYSICS, 23, 115006 (2021)

L Bradley, MJV Streeter, C Murphy, C Arran, TG Blackburn, M Galletti, S Mangles, CP Ridgers

Effect of laser temporal intensity skew on enhancing pair production in laser - electron-beam collisions

NEW JOURNAL OF PHYSICS, 23, 95004 (2021)

A Maitrallain, E Brunetti, M Streeter, B Kettle, R Spesyvtsev, G Vieux, M Shazhad, B Ersfeld, S Yoffe, A Kornaszewski, O Finlay, Y Ma, F Albert, N Bourgeois, SJ Dann, N Lemos, S Cipiccia, JM Cole, I Gallardo González, L Willingale, A Higginbotham, A Hussein, M Šmid, K Falk, K Krushelnick, NC Lopes, E Gerstmayr, C Lumsdon, O Lundh, S Mangles, Z Najmudin, PP Rajeev, D Symes, AGR Thomas, DA Jaroszynski

Parametric study of high-energy ring-shaped electron beams from a laser wakefield accelerator

NEW JOURNAL OF PHYSICS, 24, 13017 (2021)

GG Scott, GFH Indorf, MA Ennen, P Forestier-Colleoni, SJ Hawkes, L Scaife, M Sedov, DR Symes, C Thornton, F Beg, T Ma, P McKenna, AA Andreev, U Teubner, D Neely

Kinematics of femtosecond laser-generated plasma expansion: Determination of sub-micron density gradient and collisionality evolution of over-critical laser plasmas

PHYSICS OF PLASMAS, 28, 93109 (2021)

GFH Indorf, GG Scott, MA Ennen, P Forestier-Colleoni, D Haddock, SJ Hawkes, L Scaife, N Bourgeois, D Symes, C Thornton, A Andreev, U Teubner, D Neely

Investigation of the ejected mass during high-intensity laser solid interaction for improved plasma mirror generation

PLASMA PHYSICS AND CONTROLLED FUSION, 64, 34004 (2022)

HSP Thomas, RM Deas, LN Kirkham, PM Dodd, E Zemaityte, AD Hillier, D Neely

Response of nuclear track detector CR-39 to low energy muons

PLASMA PHYSICS AND CONTROLLED FUSION, 63, 124001 (2021)

A Prasselsperger, M Coughlan, N Breslin, M Yeung, C Arthur, H Donnelly, S White, M Afshari, M Speicher, R Yang, B Villagomez-Bernabe, F Currell, J Schreiber, B Dromey

Real-Time Electron Solvation Induced by Bursts of Laser-Accelerated Protons in Liquid Water

PHYSICAL REVIEW LETTERS, 127, 186001 (2021)

LASER DEVELOPMENTS

M Galimberti, FG Bisesto, M Galletti

Innovative single-shot 2D pulse front tilt diagnostic

HIGH POWER LASER SCIENCE AND ENGINEERING, 9, e16 (2021)

CN Danson, M White, JRM Barr, T Bett, P Blyth, D Bowley, C Brenner, RJ Collins, N Croxford, AEB Dangor, L Devereux, PE Dyer, A Dymoke-Bradshaw, CB Edwards, P Ewart, AI Ferguson, JM Girkin, DR Hall, DC Hanna, W Harris, DI Hillier, CJ Hooker, SM Hooker, N Hopps, J Hull, D Hunt, DA Jaroszynski, M Kempenaars, H Kessler, SPL Knight, S Knight, A Knowles, CLS Lewis, KS Lipton, A Littlechild, J Littlechild, P Maggs, GPA Malcolm, SPD Mangles, W Martin, P McKenna, RO Moore, C Morrison, Z Najmudin, D Neely, GHC New, MJ Norman, T Paine, AW Parker, RR Penman, GJ Pert, C Pietraszewski, A Randewich, NH Rizvi, N Seddon, Z Sheng, D Slater, RA Smith, C Spindloe, R Taylor, G Thomas, JWG Tisch, JS Wark, C Webb, SM Wiggins, D Willford, T Winstone

A history of high-power laser research and development in the United Kingdom

HIGH POWER LASER SCIENCE AND ENGINEERING, 9, e18 (2021)

J McConnell, G Karras, GM Archipovaite

Designing OPAs in the NIR with an all-bulk chirp control

PROCEEDINGS OF SPIE, 11777, 117770G (2021)

Y Hemani, M Galimberti, D Bleiner

EMPULSE: a compact terawatt chirped pulse amplification laser for generating coherent x-rays

PROCEEDINGS OF SPIE, 11886, 1188607 (2021)

PLASMA PHYSICS

R Scott, K Glize, L Antonelli, M Khan, W Theobald, M Wei, R Betti, C Stoeckl, A Seaton, T Arber, D Barlow, T Goffrey, K Bennett, W Garbett, S Atzeni, A Casner, D Batani, C Li, N Woolsey

Shock Ignition Laser-Plasma Interactions in Ignition-Scale Plasmas

PHYSICAL REVIEW LETTERS, 127, 65001 (2021)

S Zhang, J Li, CM Krauland, FN Beg, S Muller, W Theobald, J Palastro, T Filkins, D Turnbull, D Haberberger, C Ren, R Betti, C Stoeckl, EM Campbell, J Trela, D Batani, RHH Scott, MS Wei

Pump-depletion dynamics and saturation of stimulated Brillouin scattering in shock ignition relevant experiments

PHYSICAL REVIEW E, 103, 63208 (2021)

K Jana, AD Lad, D West, W Trickey, C Underwood, YM Ved, APL Robinson, J Pasley, GR Kumar

Femtosecond, two-dimensional spatial Doppler mapping of ultraintense laser-solid target interaction

PHYSICAL REVIEW RESEARCH, 3, 33034 (2021)

S Morris, A Robinson, C Ridgers

Highly efficient conversion of laser energy to hard x-rays in high-intensity laser-solid simulations

PHYSICS OF PLASMAS, 28, 103304 (2021)

A Tentori, A Colaitis, W Theobald, A Casner, D Raffestin, A Ruocco, J Trela, E Le Bel, K Anderson, M Wei, B Henderson, J Peebles, R Scott, S Baton, SA Pikuz, R Betti, M Khan, N Woolsey, S Zhang, D Batani

Experimental characterization of hot-electron emission and shock dynamics in the context of the shock ignition approach to inertial confinement fusion

PHYSICS OF PLASMAS, 28, 103302 (2021)

APL Robinson

A critical analysis of the 'ponderomotive snowplow' concept in direct laser acceleration of electrons

PLASMA PHYSICS AND CONTROLLED FUSION, 63, 064003 (2021)

RMGM Trines, APL Robinson, JR Wilkinson, JN Kirk, DS Hills, RM Deas, S Morris, T Goffrey, K Bennett, TD Arber

Laser-assisted propagation of a relativistic electron bunch in air

PLASMA PHYSICS AND CONTROLLED FUSION, 63, 84009 (2021)

A Ruocco, G Duchateau, VT Tikhonchuk

Self-focusing of a spatially modulated beam within the paraxial complex geometrical optics framework in low-density plasmas

PLASMA PHYSICS AND CONTROLLED FUSION, 63, 125019 (2021)

EP Alves, RMGM Trines, KA Humphrey, R Bingham, RA Cairns, F Fiúza, RA Fonseca, LO Silva

A robust plasma-based laser amplifier via stimulated Brillouin scattering

PLASMA PHYSICS AND CONTROLLED FUSION, 63, 114004 (2021)

B Brandão, JE Santos, RMGM Trines, R Bingham, LO Silva

Bandwidth effects in stimulated Brillouin scattering driven by partially incoherent light

PLASMA PHYSICS AND CONTROLLED FUSION, 63, 94003 (2021)

DR Blackman, A Adak, PK Singh, AD Lad, G Chatterjee, CP Ridgers, D Del Sorbo, RMGM Trines, APL Robinson, W Nazarov, G Ravindra Kumar, J Pasley

Formation and evolution of post-solitons following a high intensity laser-plasma interaction with a low-density foam target

PLASMA PHYSICS AND CONTROLLED FUSION, 63, 74001 (2021)

RMGM Trines, EP Alves, KA Humphrey, R Bingham, RA Cairns, F Fiúza, RA Fonseca, LO Silva

Boosting the performance of Brillouin amplification at sub-quarter-critical densities via reduction of parasitic Raman scattering

PLASMA PHYSICS AND CONTROLLED FUSION, 63, 124003 (2021)

VULCAN

G Cristoforetti, S Hüller, P Koester, L Antonelli, S Atzeni, F Baffigi, D Batani, C Baird, N Booth, M Galimberti, K Glize, A Héron, M Khan, P Loiseau, D Mancelli, M Notley, P Oliveira, O Renner, M Smid, A Schiavi, G Tran, NC Woolsey, LA Gizzi

Observation and modelling of stimulated Raman scattering driven by an optically smoothed laser beam in experimental conditions relevant for shock ignition

HIGH POWER LASER SCIENCE AND ENGINEERING, 9, e60 (2021)

C Hyland, S White, B Kettle, R Irwin, D Bailie, M Yeung, G Williams, R Heathcote, I East, C Spindloe, M Notley, D Riley

Measurements of free-free absorption in warm dense aluminium

PLASMA PHYSICS AND CONTROLLED FUSION, 63, 74003 (2021)

P Bradford, A Dearling, M Ehret, L Antonelli, N Booth, DC Carroll, RJ Clarke, K Glize, R Heathcote, M Khan, JD Moody, S Pikuz, BB Pollock, MP Read, S Ryazantsev, C Spindloe, CP Ridgers, JJ Santos, VT Tikhonchuk, NC Woolsey

Measuring magnetic fields in laser-driven coils with dual-axis proton deflectometry

PLASMA PHYSICS AND CONTROLLED FUSION, 63, 84008 (2021)

A Higginson, R Wilson, J Goodman, M King, RJ Dance, NMH Butler, CD Armstrong, M Notley, DC Carroll, Y Fang, XH Yuan, D Neely, RJ Gray, P McKenna

Influence of target-rear-side short scale length density gradients on laser-driven proton acceleration

PLASMA PHYSICS AND CONTROLLED FUSION, 63, 114001 (2021)

P Chaudhary, DC Gwynne, B Odlozilik, A McMurray, G Milluzzo, C Maiorino, D Doria, H Ahmed, L Romagnani, A Alejo, H Padda, J Green, D Carroll, N Booth, P McKenna, S Kar, G Petringa, R Catalano, FP Cammarata, GAP Cirrone, SJ McMahon, KM Prise, M Borghesi

Development of a portable hypoxia chamber for ultra-high dose rate laser-driven proton radiobiology applications

RADIATION ONCOLOGY, 17, 77 (2022)

CD Armstrong, D Neely, D Kumar, P McKenna, RJ Gray, AS Pirozhkov

Deconvolution of multi-Boltzmann x-ray distribution from linear absorption spectrometer via analytical parameter reduction

REVIEW OF SCIENTIFIC INSTRUMENTS, 92, 113102 (2021)

D Doria, P Martin, H Ahmed, A Alejo, M Cerchez, S Ferguson, J Fernandez-Tobias, JS Green, D Gwynne, F Hanton, J Jarrett, DA Maclellan, A McIlvenny, P McKenna, JA Ruiz, M Swantusch, O Willi, S Zhai, M Borghesi, S Kar

Calibration of BAS-TR image plate response to GeV gold ions

REVIEW OF SCIENTIFIC INSTRUMENTS, 93, 33304 (2022)

R Wilson, M King, NMH Butler, DC Carroll, TP Frazer, MJ Duff, A Higginson, RJ Dance, J Jarrett, ZE Davidson, CD Armstrong, H Liu, SJ Hawkes, RJ Clarke, D Neely, RJ Gray, P McKenna

Influence of spatial-intensity contrast in ultraintense laser-plasma interactions

SCIENTIFIC REPORTS, 12, 1910 (2022)

ULTRA

LA Hammarback, AL Bishop, C Jordan, G Athavan, JB Eastwood, TJ Burden, JTW Bray, F Clarke, A Robinson, J Krieger, A Whitwood, IP Clark, M Towrie, JM Lynam, IJS Fairlamb

Manganese-Mediated C-H Bond Activation of Fluorinated Aromatics and the ortho-Fluorine Effect: Kinetic Analysis by In Situ Infrared Spectroscopic Analysis and Time-Resolved Methods

ACS CATALYSIS, 12, 1532-1544 (2022)

G Ning, P Cui, IV Sazanovich, JT Pegg, Q Zhu, Z Pang, R Wei, M Towrie, KE Jelfs, MA Little, AI Cooper

Organic cage inclusion crystals exhibiting guest-enhanced multiphoton harvesting

CHEM, 7, 3157-3170 (2021)

SV Lepeshkevich, IV Sazanovich, MV Parkhats, SN Gilevich, BM Dzhagarov

Towards understanding non-equivalence of α and β subunits within human hemoglobin in conformational relaxation and molecular oxygen rebinding

CHEMICAL SCIENCE, 12, 7033-7047 (2021)

FA Baptista, D Krizsan, M Stitch, IV Sazanovich, IP Clark, M Towrie, C Long, L Martinez-Fernandez, R Improta, NAP Kane-Maguire, JM Kelly, SJ Quinn

Adenine Radical Cation Formation by a Ligand-Centered Excited State of an Intercalated Chromium Polypyridyl Complex Leads to Enhanced DNA Photo-oxidation

JOURNAL OF THE AMERICAN CHEMICAL SOCIETY, 143, 14766-14779 (2021)

L Lewis-Borrell, M Sneha, IP Clark, V Fasano, A Noble, VK Aggarwal, AJ Orr-Ewing

Direct Observation of Reactive Intermediates by Time-Resolved Spectroscopy Unravels the Mechanism of a Radical-Induced 1,2-Metalate Rearrangement

JOURNAL OF THE AMERICAN CHEMICAL SOCIETY, 143, 17191-17199 (2021)

F Dröge, FF Noakes, SA Archer, S Sreedharan, A Raza, CC Robertson, S MacNeil, JW Haycock, H Carson, AJHM Meijer, CGW Smythe, J Bernardino de la Serna, B Dietzek-Ivanšić, JA Thomas

A Dinuclear Osmium(II) Complex Near-Infrared Nanoscopy Probe for Nuclear DNA

JOURNAL OF THE AMERICAN CHEMICAL SOCIETY, 143, 20442-20453 (2021)

JH van Wonderen, K Adamczyk, X Wu, X Jiang, SEH Piper, CR Hall, MJ Edwards, TA Clarke, H Zhang, LJC Jeuken, IV Sazanovich, M Towrie, J Blumberger, SR Meech, JN Butt

Nanosecond heme-to-heme electron transfer rates in a multiheme cytochrome nanowire reported by a spectrally unique His/Met-ligated heme

PROCEEDINGS OF THE NATIONAL ACADEMY OF SCIENCES USA, 118, e2107939118 (2021)

M Pižl, BM Hunter, IV Sazanovich, M Towrie, HB Gray, S Záliš, A Vlček

Excitation-Wavelength-Dependent Photophysics of d8d8 Di-isocyanide Complexes

INORGANIC CHEMISTRY, 61, 2745-2759 (2021)

AA Seddon, JKG Karlsson, EA Gibson, L O'Reilly, M Kaufmann, JG Vos, MT Pryce

Photoelectrochemical Hydrogen Evolution Using Dye-Sensitised NiO

JOHNSON MATTHEY TECHNOLOGY REVIEW, 66, 21-31 (2021)

P Pospíšil, L Cwiklik, J Sýkora, M Hof, GM Greetham, M Towrie, A Vlček

Solvent-Dependent Excited-State Evolution of Prodan Dyes

JOURNAL OF PHYSICAL CHEMISTRY B, 125, 13858-13867 (2021)

M Sneha, A Bhattacherjee, L Lewis-Borrell, IP Clark, AJ Orr-Ewing

Structure-Dependent Electron Transfer Rates for Dihydrophenazine, Phenoxazine, and Phenothiazine Photoredox Catalysts Employed in Atom Transfer Radical Polymerization

JOURNAL OF PHYSICAL CHEMISTRY B, 125, 7 840-7854 (2021)

VL Piercy, KH Saeed, AW Prentice, G Neri, C Li, AM Gardner, Y Bai, RS Sprick, IV Sazanovich, AI Cooper, MJ Rosseinsky, MA Zwijnenburg, AJ Cowan

Time-Resolved Raman Spectroscopy of Polaron Formation in a Polymer Photocatalyst

JOURNAL OF PHYSICAL CHEMISTRY LETTERS, 12, 10899-10905 (2021)

LM Uriarte, R Vitale, S Niziński, K Hadjidemetriou, N Zala, A Lukacs, GM Greetham, IV Sazanovich, M Weik, C Ruckebusch, SR Meech, M Sliwa

Structural Information about the trans-to-cis Isomerization Mechanism of the Photoswitchable Fluorescent Protein rsEGFP2 Revealed by Multiscale Infrared Transient Absorption

JOURNAL OF PHYSICAL CHEMISTRY LETTERS, 13, 1194-1202 (2022)

J Dale, CP Howe, H Toncrova, R Fritzsch, GM Greetham, IP Clark, M Towrie, AW Parker, TC McLeish, NT Hunt

Combining steady state and temperature jump IR spectroscopy to investigate the allosteric effects of ligand binding to dsDNA

PHYSICAL CHEMISTRY CHEMICAL PHYSICS, 23, 15352-15363 (2021)

B Procacci, SH Rutherford, GM Greetham, M Towrie, AW Parker, CV Robinson, CR Howle, NT Hunt, JA Guicheteau

Sensing of bacterial spores with 2D-IR spectroscopy

PROCEEDINGS OF SPIE, 11749, 117490C (2021)

OCTOPUS

O Morana, JA Nieto-Garai, P Björkholm, J Bernardino de la Serna, O Terrones, A Arboleya, D Ciceri, I Rojo-Bartolomé, CM Blouin, C Lamaze, M Lorizate, F Contreras

Identification of a New Cholesterol-Binding Site within the IFN-γ Receptor that is Required for Signal Transduction

ADVANCED SCIENCE, 9, 2105170 (2022)

G Davies, J Driver, A Ward, L Negahdar, J McGregor

Operando Studies of Aerosol-Assisted Sol-Gel Catalyst Synthesis via Combined Optical Trapping and Raman Spectroscopy

JOURNAL OF PHYSICAL CHEMISTRY C, 125, 22591-22602 (2021)

L Mendonça, A Howe, JB Gilchrist, Y Sheng, D Sun, ML Knight, LC Zanetti-Domingues, B Bateman, A Krebs, L Chen, J Radecke, VD Li, T Ni, I Kounatidis, MA Koronfel, M Szynkiewicz, M Harkiolaki, ML Martin-Fernandez, W James, P Zhang

Correlative multi-scale cryo-imaging unveils SARS-CoV-2 assembly and egress

NATURE COMMUNICATIONS, 12, 4629 (2021)

Y Hari-Gupta, N Fili, Á dos Santos, AW Cook, RE Gough, HCW Reed, L Wang, J Aaron, T Venit, E Wait, A Grosse-Berkenbusch, JCM Gebhardt, P Percipalle, T Chew, M Martin-Fernandez, CP Toseland

Myosin VI regulates the spatial organisation of mammalian transcription initiation

NATURE COMMUNICATIONS, 13, 1346 (2022)

M Lorizate, O Terrones, JA Nieto-Garai, I Rojo-Bartolomé, D Ciceri, O Morana, J Olazar-Intxausti, A Arboleya, A Martin, M Szynkiewicz, M Calleja-Felipe, J Bernardino de la Serna, F Contreras

Super-Resolution Microscopy Using a Bioorthogonal-Based Cholesterol Probe Provides Unprecedented Capabilities for Imaging Nanoscale Lipid Heterogeneity in Living Cells

SMALL METHODS, 5, 2100430 (2021)

G Poologasundarampillai, A Haweet, SN Jayash, G Morgan, JE Moore, A Candeo

Real-time imaging and analysis of cell-hydrogel interplay within an extrusion-bioprinting capillary

BIOPRINTING, 23, e00144 (2021)

ML Martin-Fernandez

Fluorescence Imaging of Epidermal Growth Factor Receptor Tyrosine Kinase Inhibitor Resistance in Non-Small Cell Lung Cancer

CANCERS, 14, 686 (2022)

AC Benniston, D Sirbu, NV Tkachenko, L Zeng, PG Waddell, SW Botchway

Voltage-Induced Fluorescence Lifetime Imaging of a BODIPY Derivative in Giant Unilamellar Vesicles (GUVs) as Neuron Membrane Mimics

CHEMICAL COMMUNICATIONS, 57, 12631-12634 (2021)

DC Green, R Darkins, B Marzec, MA Holden, IJ Ford, SW Botchway, B Kahr, DM Duffy, FC Meldrum

Dichroic Calcite Reveals the Pathway from Additive Binding to Occlusion

CRYSTAL GROWTH & DESIGN, 21, 3746-3755 (2021)

RR Mould, SW Botchway, JRC Parkinson, EL Thomas, GW Guy, JD Bell, AVW Nunn

Cannabidiol Modulates Mitochondrial Redox and Dynamics in MCF7 Cancer Cells: A Study Using Fluorescence Lifetime Imaging Microscopy of NAD(P)H

FRONTIERS IN MOLECULAR BIOSCIENCES, 8, 630107 (2021)

M Claes, JRF Santos, L Masin, L Cools, BM Davis, L Arckens, K Farrow, L De Groef, L Moons

A Fair Assessment of Evaluation Tools for the Murine Microbead Occlusion Model of Glaucoma

INTERNATIONAL JOURNAL OF MOLECULAR SCIENCES, 22, 5633 (2021)

M Bernabé-Rubio, M Bosch-Fortea, MA Alonso, J Bernardino de la Serna

Multi-dimensional and spatiotemporal correlative imaging at the plasma membrane of live cells to determine the continuum nano-to-micro scale lipid adaptation and collective motion

METHODS, 193, 136-147 (2021)

V Kriechbaumer, SW Botchway

Methods for Detection of Protein Interactions with Plasmodesmata-Localized Reticulons

METHODS IN MOLECULAR BIOLOGY, p209-218 (2022)

JF McKenna

Quantifying the Organization and Dynamics of the Plant Plasma Membrane Across Scales Using Light Microscopy

METHODS IN MOLECULAR BIOLOGY, p233-251 (2022)

MR McGrory, RH Shepherd, MD King, N Davidson, FD Pope, IM Watson, RG Grainger, AC Jones, AD Ward

Mie scattering from optically levitated mixed sulfuric acid-silica core-shell aerosols: observation of core-shell morphology for atmospheric science

PHYSICAL CHEMISTRY CHEMICAL PHYSICS, 24, 5813-5822 (2022)

Z Savage, C Duggan, A Toufexi, P Pandey, Y Liang, ME Segretin, LH Yuen, DCA Gaboriau, AY Leary, Y Tumtas, V Khandare, AD Ward, SW Botchway, BC Bateman, I Pan, M Schattat, I Sparkes, TO Bozkurt

Chloroplasts alter their morphology and accumulate at the pathogen interface during infection by Phytophthora infestans

PLANT JOURNAL, 107, 1771-1787 (2021)

Individual contributions and collaborative science

J Dobkowski, M Kijak, S Gawinkowski, E Karpiuk, M Pietrzak, IV Sazanovich, J Waluk

Solving the Puzzle of Unusual Excited-State Proton Transfer in 2,5-Bis(6-methyl-2-benzoxazolyl)phenol

JOURNAL OF PHYSICAL CHEMISTRY A, 126, 1823-1836 (2022)

AD Crawshaw, EV Beale, AJ Warren, A Stallwood, G Duller, J Trincao, G Evans

A Sample Preparation Pipeline for Microcrystals at the VMXm Beamline

JOURNAL OF VISUALIZED EXPERIMENTS, 172, e62306 (2021)

C Ruyer, A Debayle, P Loiseau, PE Masson-Laborde, J Fuchs, M Casanova, JR Marquès, L Romagnani, P Antici, N Bourgeois, M Nakatsutsumi, M Safronova, M Starodubtsev, T Lin

Forward scattering and filamentation of a spatially smoothed laser pulse in the hydrodynamic and kinetic frameworks

PHYSICS OF PLASMAS, 28, 52701 (2021)

P Chaudhary, G Milluzzo, H Ahmed, B Odlozilik, A McMurray, KM Prise, M Borghesi

Radiobiology Experiments with Ultra-high Dose Rate Laser-Driven Protons: Methodology and State-of-the-Art

FRONTIERS IN PHYSICS, 9, 624963 (2021)

AR Bell, JH Matthews

Echoes of the past: ultra-high-energy cosmic rays accelerated by radio galaxies, scattered by starburst galaxies

MONTHLY NOTICES OF THE ROYAL ASTRONOMICAL SOCIETY, 511, 448-456 (2022)

B Eliasson, A Senior, M Rietveld, ADR Phelps, RA Cairns, K Ronald, DC Speirs, RMGM Trines, I McCrea, R Bamford, JT Mendonça, R Bingham

Controlled beat-wave Brillouin scattering in the ionosphere

NATURE COMMUNICATIONS, 12, 6209 (2021)

J Meinecke, P Tzeferacos, JS Ross, AFA Bott, S Feister, H Park, AR Bell, R Blandford, RL Berger, R Bingham, A Casner, LE Chen, J Foster, DH Froula, C Goyon, D Kalantar, M Koenig, B Lahmann, C Li, Y Lu, CAJ Palmer, RD Petrasso, H Poole, B Remington, B Reville, A Reyes, A Rigby, D Ryu, G Swadling, A Zylstra, F Miniati, S Sarkar, AA Schekochihin, DQ Lamb, G Gregori

Strong suppression of heat conduction in a laboratory replica of galaxy-cluster turbulent plasmas

SCIENCE ADVANCES, 8, eabj6799 (2022)

T Nonnenmacher, T Dascalu, R Bingham, CL Cheung, H Lau, K Long, J Pozimski, C Whyte

Anomalous Beam Transport through Gabor (Plasma) Lens Prototype

APPLIED SCIENCES, 11, 4357 (2021)

L Perrone, G Gregori, B Reville, L Silva, R Bingham

Neutrino-electron magnetohydrodynamics in an expanding universe

PHYSICAL REVIEW D, 104, 123013 (2021)

K Beyer, G Marocco, R Bingham, G Gregori

Light-shining-through-wall axion detection experiments with a stimulating laser

PHYSICAL REVIEW D, 105, 35031 (2022)

CD Arrowsmith, N Shukla, N Charitonidis, R Boni, H Chen, T Davenne, A Dyson, DH Froula, JT Gudmundsson, BT Huffman, Y Kadi, B Reville, S Richardson, S Sarkar, JL Shaw, LO Silva, P Simon, RMGM Trines, R Bingham, G Gregori

Generating ultradense pair beams using 400 GeV/c protons

PHYSICAL REVIEW RESEARCH, 3, 23103 (2021)

C Perico, H Gao, KJ Heesom, SW Botchway, IA Sparkes

Arabidopsis thaliana myosin XIK is recruited to the Golgi through interaction with a MyoB receptor

COMMUNICATIONS BIOLOGY, 4, 1182 (2021)

AV Nunn, GW Guy, SW Botchway, JD Bell

SARS-CoV-2 and EBV; the cost of a second mitochondrial "whammy"?

IMMUNITY & AGEING, 18, 40 (2021)

R Sugumar, C Armstrong, S Sarkar, M Krishnamurthy, PP Rajeev, D Neely, V Sharma, S Krishnan

Design of activation based detection scheme for pulsed gamma ray emission from intense laser plasmas

AIP CONFERENCE PROCEEDINGS, 2352, 50034- (2022)

RA Simpson, DA Mariscal, J Kim, GG Scott, GJ Williams, E Grace, C McGuffey, S Wilks, A Kemp, N Lemos, BZ Djordjevic, E Folsom, D Kalantar, R Zacharias, B Pollock, J Moody, F Beg, A Morace, N Iwata, Y Sentoku, MJ Manuel, M Mauldin, M Quinn, K Youngblood, M Gatu-Johnson, B Lahmann, C Haefner, D Neely, T Ma

Demonstration of TNSA proton radiography on the National Ignition Facility Advanced Radiographic Capability (NIF-ARC) laser

PLASMA PHYSICS AND CONTROLLED FUSION, 63, 124006 (2021)

T Ma, D Mariscal, R Anirudh, T Bremer, BZ Djordjevic, T Galvin, E Grace, S Herriot, S Jacobs, B Kailkhura, R Hollinger, J Kim, S Liu, J Ludwig, D Neely, JJ Rocca, GG Scott, RA Simpson, BS Spears, TS Spinka, K Swanson, JJ Thiagarajan, B Van Essen, S Wang, SC Wilks, GJ Williams, J Zhang, MC Herrmann, C Haefner

Accelerating the rate of discovery: toward high-repetition-rate HED science

PLASMA PHYSICS AND CONTROLLED FUSION, 63, 104003 (2021)

BT Spiers, R Aboushelbaya, Q Feng, MW Mayr, I Ouatu, RW Paddock, R Timmis, RH Wang, PA Norreys

Methods for extremely sparse-angle proton tomography

PHYSICAL REVIEW E, 104, 45201 (2021)

CH Allen, M Oliver, L Divol, OL Landen, Y Ping, M Schölmerich, R Wallace, R Earley, W Theobald, TG White, T Döppner

Toward an integrated platform for characterizing laser-driven, isochorically heated plasmas with 1 μm spatial resolution

APPLIED OPTICS, 61, 1987-1993 (2022)

A Botteon, W Kim, C Colombo, M Realini, C Castiglioni, P Matousek, B Kim, T Kwon, C Conti

Non-destructive Monitoring of Dye Depth Profile in Mesoporous TiO_2 Electrodes of Solar Cells with Micro-SORS

ANALYTICAL CHEMISTRY, 94, 2966-2972 (2022)

S Mosca, P Dey, M Salimi, B Gardner, F Palombo, N Stone, P Matousek

Spatially Offset Raman Spectroscopy – How Deep?

ANALYTICAL CHEMISTRY, 93, 6755-6762 (2021)

M Varnasseri, H Muhamadali, Y Xu, PIC Richardson, N Byrd, DI Ellis, P Matousek, R Goodacre

Portable through Bottle SORS for the Authentication of Extra Virgin Olive Oil

APPLIED SCIENCES, 11, 8347 (2021)

MJ Dooley, T Paterson, L Dexter, P Matousek, H Dehghani, I Notingher

Model-Based Optimization of Laser Excitation and Detection Improves Spectral Contrast in Non-Invasive Diffuse Raman Spectroscopy

APPLIED SPECTROSCOPY, 76, 370282110729 (2022)

A Botteon, M Realini, C Colombo, C Conti, P Matousek, C Castiglioni

Micro-SORS, diffusion processes and heritage science: a non-destructive and systematic investigation

EUROPEAN PHYSICAL JOURNAL PLUS, 136, 880 (2021)

M Salimi, S Mosca, B Gardner, F Palombo, P Matousek, N Stone

Nanoparticle-Mediated Photothermal Therapy Limitation in Clinical Applications Regarding Pain Management

NANOMATERIALS, 12, 922 (2022)

P Dey, A Vaideanu, S Mosca, M Salimi, B Gardner, F Palombo, I Uchegbu, J Baumberg, A Schatzlein, P Matousek, N Stone

Surface enhanced deep Raman detection of cancer tumour through 71 mm of heterogeneous tissue

NANOTHERANOSTICS, 6, 337-349 (2022)

L Bignardis, SK Mahatha, D Lizzit, H Bana, E Travaglia, P Lacovig, C Sanders, A Baraldi, P Hofmann, S Lizzit

Anisotropic strain in epitaxial single-layer molybdenum disulfide on Ag(110)

NANOSCALE, 13, 18789-18798 (2021)

D Curcio, S Pakdel, K Volckaert, JA Miwa, S Ulstrup, N Lanatà, M Bianchi, D Kutnyakhov, F Pressacco, G Brenner, S Dziarzhytski, H Redlin, SY Agustsson, K Medjanik, D Vasilyev, H Elmers, G Schönhense, C Tusche, Y Chen, F Speck, T Seyller, K Bühlmann, R Gort, F Diekmann, K Rossnagel, Y Acremann, J Demsar, W Wurth, D Lizzit, L Bignardi, P Lacovig, S Lizzit, CE Sanders, P Hofmann

Ultrafast electronic linewidth broadening in the C 1s core level of graphene

PHYSICAL REVIEW B, 104, L161104 (2021)

J Zhao, Y Hu, Y Lu, H Zhang, L Hu, X Zhu, Z Sheng, ICE Turcu, A Pukhov, F Shao, T Yu

All-optical quasi-monoenergetic GeV positron bunch generation by twisted laser fields

COMMUNICATIONS PHYSICS, 5, 15 (2022)

J Lee, M Kim, G Kang, SM Vinko, L Bae, MS Cho, H Chung, S Kwon, G Lee, C Nam, S Park, JH Sohn, SH Yang, U Zastrau, BI Cho

Investigation of Nonequilibrium Electronic Dynamics of Warm Dense Copper with Femtosecond X-Ray Absorption Spectroscopy

PHYSICAL REVIEW LETTERS, 127, 175003 (2021)

M Kasim, S Vinko

Learning the Exchange-Correlation Functional from Nature with Fully Differentiable Density Functional Theory

PHYSICAL REVIEW LETTERS, 127, 126403 (2021)

P Hollebon, JS Wark, SM Vinko

Excited-state potentials for modelling dense plasmas from first principles

PLASMA PHYSICS AND CONTROLLED FUSION, 63, 114006 (2021)

MF Kasim, S Lehtola, SM Vinko

DQC: A Python program package for differentiable quantum chemistry

THE JOURNAL OF CHEMICAL PHYSICS, 156, 84801 (2022)

A Milsom, AM Squires, AD Ward, C Pfrang

The impact of molecular self-organisation on the atmospheric fate of a cooking aerosol proxy

ATMOSPHERIC CHEMISTRY AND PHYSICS, 22, 4895-4907 (2022)

A Milsom, AM Squires, JA Boswell, NJ Terrill, AD Ward, C Pfrang

An organic crystalline state in ageing atmospheric aerosol proxies: spatially resolved structural changes in levitated fatty acid particles

ATMOSPHERIC CHEMISTRY AND PHYSICS, 21, 15003-15021 (2021)

ER Barber, MR Ward, AD Ward, AJ Alexander

Laser-induced nucleation promotes crystal growth of anhydrous sodium bromide

CRYSTENGCOMM, 23, 8451-8461 (2021)

CA Johnson, AW Parker, PM Donaldson, S Garrett-Roe

An ultrafast vibrational study of dynamical heterogeneity in the protic ionic liquid ethyl-ammonium nitrate. I. Room temperature dynamics

THE JOURNAL OF CHEMICAL PHYSICS, 154, 134502 (2021)

S Bodian, RJ Colchester, TJ Macdonald, F Ambroz, M Briceno de Gutierrez, SJ Mathews, YMM Fong, E Maneas, KA Welsby, RJ Gordon, P Collier, EZ Zhang, PC Beard, IP Parkin, AE Desjardins, S Noimark

$CuInS_2$ Quantum Dot and Polydimethylsiloxane Nanocomposites for All-Optical Ultrasound and Photoacoustic Imaging

ADVANCED MATERIALS INTERFACES, 8, 2100518 (2021)

AJU Holt, S Pakdel, J Rodríguez-Fernández, Y Zhang, D Curcio, Z Sun, P Lacovig, Y Yao, JV Lauritsen, S Lizzit, N Lanatà, P Hofmann, M Bianchi, CE Sanders

Electronic properties of single-layer CoO_2/Au(111)

2D MATERIALS, 8, 35050 (2021)

AJ Tanner, B Wen, J Ontaneda, Y Zhang, R Grau-Crespo, HH Fielding, A Selloni, G Thornton

Polaron-Adsorbate Coupling at the TiO_2(110)-Carboxylate Interface

JOURNAL OF PHYSICAL CHEMISTRY LETTERS, 12, 3571-3576 (2021)

TARGET FABRICATION

ER Tubman, AS Joglekar, AFA Bott, M Borghesi, B Coleman, G Cooper, CN Danson, P Durey, JM Foster, P Graham, G Gregori, ET Gumbrell, MP Hill, T Hodge, S Kar, RJ Kingham, M Read, CP Ridgers, J Skidmore, C Spindloe, AGR Thomas, P Treadwell, S Wilson, L Willingale, NC Woolsey

Observations of pressure anisotropy effects within semi-collisional magnetized plasma bubbles

NATURE COMMUNICATIONS, 12, 334 (2021)

A Bott, L Chen, G Boutoux, T Caillaud, A Duval, M Koenig, B Khiar, I Lantuéjoul, L Le-Deroff, B Reville, R Rosch, D Ryu, C Spindloe, B Vauzour, B Villette, A Schekochihin, D Lamb, P Tzeferacos, G Gregori, A Casner

Inefficient Magnetic-Field Amplification in Supersonic Laser-Plasma Turbulence

PHYSICAL REVIEW LETTERS, 127, 175002 (2021)

F Suzuki-Vidal, T Clayson, C Stehlé, U Chaulagain, JWD Halliday, M Sun, L Ren, N Kang, H Liu, B Zhu, J Zhu, C De Almeida Rossi, T Mihailescu, P Velarde, M Cotelo, JM Foster, CN Danson, C Spindloe, JP Chittenden, C Kuranz

First radiative shock experiments on the SG-II laser

HIGH POWER LASER SCIENCE AND ENGINEERING, 9, e27 (2021)

Theses

ARTEMIS

Downes-Ward, B.

Generation of XUV photons and their application in time-resolved photoelectron spectroscopy

University of Southampton (2021)

Krause, R.

Ultrafast charge transfer in WS_2/graphene heterostructures

Universität Regensburg (2021)

GEMINI

Watt, R.

Monte Carlo Modelling of QED Interactions in Laser-Plasma Experiments

Imperial College London (2021)

Baird, C.

Applications of laser wakefield acceleration to high-field physics and industrial radiography

University of York (2021)

Picksley, A.

Low Density Plasma Waveguides for Multi-GeV Laser Wakefield Accelerators

University of Oxford (2021)

Jonnerby, J.

Multi-pulse laser wakefield acceleration

University of Oxford (2021)

VULCAN

Polin, K.

Ion dosimetry for radiobiology experiments employing laser-accelerated beams

Queen's University Belfast (2021)

Maiorino, C.

Pre-clinical evaluation of lethal and sublethal DNA damage in human cell cultures by ultrashort pulse and ultra-high dose rate laser accelerated protons

Queen's University Belfast (2021)

Bradford, P.

Laser-driven discharges and electromagnetic fields

University of York (2021)

Jarrett, J.

Optical diagnosis of dense plasma evolution during irradiation by ultra-intense laser pulses

University of Strathclyde (2021)

Frazer, T.

Investigation of laser-solid interaction physics with tightly focused, ultra-intense laser pulses

University of Strathclyde (2021)

Ferguson, S.

Novel Approach to Laser-Driven Multi-Stage Ion Acceleration

Queen's University Belfast (2021)

ULTRA

Campbell, E.

Hydrocarbon Pool Mechanisms in zeolite catalysts studied by Kerr-gated Raman Spectroscopy

University College London (2021)

Carson, H.

Computational Investigations of Electron Transfer in Transition Metal Complexes

University of Sheffield (2021)

Tolentino-Collado, J.

Molecular Eyes – Proteins that Translate Light into Biological Signals

Stony Brook University (2021)

Phelps, R.

Exploring the Role of Solvents on the Chemical Dynamics of Reactive Intermediates using Ultrafast Transient Absorption Spectroscopy

University of Bristol (2021)

Lewis-Borrell, L.

Mapping Photochemical Reaction Pathways by Application of Transient Absorption Spectroscopy

University of Bristol (2021)

Hsien Kao, M.

Transient Absorption Spectroscopy Studies of Photochemical Reactions Initiated by Electron Transfer

University of Bristol (2021)

Piercy, V.

Photocatalytic Materials for the Reduction of CO_2 to Fuels

University of Liverpool (2021)

OCTOPUS

McGrory, M.

Optical Properties of Atmospheric Aerosol using Laser Tweezers

Royal Holloway, University of London (2021)

Santos, A.

Spatial and physical organisation of the mammalian nucleus

University of Sheffield (2021)

Wojcik, S.

Beyond membrane curvature; Clade 6 reticulons and their role within the plant endoplasmic reticulum

Oxford Brookes University (2021)

Spatola Rossi, T.

Expression of particulate methane monooxygenase (pMMO) proteins in plants for methane detoxification

Oxford Brookes University (2021)

Panel Membership and CLF Structure

Laser for Science Facility Access Panel 2021/22

REVIEWERS

Professor P. Kukura (Panel Chair)
Department of Chemistry
University of Oxford

Dr S. Ameer-Beg
School of Cancer and Pharmaceutical Sciences
King's College London

Professor A. Beale
Department of Chemistry
University College London

Dr J. Bernadino de la Serna
Faculty of Medicine
Imperial College London

Professor J. Bredenbeck
Johann Wolfgang Goethe-Universität
Institut für Biophysik

Dr A. Cowan
Department of Chemistry
University of Liverpool

Dr S. Cox
Faculty of Life Sciences and Medicine
King's College London

Dr I. Dobbie
Department of Biochemistry
University of Oxford

Dr M. Frogley
Diamond Light Source

Dr E. Gibson
School of Natural and Environmental Sciences
University of Newcastle

Dr M. Kuimova
Department of Chemistry
Imperial College London

Dr S. Leveque-Fort
Institut des Sciences Moléculaires d'Orsay
Université Paris-Sud

Professor G. McConnell
Centre for Biophotonics
University of Strathclyde

Professor J. Moger
University of Exeter

Professor S. Pascu
Department of Chemistry
University of Bath

Professor J. Weinstein
Department of Chemistry
University of Sheffield

RESEARCH COUNCIL REPRESENTATIVES

A. McGavigan
MRC

A. Chapman
EPSRC

J. Swarbrick (then J. Whitford)
BBSRC

M. Simons
STFC

L. Garratt then L. Bettington
NERC

SCIENCE & TECHNOLOGY FACILITIES COUNCIL REPRESENTATIVES

Dr D. T. Clarke
(Head of Lasers for Science Facility)
Central Laser Facility
Science & Technology Facilities Council

Prof J.L. Collier
(Director)
Central Laser Facility
Science & Technology Facilities Council

Professor M. Towrie
(ULTRA Group Leader)
then Dr G.M. Greetham
Central Laser Facility
Science & Technology Facilities Council

Dr M. Martin-Fernandez
(OCTOPUS Group Leader)
Central Laser Facility
Science & Technology Facilities Council

Dr E. Gozzard
ISIS & CLF User Office
Science & Technology Facilities Council

Dr S.R. Needham
(Panel Secretary)
Central Laser Facility
Science & Technology Facilities Council

Artemis Facility Access Panel 2021/22

REVIEWERS

Professor H. Fielding
(Panel Chair)
University College London, UK

Professor M. Aeschlimann
University of Kaiserslautern, Germany

Dr A. Taleb
Synchrotron SOLEIL, Essonne, France

Professor L. Perfetti
Ecole Polytechnique, 91120 Palaiseau, France

Professor P. King
University of St Andrews, UK

Dr J. Stähler
Fritz Haber Institute, Berlin, Germany

Professor J. Tisch
Imperial College, London

Professor V. Stavros
University of Warwick, UK

Dr C. Cacho
Diamond Light Source, Harwell, Didcot, UK

SCIENCE & TECHNOLOGY FACILITIES COUNCIL REPRESENTATIVES

Professor J.L. Collier
(Director)
Central Laser Facility
Science & Technology Facilities Council

Ms C. Hernandez-Gomez
(Head, High Power Laser Programme)
Central Laser Facility
Science & Technology Facilities Council

Dr E. Springate
(Artemis Group Leader)
Central Laser Facility
Science & Technology Facilities Council

Dr R.T. Chapman
(Artemis, AMO and Imaging)
Central Laser Facility
Science & Technology Facilities Council

Dr D.T Clarke
(Head of Lasers for Science Facility)
Central Laser Facility
Science & Technology Facilities Council

Professor M. Towrie
(Molecular and Structural Dynamics)
Central Laser Facility
Science & Technology Facilities Council

Vulcan, Astra TA2 & Gemini Facility Access Panel 2021/22

REVIEWERS

Professor N. Woolsey
(Panel Chair)
York Plasma Institute
University of York

Professor B. Dromey
Department of Pure and Applied Physics
Queen's University of Belfast

Professor G. Gregori
Clarendon Laboratory
University of Oxford

Dr S. Mangles
Blackett Laboratory
Imperial College London

Dr J. Pasley
York Plasma Institute
University of York

Professor B. Hidding
Department of Physics
University of Strathclyde

Professor T. Arber
Department of Physics
University of Warwick

Dr R. Kingham
Blackett Laboratory
Imperial College London

Dr A. Klisnick
Institut des Sciences Moléculaires d'Orsay
Université Paris-Saclay

Dr B. Cros
Laboratory of Gas Physics and Plasmas
Université Paris-Sud

RESEARCH COUNCIL REPRESENTATIVES

Mr C. Danson
AWE

SCIENCE & TECHNOLOGY FACILITIES COUNCIL REPRESENTATIVES

Professor J.L. Collier
(Director)
Central Laser Facility
Science & Technology Facilities Council

Ms C. Hernandez-Gomez
(Head, High Power Laser Programme)
Central Laser Facility
Science & Technology Facilities Council

Dr I.O. Musgrave
(Vulcan Group Leader)
Central Laser Facility
Science & Technology Facilities Council

Mr R.J. Clarke
(Experimental Science Group Leader)
Central Laser Facility
Science & Technology Facilities Council

Dr R. Pattathil
(Gemini Group Leader)
Central Laser Facility
Science & Technology Facilities Council

Dr D. Symes
(Gemini Target Area Section Leader)
Central Laser Facility
Science & Technology Facilities Council

Dr D. Carroll
(Panel Secretary)
Central Laser Facility
Science & Technology Facilities Council

Mr C. Spindloe
Scitech Precision

Dr E. Gozzard
ISIS Neutron & Muon Source
Science & Technology Facilities Council

Central Laser Facility Structure

Director

Professor John Collier
john.collier@stfc.ac.uk

Lasers for Science Division

Dr Dave Clarke
dave.clarke@stfc.ac.uk

CALTA Division

Dr Chris Edwards
chris.edwards@stfc.ac.uk

High Power Lasers Division

Ms Cristina Hernandez-Gomez
cristina.hernandez-gomez@stfc.ac.uk

Engineering & Technology Division

Mr Steve Blake
steve.blake@stfc.ac.uk

Ultra

Dr Greg Greetham
greg.greetham@stfc.ac.uk

Octopus

Prof Marisa Martin-Fernandez
marisa.martin-fernandez@stfc.ac.uk

Artemis

Dr Emma Springate
emma.springate@stfc.ac.uk

Gemini

Dr Rajeev Pattathil
rajeev.pattathil@stfc.ac.uk

Experimental Science

Mr Rob Clarke
rob.clarke@stfc.ac.uk

Target Fabrication

Mr Martin Tolley
martin.tolley@stfc.ac.uk

Vulcan

Dr Ian Musgrave
ian.musgrave@stfc.ac.uk

Plasma Physics

Dr Alex Robinson
alex.robinson@stfc.ac.uk

Mechanical

Mr Steve Hook
steven.hook@stfc.ac.uk

Electrical

Mr Kenny Rodgers
kenny.rodgers@stfc.ac.uk

Science and Technology Facilities Council